



CRCLEME
Cooperative Research Centre for
Landscape Evolution & Mineral Exploration



**OPEN FILE
REPORT
SERIES**



AMIRA

Australian Mineral Industries Research Association Limited ACN 004 448 266

BEASLEY CREEK ORIENTATION STUDY GEOCHEMISTRY, PETROGRAPHY AND MINERALOGY OF FERRUGINOUS LAG OVERLYING THE BEASLEY CREEK GOLD MINE - LAVERTON, WESTERN AUSTRALIA

Volume 2 - Appendices

I.D.M. Robertson

CRC LEME OPEN FILE REPORT 10

September 1998

(CSIRO Division of Exploration Geoscience Report 27R, 1989.
Second impression 1998)

CRC LEME is an unincorporated joint venture between The Australian National University, University of Canberra, Australian Geological Survey Organisation and CSIRO Exploration and Mining, established and supported under the Australian Government's Cooperative Research Centres Program.





Australian Mineral Industries Research Association Limited ACN 004 448 266



CRCLEME

Cooperative Research Centre for
Landscape Evolution & Mineral Exploration



BEASLEY CREEK ORIENTATION STUDY GEOCHEMISTRY, PETROGRAPHY AND MINERALOGY OF FERRUGINOUS LAG OVERLYING THE BEASLEY CREEK GOLD MINE -LAVERTON, WESTERN AUSTRALIA

Volume 2 - Appendices

I.D.M. Robertson

CRC LEME OPEN FILE REPORT 10

September 1998

(CSIRO Division of Exploration Geoscience Report 27R, 1989.
Second impression 1998)

© CSIRO 1989

RESEARCH ARISING FROM CSIRO/AMIRA REGOLITH GEOCHEMISTRY PROJECTS 1987-1993

In 1987, CSIRO commenced a series of multi-client research projects in regolith geology and geochemistry which were sponsored by companies in the Australian mining industry, through the Australian Mineral Industries Research Association Limited (AMIRA). The initial research program, "Exploration for concealed gold deposits, Yilgarn Block, Western Australia" (1987-1993) had the aim of developing improved geological, geochemical and geophysical methods for mineral exploration that would facilitate the location of blind, buried or deeply weathered gold deposits. The program included the following projects:

P240: Laterite geochemistry for detecting concealed mineral deposits (1987-1991). Leader: Dr R.E. Smith. Its scope was development of methods for sampling and interpretation of multi-element laterite geochemistry data and application of multi-element techniques to gold and polymetallic mineral exploration in weathered terrain. The project emphasised viewing laterite geochemical dispersion patterns in their regolith-landform context at local and district scales. It was supported by 30 companies.

P241: Gold and associated elements in the regolith - dispersion processes and implications for exploration (1987-1991). Leader: Dr C.R.M. Butt.

The project investigated the distribution of ore and indicator elements in the regolith. It included studies of the mineralogical and geochemical characteristics of weathered ore deposits and wall rocks, and the chemical controls on element dispersion and concentration during regolith evolution. This was to increase the effectiveness of geochemical exploration in weathered terrain through improved understanding of weathering processes. It was supported by 26 companies.

These projects represented "an opportunity for the mineral industry to participate in a multi-disciplinary program of geoscience research aimed at developing new geological, geochemical and geophysical methods for exploration in deeply weathered Archaean terrains". This initiative recognised the unique opportunities, created by exploration and open-cut mining, to conduct detailed studies of the weathered zone, with particular emphasis on the near-surface expression of gold mineralisation. The skills of existing and specially recruited research staff from the Floreat Park and North Ryde laboratories (of the then Divisions of Minerals and Geochemistry, and Mineral Physics and Mineralogy, subsequently Exploration Geoscience and later Exploration and Mining) were integrated to form a task force with expertise in geology, mineralogy, geochemistry and geophysics. Several staff participated in more than one project. Following completion of the original projects, two continuation projects were developed.

P240A: Geochemical exploration in complex lateritic environments of the Yilgarn Craton, Western Australia (1991-1993). Leaders: Drs R.E. Smith and R.R. Anand.

The approach of viewing geochemical dispersion within a well-controlled and well-understood regolith-landform and bedrock framework at detailed and district scales continued. In this extension, focus was particularly on areas of transported cover and on more complex lateritic environments typified by the Kalgoorlie regional study. This was supported by 17 companies.

P241A: Gold and associated elements in the regolith - dispersion processes and implications for exploration. Leader: Dr. C.R.M. Butt.

The significance of gold mobilisation under present-day conditions, particularly the important relationship with pedogenic carbonate, was investigated further. In addition, attention was focussed on the recognition of primary lithologies from their weathered equivalents. This project was supported by 14 companies.

Although the confidentiality periods of the research reports have expired, the last in December 1994, they have not been made public until now. Publishing the reports through the CRC LEME Report Series is seen as an appropriate means of doing this. By making available the results of the research and the authors' interpretations, it is hoped that the reports will provide source data for future research and be useful for teaching. CRC LEME acknowledges the Australian Mineral Industries Research Association and CSIRO Division of Exploration and Mining for authorisation to publish these reports. It is intended that publication of the reports will be a substantial additional factor in transferring technology to aid the Australian Mineral Industry.

This report (CRC LEME Open File Report 10) is a first revision of CSIRO, Division of Exploration Geoscience Restricted Report 027R, first issued in 1989, which formed part of the CSIRO/AMIRA Project P240.

Copies of this publication can be obtained from:

The Publication Officer, CRC LEME, CSIRO Exploration and Mining, PMB, Wembley, WA 6014, Australia. Information on other publications in this series may be obtained from the above or from <http://leme.anu.edu.au/>

Bibliographic reference:

This publication should be referred to as Robertson, I.D.M., 1998. Geochemistry, petrography and mineralogy of ferruginous lag overlying the Beasley Creek Gold Mine - Laverton WA. Open File Report 10, Cooperative Research Centre for Landscape Evolution and Mineral Exploration, Perth, Australia.

Cataloguing-in-Publication:

Robertson, I.D.M.

Geochemistry, petrography and mineralogy of ferruginous lag overlying the Beasley Creek Gold Mine - Laverton WA
ISBN v1: 0 642 28224 2 v2: 0 642 28230 7 set: 0 642 28236 6

1. Geochemistry 2. Laterite 3. Mineralogy 4. Gold - Western Australia.

I. Title

CRC LEME Open File Report 10.

ISSN 1329-4768

APPENDIX 1

Coarse Lag

Tabulated Geochemistry

Oxides in weight %

Trace elements in ppm

Mine co-ordinates in metres

COARSE LAGS

LINE 38820

Sample Numbers			Co-ordinates		ICP	ICP	XRF	ICP	ICP	ICP	XRF	ICP
Field No	Lab Seq	Lib No	East	North	SiO ₂	Al ₂ O ₃	Fe ₂ O ₃	Fe ₂ O ₃	MgO	CaO	TiO ₂	TiO ₂
BC 001	L08-0120	08-082	33600	38820	8.06	4.84	69.34	74.00	0.12	0.11	0.40	0.32
BC 002	L08-0112	08-083	33650	38820	7.84	4.70	70.34	75.00	0.11	0.10	0.36	0.29
BC 003	L08-0117	08-084	33700	38820	7.46	3.92	72.06	80.00	0.11	0.11	0.31	0.25
BC 004	L08-0097	08-085	33750	38820	7.68	3.76	71.06	75.40	0.12	0.13	0.48	0.39
BC 005	L08-0093	08-086	33800	38820	7.38	4.58	70.06	71.80	0.14	0.17	0.41	0.32
BC 006	L08-0116	08-087	33850	38820	7.26	4.06	72.20	77.80	0.16	0.27	0.34	0.27
BC 007	L08-0087	08-088	33900	38820	7.94	3.74	69.05	70.60	0.16	0.27	0.41	0.31
BC 008	L08-0099	08-089	33925	38820	8.48	3.00	71.06	70.40	0.15	0.27	0.30	0.23
BC 009	L08-0091	08-090	33950	38820	6.22	3.22	72.34	75.80	0.14	0.26	0.30	0.25
BC 010	L08-0115	08-091	33975	38820	7.54	3.87	70.20	68.80	0.14	0.20	0.48	0.34
BC 011	L08-0089	08-092	34000	38820	5.18	3.62	71.63	74.40	0.14	0.20	0.46	0.34
BC 012	L08-0113	08-093	34025	38820	6.48	4.14	71.91	76.80	0.14	0.23	0.34	0.27
BC 013	L08-0084	08-094	34050	38820	6.90	5.34	67.05	66.60	0.15	0.12	0.52	0.38
BC 014	L08-0109	08-095	34075	38820	6.26	6.68	71.06	72.40	0.09	0.08	0.46	0.34
BC 015	L08-0094	08-096	34100	38820	6.30	5.20	70.20	71.60	0.12	0.08	0.46	0.35
BC 016	L08-0123	08-097	34150	38820	7.54	6.00	70.06	79.80	0.11	0.08	0.37	0.32
BC 017	L08-0086	08-098	34200	38820	6.02	4.24	71.91	73.00	0.12	0.10	0.29	0.23
BC 018	L08-0082	08-099	34250	38820	5.90	3.66	72.77	72.00	0.12	0.11	0.33	0.25
BC 706	L08-0474	08-440	34350	38820	11.60	8.13	66.34	70.80	0.08	0.08	0.75	0.60
BC 707	L08-0440	08-441	34450	38820	9.92	8.31	67.05	68.30	0.08	0.07	0.75	0.53
BC 708	L08-0466	08-442	34550	38820	12.30	8.87	67.77	77.90	0.06	0.08	0.87	0.71
BC 709	L08-0452	08-443	34650	38820	14.30	7.82	64.91	71.10	0.09	0.08	0.89	0.67
BC 710	L08-0475	08-444	34750	38820	13.04	5.51	66.34	68.11	0.08	0.07	0.67	0.48
Min			33600	38820	5.18	3.00	64.91	66.60	0.06	0.07	0.29	0.23
Max			34750	38820	14.30	8.87	72.77	80.00	0.16	0.27	0.89	0.71

COARSE LAGS

LINE 38820

Sample	XRF	INAA	INAA	ICP	ICP	XRF	INAA	XRF	INAA	ICP	INAA	ICP	XRF	XRF	XRF	INAA	ICP	XRF	
Lib No	Ag	As	Au	Ba	Be	Bi	Ce	Cd	Co	Cr	Cr	Cu	Cu	Ga	Ge	In	La	Mn	Mn
08-082	9	229	1.869	396	0	0	25.5	0	22.8	260	243	109	81	4	0	0	15.2	768	587
08-083	2	382	1.596	216	1	1	21.2	0	26.4	262	243	179	124	3	1	0	12.8	870	659
08-084	1	246	0.907	111	1	0	18.5	1	176.7	266	236	216	95	0	0	0	11.6	946	583
08-085	0	193	3.200	134	0	0	19.0	0	25.7	220	219	170	140	3	0	0	11.0	846	625
08-086	5	182	0.789	552	0	2	21.5	3	24.4	167	181	167	113	2	0	3	10.9	806	649
08-087	0	180	1.011	540	0	0	19.7	0	23.5	169	143	242	102	1	0	1	11.6	950	705
08-088	0	148	1.430	674	0	1	14.5	0	20.6	185	161	150	140	10	0	1	9.7	620	504
08-089	2	171	2.788	738	0	0	20.2	2	25.3	168	179	181	134	0	0	0	11.6	868	683
08-090	0	228	1.273	770	0	1	18.6	0	29.8	122	124	558	102	0	0	2	10.6	1542	1171
08-091	0	339	2.666	648	0	1	15.0	0	43.1	212	191	141	119	2	0	1	7.6	9510	7624
08-092	0	324	0.456	382	0	1	15.6	2	46.3	204	181	142	103	0	5	0	8.8	20296	14849
08-093	0	278	12.450	197	2	1	9.4	0	24.3	216	179	166	100	0	0	0	7.8	3060	2311
08-094	1	139	0.713	850	0	1	24.4	0	64.9	464	456	136	134	5	0	1	9.5	36090	27899
08-095	1	229	0.467	54	0	2	10.1	0	22.1	554	560	185	125	7	0	0	6.8	738	606
08-096	0	117	0.891	244	0	0	9.5	1	20.3	314	341	126	125	4	0	1	9.3	1158	910
08-097	0	293	1.840	101	0	0	17.7	0	25.4	474	446	123	105	2	0	0	9.7	800	575
08-098	1	246	1.062	71	0	0	12.6	0	28.9	446	445	166	144	6	1	0	8.2	590	500
08-099	0	173	1.057	86	0	0	1.7	1	34.8	224	233	127	97	5	0	2	11.2	826	696
08-440	0	81	0.345	112	0	1	20.4	1	21.3	728	711	118	107	24	2	0	12.7	556	452
08-441	0	75	0.183	52	0	0	24.0	0	12.5	872	880	99	85	39	5	0	13.1	426	355
08-442	0	76	0.104	156	0	0	38.0	0	7.7	906	826	86	69	47	2	0	19.7	492	377
08-443	0	25	0.007	825	0	3	19.1	0	16.3	520	516	114	101	40	3	0	11.8	957	769
08-444	0	22	0.035	1646	0	0	31.0	1	21.6	366	368	98	128	19	0	0	17.7	467	376
Min	0	22	0.007	52	0	0	1.7	0	7.7	122	124	86	69	0	0	0	6.8	426	355
Max	9	382	12.450	1646	2	3	38.0	3	176.7	906	880	558	144	47	5	3	19.7	36090	27899

COARSE LAGS

LINE 38820

Sample Lib No	INAA Mo	XRF Nb	ICP Ni	XRF Ni	XRF Pb	XRF Rb	INAA Sb	XRF Se	XRF Sn	XRF Sr	ICP V	XRF V	INAA W	XRF Y	XRF Zn	ICP Zr	XRF Zr
08-082	5.5	0	103	64	18	10	2.6	3	1	9	228	283	5.2	37	314	0	29
08-083	5.6	4	135	75	16	7	1.8	3	0	6	392	452	2.4	37	334	0	23
08-084	5.5	2	185	74	29	5	0.9	1	0	3	326	357	8.7	30	210	0	22
08-085	6.4	0	114	84	14	2	1.1	0	0	3	278	366	5.0	43	235	0	28
08-086	5.8	0	70	39	26	12	2.4	1	0	19	334	432	4.1	34	240	0	21
08-087	5.4	0	124	78	27	5	0.8	0	0	17	378	438	8.4	25	252	0	21
08-088	3.6	2	80	67	28	3	2.3	3	3	24	548	668	6.0	29	249	0	22
08-089	6.2	0	119	68	24	5	1.0	1	3	20	364	474	14.8	28	230	0	15
08-090	5.8	0	76	55	25	7	0.5	1	3	22	220	300	8.7	30	205	0	19
08-091	4.7	0	72	41	26	10	0.8	5	2	23	241	285	5.6	22	185	0	21
08-092	3.8	0	77	50	33	8	0.7	2	0	17	300	384	3.6	26	210	0	20
08-093	5.0	1	71	49	51	8	1.6	0	1	10	392	446	13.5	28	303	0	20
08-094	5.8	1	74	58	34	12	0.8	2	0	24	288	384	8.3	23	204	71	50
08-095	4.2	2	82	51	14	0	0.6	2	0	6	532	610	2.4	20	192	0	30
08-096	6.0	2	97	79	113	8	1.6	0	0	4	398	497	8.3	29	285	0	29
08-097	5.7	0	143	107	30	7	1.1	2	0	0	412	446	6.0	25	302	0	29
08-098	5.8	1	129	98	28	7	2.4	1	0	5	418	512	10.6	26	447	0	23
08-099	4.2	0	346	292	41	9	1.1	0	0	7	294	366	9.8	47	594	0	24
08-440	4.8	3	83	55	51	3	1.5	4	2	5	903	1071	3.8	18	214	41	63
08-441	5.4	1	51	26	36	1	1.4	6	0	3	1013	1455	3.6	9	101	54	67
08-442	4.8	6	42	17	46	1	1.5	3	2	6	1606	1970	3.5	7	50	124	125
08-443	8.0	0	46	20	44	2	1.6	5	0	16	1332	1854	4.3	9	91	86	85
08-444	3.6	0	55	45	51	0	0.4	5	1	26	958	1324	4.0	12	169	139	82
Min	3.6	0	42	17	14	0	0.4	0	0	0	220	283	2.4	7	50	0	15
Max	8.0	6	346	292	113	12	2.6	6	3	26	1606	1970	14.8	47	594	139	125

COARSE LAGS

LINE 38940

Sample Numbers				Co-ordinates		ICP	ICP	XRF	ICP	ICP	ICP	XRF	ICP
Field No	Lab Seq	Lib No		East	North	SiO ₂	Al ₂ O ₃	Fe ₂ O ₃	Fe ₂ O ₃	MgO	CaO	TiO ₂	TiO ₂
BC 021	L08-0119	08-100		33650	38940	14.20	5.16	65.05	69.60	0.12	0.15	0.43	0.36
BC 022	L08-0090	08-101		33700	38940	8.00	5.96	69.34	72.80	0.13	0.16	0.40	0.32
BC 023	L08-0105	08-102		33750	38940	7.82	5.28	71.91	75.40	0.12	0.18	0.56	0.45
BC 024	L08-0103	08-103		33800	38940	8.96	3.54	69.20	69.40	0.21	0.35	0.31	0.24
BC 025	L08-0110	08-104		33850	38940	7.84	3.96	70.48	74.40	0.19	0.30	0.39	0.30
BC 026	L08-0083	08-105		33900	38940	7.62	3.16	71.49	74.00	0.15	0.21	0.29	0.23
BC 027	L08-0098	08-106		33925	38940	6.70	3.80	69.63	72.80	0.15	0.25	0.32	0.24
BC 028	L08-0114	08-107		33950	38940	9.58	5.66	67.62	74.80	0.20	0.41	0.71	0.54
BC 029	L08-0118	08-108		33975	38940	9.24	5.06	66.34	72.80	0.35	1.35	0.58	0.46
BC 030	L08-0107	08-109		34000	38940	9.88	4.26	69.48	74.00	0.18	0.32	0.42	0.33
BC 031	L08-0108	08-110		34025	38940	6.88	4.34	71.34	77.20	0.13	0.21	0.41	0.33
BC 032	L08-0122	08-111		34050	38940	10.10	8.26	67.20	77.40	0.12	0.16	0.52	0.47
BC 033	L08-0102	08-112		34100	38940	8.46	8.04	68.05	66.80	0.08	0.08	0.73	0.53
BC 034	L08-0100	08-113		34150	38940	8.64	7.96	68.63	68.60	0.10	0.08	0.67	0.50
BC 035	L08-0095	08-114		34200	38940	11.70	9.68	65.05	69.80	0.09	0.11	0.65	0.53
BC 036	L08-0121	08-115		34250	38940	10.10	8.80	67.77	74.40	0.10	0.13	0.59	0.49
BC 037	L08-0101	08-116		34300	38940	7.94	7.12	69.77	70.80	0.08	0.08	0.62	0.46
BC 701	L08-0460	08-435		34400	38940	11.10	8.44	67.34	74.40	0.10	0.14	0.86	0.65
BC 702	L08-0471	08-436		34500	38940	13.70	5.96	64.05	71.40	0.12	0.10	0.78	0.65
BC 703	L08-0453	08-437		34600	38940	21.60	5.35	60.33	66.10	0.11	0.13	0.60	0.47
BC 704	L08-0469	08-438		34700	38940	20.80	4.02	60.76	67.60	0.12	0.12	0.34	0.28
BC 705	L08-0439	08-439		34800	38940	18.30	4.37	61.05	60.80	0.11	0.10	1.05	0.76
Min				33650	38940	6.70	3.16	60.33	60.80	0.08	0.08	0.29	0.23
Max				34800	38940	21.60	9.68	71.91	77.40	0.35	1.35	1.05	0.76

COARSE LAGS

LINE 38940

Sample Lib No	XRF Ag	INAA As	INAA Au	ICP Ba	ICP Be	XRF Bi	INAA Ce	XRF Cd	INAA Co	ICP Cr	INAA Cr	ICP Cu	XRF Cu	XRF Ga	XRF Ge	XRF In	INAA La	ICP Mn	XRF Mn
08-100	1	95	0.395	1480	0	0	27.0	0	27.5	382	372	146	117	9	3	0	15.3	708	537
08-101	3	185	1.359	1260	0	0	31.8	1	27.3	342	344	121	112	7	0	0	18.4	880	692
08-102	1	219	0.085	1420	1	0	54.5	1	27.1	504	512	149	99	11	0	1	29.6	664	515
08-103	0	160	0.633	920	0	1	31.6	0	70.4	174	196	206	160	0	0	2	14.0	1892	1501
08-104	0	164	0.288	-	-	0	18.2	0	31.9	282	285	-	140	0	0	4	10.6	1322	1020
08-105	2	313	6.196	562	0	0	2.9	0	26.8	161	152	236	134	0	0	1	9.8	1590	1279
08-106	1	288	2.741	736	0	0	37.3	0	89.1	178	186	256	198	1	0	1	13.3	8110	5940
08-107	3	1041	12.047	364	0	0	11.2	0	18.6	462	410	290	178	2	0	0	8.9	1082	822
08-108	5	822	8.826	1000	1	0	16.0	0	13.5	436	399	214	155	14	0	0	9.8	828	653
08-109	0	407	2.295	654	0	0	13.5	1	17.7	284	262	226	164	9	0	1	10.8	1038	815
08-110	0	322	5.188	614	1	1	16.6	0	23.5	350	321	220	120	9	0	0	9.9	1866	1446
08-111	0	80	1.322	1386	0	0	7.8	0	15.1	484	451	86	64	19	1	4	5.1	1154	792
08-112	1	82	0.520	316	0	0	7.3	0	14.7	702	765	103	66	30	3	3	4.3	634	476
08-113	3	86	0.231	35	0	0	10.5	1	16.5	764	803	113	123	27	4	1	4.9	934	725
08-114	0	57	0.077	48	0	2	13.6	1	16.5	748	686	86	71	26	3	1	6.4	506	383
08-115	3	110	0.300	140	0	0	13.8	0	15.2	722	668	111	91	32	3	0	7.9	604	441
08-116	2	234	0.432	159	0	1	20.5	0	18.3	502	532	163	88	18	3	0	10.2	628	503
08-435	0	38	0.180	2346	0	1	57.0	0	8.5	600	577	88	57	48	2	0	35.9	440	362
08-436	1	41	0.006	2243	0	0	34.3	2	33.7	387	347	196	167	16	4	0	22.2	466	367
08-437	0	35	0.006	1000	0	1	25.6	1	37.6	393	374	200	199	14	2	0	17.8	469	398
08-438	0	34	0.066	1728	0	1	29.3	0	33.4	292	253	214	177	8	0	0	20.1	570	461
08-439	0	69	0.006	1509	0	0	28.8	1	37.2	313	301	195	197	15	0	2	19.7	538	488
Min	0	34	0.006	35	0	0	2.9	0	8.5	161	152	86	57	0	0	0	4.3	440	362
Max	5	1041	12.047	2346	1	2	57.0	2	89.1	764	803	290	199	48	4	4	35.9	8110	5940

COARSE LAGS

LINE 38940

Sample Lib No	INAA Mo	XRF Nb	ICP Ni	XRF Ni	XRF Pb	XRF Rb	INAA Sb	XRF Se	XRF Sn	XRF Sr	ICP V	XRF V	INAA W	XRF Y	XRF Zn	ICP Zr	XRF Zr
08-100	5.0	5	109	88	23	9	1.3	5	1	27	550	611	5.5	19	200	0	31
08-101	5.9	1	69	41	32	9	2.4	4	0	18	502	575	6.9	25	213	0	34
08-102	6.6	5	82	45	32	6	3.6	3	0	23	896	961	4.9	27	136	7	56
08-103	6.2	0	87	82	22	5	1.1	3	1	36	356	461	2.1	30	281	0	18
08-104	5.4	3	113	76	22	5	0.6	2	1	29	348	415	5.1	27	198	0	24
08-105	6.9	0	66	54	26	6	0.4	1	0	16	322	396	2.6	25	192	0	14
08-106	6.6	2	117	94	25	8	0.4	1	1	20	308	396	4.8	34	262	0	16
08-107	5.5	0	55	24	41	11	0.9	6	0	34	856	944	8.7	29	202	0	33
08-108	6.0	0	41	19	47	11	0.8	6	0	86	712	765	8.3	30	192	0	43
08-109	5.3	2	73	55	37	9	0.5	4	1	25	468	537	6.2	29	292	0	23
08-110	6.1	0	81	39	26	2	0.8	0	2	17	688	725	6.2	24	216	0	28
08-111	5.0	0	56	35	17	6	1.4	1	0	13	790	816	5.0	11	123	0	33
08-112	5.5	1	50	32	18	8	1.2	4	1	9	1106	1255	4.3	9	107	0	55
08-113	6.1	0	51	62	22	4	1.2	3	2	4	1014	1154	5.3	9	100	0	50
08-114	6.0	4	77	67	23	5	1.0	5	0	3	968	1046	5.0	12	125	0	49
08-115	6.0	0	58	43	25	2	1.3	5	2	8	990	1057	3.5	10	97	0	48
08-116	5.9	5	35	42	21	4	1.0	3	2	7	836	972	4.7	10	76	0	48
08-435	4.9	1	38	22	58	3	0.9	4	0	54	1660	2446	3.4	7	69	90	84
08-436	4.9	1	114	75	58	3	1.1	3	2	54	934	1079	8.8	20	237	20	52
08-437	5.5	1	98	65	51	2	1.6	2	1	25	646	790	14.7	15	203	94	87
08-438	5.0	0	125	81	54	1	1.0	1	2	45	626	670	7.0	21	251	8	46
08-439	5.1	5	114	95	48	6	2.7	1	0	33	619	821	16.9	20	183	83	89
Min	4.9	0	35	19	17	1	0.4	0	0	3	308	396	2.1	7	69	0	14
Max	6.9	5	125	95	58	11	3.6	6	2	86	1660	2446	16.9	34	292	94	89

KHAKI LAG

Sample Numbers			Co-ordinates		ICP	ICP	XRF	ICP	ICP	ICP	XRF	ICP
Field No	Lab Seq	Lib No	East	North	SiO ₂	Al ₂ O ₃	Fe ₂ O ₃	Fe ₂ O ₃	MgO	CaO	TiO ₂	TiO ₂
BC 112	L08-0126	08-124	34025	38820	13.80	16.40	53.47	57.20	0.18	0.16	1.45	1.15
BC 113	L08-0132	08-125	34050	38820	12.90	15.20	54.47	58.20	0.14	0.11	1.31	1.08
BC 114	L08-0125	08-126	34075	38820	7.50	12.10	66.20	71.20	0.09	0.08	0.99	0.75
BC 116	L08-0129	08-127	34150	38820	12.70	12.10	58.76	61.40	0.15	0.10	0.80	0.63
BC 117	L08-0128	08-128	34200	38820	13.70	11.40	58.76	60.60	0.10	0.10	0.72	0.56
BC 118	L08-0133	08-129	34250	38820	13.60	11.10	60.05	62.00	0.11	0.10	0.68	0.51
BC 131	L08-0127	08-130	34025	38940	12.20	21.00	47.61	49.80	0.20	0.14	2.54	1.99
BC 132	L08-0134	08-131	34050	38940	9.40	16.70	54.47	58.20	0.13	0.09	2.17	1.64
BC 133	L08-0124	08-132	34100	38940	9.74	16.30	57.33	62.60	0.13	0.08	2.04	1.59
BC 231	L08-0130	08-133	34025	38940	12.00	15.90	56.04	58.20	0.15	0.16	1.35	1.06
Min	-	-	34025	38820	7.50	11.10	47.61	49.80	0.09	0.08	0.68	0.51
Max	-	-	34250	38940	13.80	21.00	66.20	71.20	0.20	0.16	2.54	1.99

BACKGROUND DATA SET

Sample Numbers			Co-ordinates		ICP	ICP	XRF	ICP	ICP	ICP	XRF	ICP
Field No	Lab Seq	Lib No	East	North	SiO ₂	Al ₂ O ₃	Fe ₂ O ₃	Fe ₂ O ₃	MgO	CaO	TiO ₂	TiO ₂
BC 041	L08-0085	08-117	33747	39311	18.00	8.40	59.48	61.60	0.18	0.09	0.61	0.48
BC 042	L08-0106	08-118	34172	39314	16.20	6.82	64.19	68.80	0.09	0.10	0.75	0.59
BC 043	L08-0104	08-119	33545	38146	16.00	7.04	61.91	64.00	0.11	0.11	0.53	0.41
BC 044	L08-0088	08-120	34290	38110	11.20	6.04	69.05	74.00	0.07	0.10	1.42	1.05
G.Mean	-	-	-	-	15.12	7.03	63.56	66.93	0.11	0.10	0.77	0.59
Max	-	-	-	-	18.00	8.40	69.05	74.00	0.18	0.11	1.42	1.05
Min	-	-	-	-	11.20	6.04	59.48	61.60	0.07	0.09	0.53	0.41

STANDARD

Sample Numbers			Co-ordinates		ICP	ICP	XRF	ICP	ICP	ICP	XRF	ICP
Field No	Lab Seq	Lib No	East	North	SiO ₂	Al ₂ O ₃	Fe ₂ O ₃	Fe ₂ O ₃	MgO	CaO	TiO ₂	TiO ₂
STD 9	L08-0477	08-477	-	-	13.36	7.06	64.48	66.14	0.12	0.13	0.69	0.50
STD 9	L08-0111	08-121	-	-	-	-	-	-	-	-	-	-
STD 9	L08-0092	08-122	-	-	-	-	-	-	-	-	-	-
STD 9	L08-0096	08-123	-	-	-	-	-	-	-	-	-	-
STD 9	L08-131	08-135	-	-	-	-	-	-	-	-	-	-
Mean	-	-	-	-	13.36	7.06	64.48	66.14	0.12	0.13	0.69	0.50
Pre Val	-	-	-	-	14.14	7.48	72.92	72.92	0.10	0.10	0.70	0.70

KHAKI LAG

Sample Lib No	XRF Ag	INAA As	INAA Au	ICP Ba	ICP Be	XRF Bi	INAA Ce	XRF Cd	INAA Co	ICP Cr	INAA Cr	ICP Cu	XRF Cu	XRF Ga	XRF Ge	XRF In	INAA La	ICP Mn	XRF Mn
08-124	2	99	2.102	254	0	0	6.4	0	19.2	1280	1218	185	172	38	0	0	3.2	706	570
08-125	4	90	0.500	430	0	0	11.1	0	15.2	920	948	195	201	41	1	0	7.3	702	570
08-126	0	98	0.725	121	0	0	12.0	1	14.1	968	943	141	151	41	0	0	9.3	1004	744
08-127	2	147	0.212	108	0	0	9.5	1	18.8	616	624	1560	143	22	0	0	5.4	572	489
08-128	4	148	0.483	63	0	0	14.5	0	27.8	426	421	126	115	7	0	1	7.5	286	224
08-129	0	39	0.477	90	1	0	18.4	3	29.9	570	603	97	97	13	1	0	8.1	274	212
08-130	0	74	1.042	694	0	1	9.4	1	8.8	630	583	130	132	78	0	0	4.9	844	649
08-131	6	375	2.213	1744	0	1	8.9	0	12.5	700	678	165	165	62	4	0	4.5	490	351
08-132	4	451	0.372	404	0	0	12.1	0	13.7	978	958	204	190	63	4	0	6.9	526	369
08-133	3	135	0.020	686	0	0	5.4	0	10.5	510	490	117	87	36	3	2	3.1	404	303
Min	0	39	0.020	63	0	0	5.4	0	8.8	426	421	97	87	7	0	0	3.1	274	212
Max	6	451	2.213	1744	1	1	18.4	3	29.9	1280	1218	1560	201	78	4	2	9.3	1004	744

BACKGROUND DATA SET

Sample Lib No	XRF Ag	INAA As	INAA Au	ICP Ba	ICP Be	XRF Bi	INAA Ce	XRF Cd	INAA Co	ICP Cr	INAA Cr	ICP Cu	XRF Cu	XRF Ga	XRF Ge	XRF In	INAA La	ICP Mn	XRF Mn
08-117	3	45	0.007	75	0	0	23.2	0	87.7	576	624	180	201	14	0.05	3	9.9	1314	1083
08-118	0	81	0.007	105	0	2	28.4	0	34.9	434	417	109	94	35	1	0	14.2	820	675
08-119	4	56	0.008	88	0	0	39.1	0	68.6	512	559	234	185	14	3	1	24.7	862	704
08-120	1	52	0.007	634	0	0	21.5	1	30.4	870	908	46	24	42	2	1	11.7	536	449
G.Mean	1.0	57	0.007	145	0	0.2	27.3	0.2	50.3	578	603	121	95.7	23.2	0.74	0.7	14.2	840	693
Max	4	81	0.008	634	0	2	39.1	1	87.7	870	908	234	201	42	3	3	24.7	1314	1083
Min	0	45	0.007	75	0	0	21.5	0	30.4	434	417	46	24	14	0	0	9.9	536	449

STANDARD

Sample Lib No	XRF Ag	INAA As	INAA Au	ICP Ba	ICP Be	XRF Bi	INAA Ce	XRF Cd	INAA Co	ICP Cr	INAA Cr	ICP Cu	XRF Cu	XRF Ga	XRF Ge	XRF In	INAA La	ICP Mn	XRF Mn
08-477	2	-	-	304	0	2	-	0	-	446	-	102	141	28	0	2	-	1757	1581
08-121	4	-	-	-	-	2	-	1	-	-	-	-	-	-	-	0	-	-	
08-122	0	-	-	-	-	0	-	0	-	-	-	-	-	-	-	0	-	-	
08-123	0	-	-	-	-	1	-	0	-	-	-	-	-	-	-	0	-	-	
08-135	0	-	-	-	-	2	-	2	-	-	-	-	-	-	-	3	-	-	
Mean	1.2	-	-	304	0	1.4	-	0.6	-	446	-	102	141	28	0	1	-	1757	1581
Pre Val	1.09	437	0.088	270	0	1.33	18.0	0.74	18.0	469	469	141	141	25	1	0.25	12.0	1557	1557

KHAKI LAG

Sample Lib No	INAA Mo	XRF Nb	ICP Ni	XRF Ni	XRF Pb	XRF Rb	INAA Sb	XRF Se	XRF Sn	XRF Sr	ICP V	XRF V	INAA W	XRF Y	XRF Zn	ICP Zr	XRF Zr
08-124	6.4	6	46	49	19	3	0.5	3	2	10	1252	1434	9.7	6	128	46	107
08-125	5.7	1	43	42	14	2	0.8	2	1	8	1212	1353	7.5	5	83	46	107
08-126	6.0	2	30	30	21	3	1.4	1	0	3	1656	1808	4.9	9	69	31	90
08-127	4.5	4	99	82	47	11	0.9	3	0	4	798	883	2.6	15	331	1	62
08-128	4.4	0	102	78	8	5	1.1	2	1	6	362	410	2.0	40	503	0	34
08-129	4.3	0	117	93	6	6	0.4	1	0	6	356	419	3.8	35	466	0	36
08-130	5.4	8	24	43	20	2	0.9	5	0	17	1658	1844	7.8	10	48	105	169
08-131	6.5	5	28	20	25	5	1.0	5	1	15	1612	1796	8.9	4	60	99	159
08-132	6.6	9	39	50	31	4	0.7	3	0	6	1806	1945	21.3	6	63	90	150
08-133	3.6	5	63	54	10	4	0.7	6	0	22	786	888	4.3	2	39	24	87
Min	3.6	0	24	20	6	2	0.4	1	0	3	356	410	2.0	2	39	0	34
Max	6.6	9	117	93	47	11	1.4	6	2	22	1806	1945	21.3	40	503	105	169

BACKGROUND DATA SET

Sample Lib No	INAA Mo	XRF Nb	ICP Ni	XRF Ni	XRF Pb	XRF Rb	INAA Sb	XRF Se	XRF Sn	XRF Sr	ICP V	XRF V	INAA W	XRF Y	XRF Zn	ICP Zr	XRF Zr
08-117	5.7	1	164	133	18	4	4.0	4	0	5	912	1006	2.3	17	198	0	51
08-118	4.9	0	63	59	21	3	1.4	4	0	3	1490	1581	9.0	22	141	54	86
08-119	6.2	2	136	112	20	3	1.6	6	0	3	836	924	4.7	54	162	0	44
08-120	5.8	4	47	36	20	4	5.3	4	1	14	1942	2115	2.3	12	82	120	170
G.Mean	5.6	1	90	75	19.7	3.5	2.6	4.4	0.2	5.0	1219	1328	3.9	22.2	139	2	76
Max	6.2	4	164	133	21	4	5.3	6	1	14	1942	2115	9.0	54	198	120	170
Min	4.9	0	47	36	18	3	1.4	4	0	3	836	924	2.3	12	82	0	44

STANDARD

Sample Lib No	INAA Mo	XRF Nb	ICP Ni	XRF Ni	XRF Pb	XRF Rb	INAA Sb	XRF Se	XRF Sn	XRF Sr	ICP V	XRF V	INAA W	XRF Y	XRF Zn	ICP Zr	XRF Zr
08-477	-	1	46	23	57	6	-	2	1	11	693	946	-	13	298	155	96
08-121	-	-	-	-	-	-	-	7	2	-	-	-	-	-	-	-	
08-122	-	-	-	-	-	-	-	2	2	-	-	-	-	-	-	-	
08-123	-	-	-	-	-	-	-	5	3	-	-	-	-	-	-	-	
08-135	-	-	-	-	-	-	-	5	0	-	-	-	-	-	-	-	
Mean	-	1	46	23	57	6	-	4.2	1.6	11	693	946	-	13	298	155	96
Pre Val	5.2	2	28	28	57	5	0.6	5	1.62	12	948	948	7.9	13	297	89	89

APPENDIX 2

Fine Lag - All Fractions Tabulated Geochemistry

Oxides in weight %
Trace elements in ppm
Mine co-ordinates in metres

FINE LAG

LINE 38820

Sample Numbers				% of Total	Co-ordinates		ICP	ICP	XRF	ICP	ICP	ICP	XRF	ICP
Field No	Lab Seq	Lib No			East	North	SiO ₂	Al ₂ O ₃	Fe ₂ O ₃	Fe ₂ O ₃	MgO	CaO	TiO ₂	TiO ₂
BC 301	L08-00213	08-190	-	33600	38820	29.50	10.30	48.04	51.40	0.08	0.05	1.01	0.75	
BC 302	L08-00211	08-191	-	33650	38820	23.60	10.20	53.76	56.90	0.07	0.05	1.08	0.79	
BC 303	L08-00195	08-192	-	33700	38820	28.60	10.20	49.04	55.50	0.08	0.05	0.99	0.81	
BC 304	L08-00217	08-193	-	33750	38820	18.30	9.17	59.05	57.80	0.07	0.06	1.11	0.78	
BC 305	L08-00228	08-194	-	33800	38820	16.20	8.90	60.91	59.10	0.08	0.08	1.14	0.76	
BC 306	L08-00220	08-195	-	33850	38820	13.70	8.38	64.48	66.10	0.12	0.21	1.14	0.83	
BC 307	L08-00207	08-196	-	33900	38820	10.10	7.89	66.62	70.40	0.13	0.18	1.19	0.83	
BC 308	L08-00219	08-197	-	33925	38820	10.60	7.99	68.34	66.70	0.09	0.09	1.17	0.81	
BC 309	L08-00193	08-198	-	33950	38820	13.10	8.99	63.91	71.30	0.13	0.13	1.13	0.88	
BC 310	L08-00206	08-199	-	33975	38820	12.90	8.92	64.05	70.70	0.11	0.12	1.08	0.79	
BC 311	L08-00201	08-200	-	34000	38820	11.40	8.93	64.48	68.90	0.12	0.17	1.04	0.78	
BC 312	L08-00210	08-201	-	34025	38820	13.10	9.81	60.19	63.20	0.13	0.13	1.08	0.79	
BC 313	L08-00215	08-202	-	34050	38820	9.12	9.26	65.48	64.00	0.09	0.07	1.57	1.07	
BC 314	L08-00231	08-203	-	34075	38820	8.39	8.56	69.05	67.90	0.08	0.09	1.59	1.07	
BC 315	L08-00224	08-204	-	34100	38820	9.83	9.07	66.05	62.00	0.07	0.05	1.60	1.08	
BC 316	L08-00194	08-205	-	34150	38820	12.60	11.10	61.48	69.60	0.09	0.05	1.47	1.21	
BC 317	L08-00209	08-206	-	34200	38820	11.10	10.10	63.48	67.50	0.08	0.05	1.45	1.07	
BC 318	L08-00226	08-207	-	34250	38820	11.70	9.67	62.19	59.50	0.08	0.06	1.49	0.99	
BC 716	L08-00472	08-450	-	34350	38820	20.20	10.80	57.47	64.50	0.09	0.09	1.23	1.03	
BC 717	L08-00451	08-451	-	34450	38820	29.80	9.24	51.90	56.80	0.08	0.08	1.08	0.83	
BC 718	L08-00438	08-452	-	34550	38820	26.90	9.06	54.76	56.40	0.08	0.08	1.04	0.83	
BC 719	L08-00467	08-453	-	34650	38820	31.30	8.28	51.33	58.30	0.09	0.08	0.91	0.76	
BC 720	L08-00476	08-454	-	34750	38820	28.22	7.56	52.76	55.17	0.04	0.07	0.89	0.68	
Min				-	33600	38820	8.39	7.56	48.04	51.40	0.04	0.05	0.89	0.68
Max				-	34750	38820	31.30	11.10	69.05	71.30	0.13	0.21	1.60	1.21

FINE LAG

LINE 38820

Lib No	XRF Ag	INAA As	INAA Au	ICP Ba	ICP Be	XRF Bi	XRF Cd	INAA Ce	INAA Co	ICP Cr	INAA Cr	ICP Cu	XRF Cu	XRF Ga	XRF Ge	XRF In	INAA La	ICP Mn	XRF Mn
08-190	0	53	0.005	37	0	2	0	25.5	20.1	1236	1494	104	96	31	1	0	14.4	390	363
08-191	0	57	0.009	24	0	3	0	24.5	21.3	1275	1538	112	106	35	1	0	14.4	374	344
08-192	0	57	0.013	9	0	1	0	21.4	20.3	1403	1471	116	103	37	1	1	13.5	372	314
08-193	0	65	0.067	23	0	2	1	19.1	18.4	1356	1470	105	107	38	1	0	12.1	367	340
08-194	0	68	0.006	213	0	0	0	21.1	19.5	1216	1377	71	100	36	0	1	12.2	383	367
08-195	0	70	0.081	408	0	3	0	20.7	15.6	1207	1194	106	90	32	0	4	12.2	437	384
08-196	0	76	0.094	1577	0	1	0	20.2	14.7	993	1262	108	111	38	1	1	12.5	437	396
08-197	1	68	0.002	1249	0	1	0	18.9	15.1	1136	1181	133	116	37	0	0	10.4	425	389
08-198	3	80	0.012	1520	0	1	1	19.8	17.0	1071	1091	166	150	33	0	2	10.5	694	591
08-199	0	90	0.066	1029	0	3	0	19.2	21.9	910	1100	135	161	33	0	0	11.0	1387	1357
08-200	0	99	0.077	738	0	1	0	15.2	24.2	795	912	130	163	30	1	1	10.9	1912	1785
08-201	1	98	0.053	570	0	2	0	17.1	21.5	738	862	177	185	33	0	1	9.8	2406	2374
08-202	1	63	0.146	300	0	1	1	11.1	13.2	713	757	124	109	45	2	0	8.0	1074	966
08-203	0	67	0.150	22	0	3	0	14.3	13.8	745	782	86	98	40	0	0	8.8	874	767
08-204	0	75	0.342	62	0	0	0	16.3	14.0	769	842	96	121	38	1	0	8.6	879	817
08-205	0	78	0.161	14	0	0	0	17.0	15.1	941	976	112	118	36	1	0	9.5	1116	915
08-206	3	80	0.619	17	0	0	0	16.7	15.3	873	1077	125	120	39	2	2	9.8	1071	959
08-207	0	81	0.244	38	0	1	1	19.3	15.0	987	1104	107	115	41	1	1	10.0	1076	995
08-450	3	104	0.129	42	0	2	0	14.0	16.1	1302	1183	126	117	36	2	1	11.3	777	618
08-451	1	82	0.012	24	0	0	0	13.9	14.3	1286	1291	111	99	32	1	0	10.9	558	472
08-452	2	80	0.035	21	0	0	0	14.6	14.0	1439	1237	99	97	33	2	0	9.6	804	475
08-453	3	39	0.005	202	0	1	1	15.1	14.4	923	848	113	108	31	0	2	9.7	490	401
08-454	2	42	0.005	175	0	2	0	13.7	14.9	877	932	70	98	28	0	0	9.3	439	367
Min	0	39	0.002	9	0	0	0	11.1	13.2	713	757	70	90	28	0	0	8.0	367	314
Max	3	104	0.619	1577	0	3	1	25.5	24.2	1439	1538	177	185	45	2	4	14.4	2406	2374

FINE LAG

LINE 38820

Lib No	INAA Mo	XRF Nb	ICP Ni	XRF Ni	XRF Pb	XRF Rb	INAA Sb	XRF Se	XRF Sn	XRF Sr	ICP V	XRF V	INAA W	XRF Y	XRF Zn	ICP Zr	XRF Zr
08-190	4.6	2	52	58	29	4	3.7	4	1	9	989	1301	2.0	12	53	152	145
08-191	5.2	4	56	56	36	9	4.4	4	0	9	1105	1484	2.0	10	54	168	147
08-192	4.1	4	53	53	38	6	4.0	4	1	9	1162	1300	2.2	9	59	106	134
08-193	5.6	5	69	50	43	7	5.0	4	3	8	1068	1552	2.4	9	51	146	151
08-194	5.4	3	50	51	44	5	5.2	6	1	12	1069	1584	5.5	11	60	119	139
08-195	2.2	4	62	49	46	7	5.5	4	2	19	1230	1676	2.5	11	56	136	139
08-196	2.6	6	44	43	45	6	6.1	6	0	37	1285	1769	2.4	11	65	154	135
08-197	9.3	0	72	41	43	7	5.7	6	6	25	1213	1750	2.5	8	71	143	140
08-198	2.2	3	61	41	41	6	5.3	9	2	34	1389	1597	2.2	13	85	126	124
08-199	2.5	4	44	54	46	6	4.9	4	3	20	1219	1544	2.3	11	89	134	129
08-200	2.4	3	33	40	44	9	4.7	4	0	15	1215	1503	2.1	9	103	80	112
08-201	1.9	6	46	36	49	9	3.1	7	0	14	1109	1513	5.4	11	109	132	111
08-202	1.9	1	56	33	44	4	2.7	6	3	5	1239	1861	8.4	7	58	139	131
08-203	13.2	4	34	30	44	6	2.5	5	1	5	1323	2001	10.8	9	55	122	138
08-204	4.3	4	42	35	50	8	2.4	8	1	3	1206	1884	9.8	8	61	119	133
08-205	4.4	5	25	32	43	5	2.5	7	0	1	1491	1702	4.0	12	69	99	126
08-206	4.3	3	38	31	40	9	2.5	6	2	2	1320	1831	2.4	11	75	136	123
08-207	5.9	2	47	36	42	7	2.4	7	2	5	1208	1835	4.3	9	76	117	132
08-450	4.8	1	54	45	47	7	3.3	4	2	7	1346	1614	4.5	11	61	110	123
08-451	5.4	0	56	40	32	5	2.8	5	0	4	1081	1452	3.1	8	57	123	122
08-452	5.2	2	51	40	41	7	2.9	5	1	7	1284	1592	3.4	9	50	131	116
08-453	4.6	2	52	40	36	5	2.2	4	0	11	1143	1371	4.3	7	64	94	108
08-454	4.7	0	46	33	32	7	2.3	5	0	8	1093	1424	3.8	7	61	151	105
Min	1.9	0	25	30	29	4	2.2	4	0	1	989	1300	2.0	7	50	80	105
Max	13.2	6	72	58	50	9	6.1	9	6	37	1491	2001	10.8	13	109	168	151

FINE LAG

LINE 38940

Sample Numbers				% of Total	Co-ordinates		ICP	ICP	XRF	ICP	ICP	ICP	XRF	ICP
Field No	Lab Seq	Lib No			East	North	SiO ₂	Al ₂ O ₃	Fe ₂ O ₃	Fe ₂ O ₃	MgO	CaO	TiO ₂	TiO ₂
BC 321	L08-00205	08-208	-	33650	38940	21.30	10.00	54.76	62.20	0.10	0.09	1.16	0.89	
BC 322	L08-00204	08-209	-	33700	38940	27.50	10.00	49.32	54.20	0.09	0.07	1.03	0.79	
BC 323	L08-00225	08-210	-	33750	38940	23.00	9.13	53.90	51.70	0.08	0.07	1.10	0.77	
BC 324	L08-00221	08-211	-	33800	38940	17.80	9.13	59.19	58.50	0.11	0.12	1.17	0.81	
BC 325	L08-00190	08-212	-	33850	38940	18.40	9.41	58.62	68.80	0.14	0.17	1.07	0.87	
BC 326	L08-00199	08-213	-	33900	38940	20.60	8.75	56.47	60.40	0.14	0.21	1.02	0.80	
BC 327	L08-00200	08-214	-	33925	38940	17.40	8.63	58.19	63.20	0.15	0.15	0.98	0.75	
BC 328	L08-00214	08-215	-	33950	38940	14.30	8.02	61.62	62.40	0.23	0.55	1.09	0.78	
BC 329	L08-00227	08-216	-	33975	38940	11.80	7.03	63.76	60.70	0.28	0.74	1.05	0.68	
BC 330	L08-00216	08-217	-	34000	38940	17.50	8.71	56.33	58.00	0.42	1.08	1.19	0.87	
BC 331	L08-00218	08-218	-	34025	38940	13.10	11.10	58.62	56.20	0.24	0.31	1.62	1.13	
BC 332	L08-00223	08-219	-	34050	38940	13.30	10.60	58.76	54.50	0.11	0.06	1.55	1.03	
BC 333	L08-00197	08-220	-	34100	38940	10.20	8.31	66.48	71.00	0.09	0.06	1.48	1.07	
BC 334	L08-00191	08-221	-	34150	38940	12.60	9.74	63.76	72.70	0.09	0.07	1.41	1.09	
BC 335	L08-00229	08-222	-	34200	38940	12.30	9.13	64.91	63.90	0.08	0.06	1.41	0.98	
BC 336	L08-00212	08-223	-	34250	38940	14.50	9.27	63.05	65.10	0.08	0.06	1.34	0.92	
BC 337	L08-00208	08-224	-	34300	38940	29.60	9.18	47.32	51.60	0.08	0.07	1.01	0.76	
BC 711	L08-00461	08-445	-	34400	38940	22.40	9.99	56.90	62.50	0.09	0.11	1.03	0.79	
BC 712	L08-00435	08-446	-	34500	38940	33.00	9.96	48.90	48.60	0.12	0.10	0.91	0.72	
BC 713	L08-00450	08-447	-	34600	38940	19.30	9.25	61.05	67.30	0.09	0.13	1.02	0.77	
BC 715	L08-00449	08-449	-	34800	38940	35.10	6.16	48.61	54.10	0.09	0.09	0.68	0.56	
Min				-	33650	38940	10.20	6.16	47.32	48.60	0.08	0.06	0.68	0.56
Max				-	34800	38940	35.10	11.10	66.48	72.70	0.42	1.08	1.62	1.13

BACKGROUND DATA SET - FINE LAG

Sample Numbers				% of Total	Co-ordinates		ICP	ICP	XRF	ICP	ICP	ICP	XRF	ICP
Field No	Lab Seq	Lib No			East	North	SiO ₂	Al ₂ O ₃	Fe ₂ O ₃	Fe ₂ O ₃	MgO	CaO	TiO ₂	TiO ₂
BC 341	L08-00222	08-225	-	33747	39311	23.50	10.10	51.90	50.80	0.07	0.04	1.09	0.77	
BC 342	L08-00192	08-226	-	34172	39314	24.50	11.00	49.18	56.30	0.08	0.07	1.05	0.81	
BC 343	L08-00198	08-227	-	33545	38146	48.40	7.92	33.17	37.30	0.11	0.09	0.70	0.60	
BC 344	L08-00196	08-228	-	34290	38110	21.10	8.76	57.76	64.90	0.09	0.07	1.23	0.98	
Max				-	-	-	48.40	11.00	57.76	64.90	0.11	0.09	1.23	0.98
Min				-	-	-	21.10	7.92	33.17	37.30	0.07	0.04	0.70	0.60
G.Mean				-	-	-	27.69	9.37	47.02	51.30	0.09	0.06	1.00	0.78

FINE LAG

LINE 38940

Lib No	XRF Ag	INAA As	INAA Au	ICP Ba	ICP Be	XRF Bi	XRF Cd	INAA Ce	INAA Co	ICP Cr	INAA Cr	ICP Cu	XRF Cu	XRF Ga	XRF Ge	XRF In	INAA La	ICP Mn	XRF Mn
08-208	0	63	0.008	166	0	2	1	23.8	19.7	1262	1558	91	100	34	0	0	14.7	344	313
08-209	0	61	0.007	156	0	3	0	21.0	21.9	1208	1502	112	107	32	1	0	14.5	343	312
08-210	0	58	0.014	241	0	2	0	19.8	19.5	1290	1430	91	115	36	0	1	12.8	311	313
08-211	0	62	0.006	362	0	1	1	21.7	19.2	1322	1405	98	116	33	0	1	14.2	372	344
08-212	0	61	0.032	709	0	0	3	21.8	21.1	1265	1268	191	128	34	1	0	13.8	481	402
08-213	0	66	0.007	747	0	1	1	20.4	22.6	998	1120	158	171	30	0	1	14.1	620	568
08-214	3	83	0.016	1095	0	1	1	21.0	26.6	900	1045	177	222	25	0	0	14.8	864	877
08-215	0	119	0.887	1704	0	2	0	28.5	21.3	996	1077	165	169	33	0	1	17.5	895	826
08-216	0	252	0.086	1613	0	0	0	21.7	26.6	831	937	190	211	37	0	0	12.3	1175	1138
08-217	1	304	0.288	885	0	1	3	17.5	14.1	771	793	221	219	37	1	0	9.1	1032	895
08-218	0	165	0.117	641	0	0	0	15.7	15.6	815	845	158	143	48	0	2	9.8	795	723
08-219	0	140	0.217	1328	0	0	1	17.1	16.9	763	850	114	151	40	3	1	8.9	842	795
08-220	1	123	0.314	288	0	1	1	10.5	14.6	876	950	104	108	38	0	3	7.6	688	558
08-221	0	130	0.372	26	0	2	1	15.9	12.9	1016	1018	204	131	42	0	0	8.8	700	561
08-222	1	125	0.260	15	0	3	0	17.4	15.8	1072	1160	98	112	43	0	0	12.2	739	650
08-223	4	117	0.045	5	0	3	0	17.9	15.6	982	1205	110	100	32	0	1	10.0	681	614
08-224	2	74	0.044	25	0	1	1	17.7	18.6	1090	1384	119	101	30	1	1	11.7	594	540
08-445	0	59	0.015	76	0	0	0	16.7	19.4	1389	1329	107	108	35	1	0	12.0	486	407
08-446	0	44	0.006	134	0	1	0	23.7	21.4	1226	1184	119	117	31	0	0	15.7	596	395
08-447	0	48	0.008	355	0	1	0	19.7	15.1	1079	1073	111	101	34	0	0	11.7	430	358
08-449	0	38	0.006	336	0	3	0	13.2	16.5	838	809	124	126	21	0	0	8.5	346	301
Min	0	38	0.006	5	0	0	0	10.5	12.9	763	793	91	100	21	0	0	7.6	311	301
Max	4	304	0.887	1704	0	3	3	28.5	26.6	1389	1558	221	222	48	3	3	17.5	1175	1138

BACKGROUND DATA SET - FINE LAG

Lib No	XRF Ag	INAA As	INAA Au	ICP Ba	ICP Be	XRF Bi	XRF Cd	INAA Ce	INAA Co	ICP Cr	INAA Cr	ICP Cu	XRF Cu	XRF Ga	XRF Ge	XRF In	INAA La	ICP Mn	XRF Mn
08-225	0	55	0.006	17	0	4	0	23.9	20.3	1365	1453	89	113	39	0	0	14.2	342	318
08-226	0	55	0.007	19	0	1	2	22.1	22.3	1429	1524	205	122	35	2	0	13.2	385	333
08-227	2	38	0.002	29	0	0	0	20.1	18.6	950	1057	57	81	23	0	0	12.0	393	361
08-228	0	53	0.008	81	0	0	0	16.5	13.4	1081	1123	80	85	36	0	1	9.0	537	436
Max	2	55	0.008	81	0	4	2	23.9	22.3	1429	1524	205	122	39	2	1	14.2	537	436
Min	0	38	0.002	17	0	0	0	16.5	13.4	950	1057	57	81	23	0	0	9.0	342	318
G.Mean	0	50	0.005	30	-	0	0	20.5	18.3	1190	1273	95	99	33	-	0	11.9	408	359

FINE LAG

LINE 38940

Lib No	INAA	XRF	ICP	XRF	XRF	ICP	XRF	XRF	XRF	ICP	XRF	INAA	XRF	XRF	ICP	XRF
	Mo	Nb	Ni	Ni	Pb	Rb	Sb	Se	Sn	Sr	V	V	W	Y	Zn	Zr
08-208	2.4	6	54	60	45	4	5.3	7	0	13	1222	1555	2.2	12	54	168
08-209	2.3	4	58	59	37	5	4.1	5	2	9	1075	1357	2.1	12	58	143
08-210	2.3	3	56	51	37	6	4.9	7	0	10	1001	1477	2.5	9	53	120
08-211	2.0	1	58	60	38	7	5.6	3	4	16	1144	1620	2.5	11	65	130
08-212	2.2	3	87	53	44	7	4.6	4	2	23	1388	1570	2.0	11	76	165
08-213	2.2	6	51	53	39	7	4.0	5	0	21	1198	1464	2.9	14	96	88
08-214	2.3	4	40	51	41	5	3.9	4	0	24	1198	1484	2.0	15	111	75
08-215	2.0	1	71	47	38	7	5.1	6	1	50	1112	1584	2.3	13	85	131
08-216	3.0	2	46	48	43	8	5.8	10	0	80	1036	1541	2.7	13	78	105
08-217	6.6	6	67	29	39	6	3.6	11	3	48	1233	1714	6.2	11	75	125
08-218	3.5	7	58	27	36	6	3.2	9	3	27	1267	1932	8.9	13	79	139
08-219	10.6	3	41	52	36	7	3.3	4	3	17	1111	1745	5.1	10	79	112
08-220	2.3	4	40	30	40	4	2.8	8	3	5	1597	1964	2.4	7	61	111
08-221	5.5	3	79	37	47	8	2.8	6	1	1	1583	1836	4.0	9	65	167
08-222	6.9	5	43	35	42	3	3.3	8	3	5	1267	1882	8.3	13	67	122
08-223	5.1	2	45	44	48	5	3.4	7	2	4	1344	1933	5.8	10	63	153
08-224	2.3	5	56	55	30	4	3.0	5	2	9	1019	1329	2.2	7	60	126
08-445	4.8	5	68	46	50	6	4.1	5	0	8	1161	1572	3.5	10	56	143
08-446	5.0	0	73	58	38	4	3.1	7	2	15	1008	1271	2.7	13	72	120
08-447	5.8	2	59	46	44	6	3.6	5	1	13	1257	1729	3.4	9	65	127
08-449	4.7	0	56	38	35	5	1.8	2	0	12	842	1080	3.5	7	87	91
Min	2.0	0	40	27	30	3	1.8	2	0	1	842	1080	2.0	7	53	75
Max	10.6	7	87	60	50	8	5.8	11	4	80	1597	1964	8.9	15	111	168

BACKGROUND DATA SET - FINE LAG

Lib No	INAA	XRF	ICP	XRF	XRF	ICP	XRF	XRF	XRF	ICP	XRF	INAA	XRF	XRF	ICP	XRF
	Mo	Nb	Ni	Ni	Pb	Rb	Sb	Se	Sn	Sr	V	V	W	Y	Zn	Zr
08-225	8.8	3	62	60	37	6	4.5	4	3	3	1002	1413	0.8	9	48	128
08-226	3.9	3	108	59	33	4	4.4	4	4	7	1229	1414	2.0	9	58	165
08-227	2.0	5	36	49	22	11	2.8	2	1	7	759	864	1.9	9	44	66
08-228	4.7	3	40	36	25	11	4.2	6	2	7	1358	1556	2.3	8	51	92
Max	8.8	5	108	60	37	11	4.5	6	4	7	1358	1556	2.3	9	58	155
Min	2.0	3	36	36	22	4	2.8	2	1	3	759	864	0.8	8	44	112
G.Mean	4.2	3	56	50	29	7	3.9	4	2	6	1061	1280	1.6	9	50	130

FINE LAG - NON-MAGNETIC FRACTION

LINE 38820

Sample Numbers				% of Total	Co-ordinates		ICP	ICP	XRF	ICP	ICP	ICP	XRF	ICP
Field No	Lab Seq	Lib No			East	North	SiO ₂	Al ₂ O ₃	Fe ₂ O ₃	Fe ₂ O ₃	MgO	CaO	TiO ₂	TiO ₂
BC 701	L08-00299	08-232	83.6	33600	38820	35.50	11.20	43.75	45.90	0.08	0.04	0.93	0.76	
BC 702	L08-00280	08-233	76.8	33650	38820	30.70	11.80	48.04	53.40	0.08	0.05	0.98	0.81	
BC 703	L08-00276	08-234	76.8	33700	38820	31.50	10.30	44.75	46.20	0.07	0.05	0.89	0.69	
BC 704	L08-00301	08-235	73.3	33750	38820	24.10	10.70	52.76	54.00	0.08	0.06	0.99	0.76	
BC 705	L08-00308	08-236	67.6	33800	38820	22.90	10.40	54.33	56.20	0.09	0.09	1.02	0.78	
BC 706	L08-00272	08-237	63.7	33850	38820	17.10	9.28	60.62	62.10	0.13	0.23	1.07	0.76	
BC 707	L08-00278	08-238	62.0	33900	38820	13.50	9.35	63.76	71.80	0.14	0.19	1.07	0.86	
BC 708	L08-00311	08-239	65.1	33925	38820	14.10	9.59	61.91	67.80	0.11	0.10	1.05	0.84	
BC 709	L08-00281	08-240	66.5	33950	38820	15.20	9.64	61.76	66.40	0.13	0.14	1.07	0.82	
BC 710	L08-00235	08-241	68.5	33975	38820	15.00	9.13	60.62	61.30	0.11	0.10	0.99	0.71	
BC 711	L08-00305	08-242	68.8	34000	38820	13.10	9.23	62.91	63.30	0.14	0.25	1.01	0.75	
BC 712	L08-00262	08-243	80.6	34025	38820	14.50	10.40	59.05	59.20	0.15	0.14	1.09	0.79	
BC 713	L08-00290	08-244	65.5	34050	38820	12.40	11.40	62.62	63.70	0.10	0.07	1.46	1.11	
BC 714	L08-00268	08-245	60.2	34075	38820	12.10	10.40	64.34	68.70	0.11	0.12	1.34	1.03	
BC 715	L08-00252	08-246	69.3	34100	38820	13.10	11.30	62.19	67.70	0.10	0.07	1.49	1.11	
BC 716	L08-00241	08-247	75.9	34150	38820	14.00	11.10	59.76	59.30	0.10	0.06	1.43	1.00	
BC 717	L08-00289	08-248	78.9	34200	38820	13.00	11.40	61.76	62.30	0.09	0.05	1.38	1.06	
BC 718	L08-00250	08-249	82.7	34250	38820	14.70	12.60	61.48	70.50	0.10	0.07	1.45	1.17	
BC 736	L08-00463	08-470	89.1	34350	38820	21.60	10.90	55.19	59.90	0.09	0.09	1.23	0.99	
BC 737	L08-00458	08-471	86.8	34450	38820	31.50	9.38	47.89	52.40	0.08	0.08	0.98	0.77	
BC 738	L08-00454	08-472	85.8	34550	38820	30.70	9.36	49.90	55.60	0.08	0.08	0.96	0.77	
BC 739	L08-00464	08-473	82.1	34650	38820	32.70	8.03	48.18	51.10	0.08	0.07	0.84	0.67	
BC 740	L08-00447	08-474	82.5	34750	38820	34.50	8.49	47.89	53.50	0.08	0.07	0.81	0.67	
Min				-	33600	38820	12.10	8.03	43.75	45.90	0.07	0.04	0.81	0.67
Max				-	34750	38820	35.50	12.60	64.34	71.80	0.15	0.25	1.49	1.17

FINE LAG - NON-MAGNETIC FRACTION

LINE 38820

Lib No	XRF Ag	INAA As	INAA Au	ICP Ba	ICP Be	XRF Bi	XRF Cd	INAA Ce	INAA Co	ICP Cr	INAA Cr	ICP Cu	XRF Cu	XRF Ga	XRF Ge	XRF In	INAA La	ICP Mn	XRF Mn
08-232	1	54	0.006	52	0	2	0	22.0	23.0	1672	1456	133	120	27	0	0	14.7	448	388
08-233	2	58	0.010	30	0	1	0	20.2	23.7	1706	1537	147	115	31	1	3	15.6	375	330
08-234	0	59	0.009	24	0	2	0	20.9	21.2	1418	1397	133	121	26	1	1	14.4	358	334
08-235	0	66	0.012	35	0	2	0	17.7	23.7	1615	1476	148	127	29	0	1	13.7	398	339
08-236	0	69	0.033	240	0	1	0	19.6	23.0	1545	1414	141	128	32	0	2	16.2	432	370
08-237	0	72	0.183	480	0	2	2	18.1	17.6	1223	1162	133	120	35	2	3	13.3	453	408
08-238	1	77	0.044	1876	0	1	0	18.4	19.6	1237	1130	176	143	31	2	2	12.9	534	428
08-239	0	72	0.009	1254	0	1	0	16.2	17.9	1163	1089	175	156	29	0	0	11.7	500	413
08-240	2	79	0.016	1359	0	1	0	14.7	20.2	1055	937	217	172	29	3	0	11.5	684	580
08-241	0	102	0.073	970	0	3	0	19.1	22.9	951	950	199	196	28	3	0	10.4	1475	1328
08-242	2	127	0.206	638	0	0	0	15.0	24.7	900	820	217	182	27	0	2	11.1	2131	1857
08-243	0	116	0.046	525	0	3	2	16.4	24.0	772	776	222	214	26	1	2	11.0	3829	3597
08-244	2	74	0.254	282	0	0	0	11.6	16.9	844	686	167	156	37	3	1	8.3	1428	1286
08-245	0	84	0.325	69	0	3	0	12.2	15.0	856	830	159	134	30	1	1	9.3	1220	1016
08-246	6	90	0.120	68	0	0	0	16.3	15.9	860	853	125	135	31	0	3	9.3	1007	892
08-247	4	78	0.152	49	0	0	1	16.4	17.4	875	918	155	150	35	2	2	8.8	1092	1026
08-248	4	83	0.096	27	0	0	0	14.3	15.6	1122	1013	171	152	37	0	0	9.2	1183	1058
08-249	1	83	0.218	40	0	2	0	20.7	15.8	1201	1074	129	133	40	0	0	10.2	1147	996
08-470	4	96	0.113	46	0	3	0	16.4	15.9	1243	1174	134	127	38	2	1	11.6	767	664
08-471	0	76	0.104	29	0	2	0	14.0	15.1	1292	1263	116	105	33	1	2	10.9	533	454
08-472	1	85	0.085	41	0	0	2	12.7	17.3	1282	1339	110	109	28	0	0	9.9	566	476
08-473	0	40	0.010	164	0	2	0	14.4	14.5	832	815	127	127	27	0	2	9.4	459	396
08-474	0	38	0.005	117	0	1	0	12.6	14.6	916	869	130	111	26	0	0	8.5	415	345
Min	0	38	0.005	24	0	0	0	11.6	14.5	772	686	110	105	26	0	0	8.3	358	330
Max	6	127	0.325	1876	0	3	2	22.0	24.7	1706	1537	222	214	40	3	3	16.2	3829	3597

FINE LAG - NON-MAGNETIC FRACTION

LINE 38820

Lib No	INAA Mo	XRF Nb	ICP Ni	XRF Ni	XRF Pb	XRF Rb	INAA Sb	XRF Se	XRF Sn	XRF Sr	ICP V	XRF V	INAA W	XRF Y	XRF Zn	ICP Zr	XRF Zr
08-232	1.9	6	86	57	33	8	3.3	6	1	5	1022	1224	2.2	10	54	127	144
08-233	4.6	3	85	56	29	7	3.6	6	1	7	1100	1332	3.1	12	59	161	154
08-234	4.5	0	77	56	34	5	3.7	5	1	6	914	1190	3.5	9	62	115	128
08-235	2.0	1	91	63	34	7	3.9	6	1	3	1149	1427	2.4	11	69	117	133
08-236	2.1	7	77	56	40	8	4.0	7	0	10	1191	1463	0.9	11	69	113	127
08-237	4.4	4	73	50	43	5	4.4	5	1	20	1142	1541	2.1	12	76	133	128
08-238	7.2	4	77	52	44	7	4.4	5	1	36	1359	1706	7.4	12	87	156	142
08-239	3.6	3	74	48	42	5	4.4	5	3	25	1323	1624	0.9	11	90	123	125
08-240	7.6	4	79	56	37	6	4.3	8	2	31	1234	1594	5.4	13	102	117	114
08-241	4.1	3	77	54	36	6	3.6	6	1	20	1113	1489	1.0	11	109	97	107
08-242	9.3	4	76	37	38	6	3.7	6	1	16	1161	1442	5.2	12	110	100	108
08-243	2.0	3	59	42	43	8	3.0	8	3	13	1020	1409	3.4	14	127	104	104
08-244	5.6	5	59	30	41	6	2.4	5	1	7	1302	1675	7.3	9	83	117	118
08-245	2.9	1	55	32	41	5	2.7	6	3	3	1302	1693	6.8	9	76	114	113
08-246	1.4	4	46	30	38	6	2.5	6	2	3	1234	1714	4.0	7	75	118	125
08-247	6.1	5	70	28	41	7	2.4	5	2	4	1045	1588	2.8	9	80	143	118
08-248	4.8	3	63	34	42	6	2.4	8	2	4	1288	1684	8.1	13	86	111	119
08-249	6.2	4	55	39	37	5	2.1	6	0	4	1347	1789	3.4	10	79	130	125
08-470	4.7	3	58	46	37	8	2.3	5	3	7	1238	1602	3.5	8	67	112	120
08-471	4.2	5	57	39	28	4	2.3	6	0	5	1014	1360	2.8	8	58	109	111
08-472	5.4	5	62	40	35	3	2.7	5	1	4	1072	1432	3.2	10	63	116	111
08-473	4.4	5	58	40	30	8	1.9	3	1	7	983	1247	3.2	7	79	82	104
08-474	4.9	5	49	36	30	8	2.2	6	0	10	1008	1317	3.4	5	64	105	110
Min	1.4	0	46	28	28	3	1.9	3	0	3	914	1190	0.9	5	54	82	104
Max	9.3	7	91	63	44	8	4.4	8	3	36	1359	1789	8.1	14	127	161	154

FINE LAG - NON-MAGNETIC FRACTION

LINE 38940

Sample Numbers			% of Total	Co-ordinates		ICP	ICP	XRF	ICP	ICP	ICP	XRF	ICP
Field No	Lab Seq	Lib No		East	North	SiO ₂	Al ₂ O ₃	Fe ₂ O ₃	Fe ₂ O ₃	MgO	CaO	TiO ₂	TiO ₂
BC 721	L08-00283	08-250	73.5	33650	38940	24.40	10.10	51.61	52.10	0.09	0.10	1.04	0.75
BC 722	L08-00292	08-251	79.7	33700	38940	32.90	10.70	45.46	46.70	0.09	0.06	0.89	0.73
BC 723	L08-00255	08-252	77.5	33750	38940	31.60	10.80	47.75	52.10	0.10	0.10	0.95	0.74
BC 724	L08-00286	08-253	73.4	33800	38940	21.00	9.89	54.19	51.80	0.11	0.12	1.04	0.75
BC 725	L08-00257	08-254	72.8	33850	38940	22.50	10.10	56.33	62.80	0.14	0.14	0.97	0.78
BC 726	L08-00285	08-255	77.9	33900	38940	24.70	9.03	52.47	56.20	0.16	0.31	0.89	0.70
BC 727	L08-00264	08-256	77.3	33925	38940	21.10	9.24	56.19	59.50	0.17	0.18	0.90	0.68
BC 728	L08-00307	08-257	72.4	33950	38940	17.70	8.58	58.47	58.40	0.26	0.68	0.95	0.70
BC 729	L08-00265	08-258	76.1	33975	38940	15.50	8.26	59.33	65.30	0.38	1.02	0.89	0.68
BC 730	L08-00238	08-259	90.6	34000	38940	19.00	9.67	55.47	59.80	0.48	1.13	1.20	0.92
BC 731	L08-00237	08-260	87.7	34025	38940	15.30	12.90	55.62	58.10	0.28	0.40	1.67	1.24
BC 732	L08-00236	08-261	83.8	34050	38940	15.80	12.40	56.04	56.90	0.13	0.07	1.56	1.15
BC 733	L08-00261	08-262	85.3	34100	38940	11.60	9.13	66.48	73.90	0.09	0.07	1.50	1.13
BC 734	L08-00296	08-263	83.0	34150	38940	13.80	10.40	63.05	67.70	0.09	0.06	1.44	1.13
BC 735	L08-00258	08-264	82.5	34200	38940	15.40	10.50	61.76	69.10	0.09	0.07	1.38	1.08
BC 736	L08-00273	08-265	80.2	34250	38940	16.80	10.00	59.48	62.80	0.08	0.06	1.32	0.98
BC 737	L08-00248	08-266	85.0	34300	38940	36.60	10.10	44.32	49.60	0.08	0.05	0.95	0.77
BC 731	L08-00462	08-465	79.0	34400	38940	26.10	10.80	52.76	57.80	0.10	0.12	0.99	0.77
BC 732	L08-00468	08-466	84.7	34500	38940	36.20	11.40	44.61	50.80	0.13	0.11	0.84	0.72
BC 733	L08-00448	08-467	73.4	34600	38940	23.90	10.10	56.90	64.60	0.10	0.11	0.95	0.77
BC 735	L08-00443	08-469	84.5	34800	38940	40.80	6.04	44.46	48.50	0.10	0.08	0.58	0.48
Min	-	-	-	33650	38940	11.60	6.04	44.32	46.70	0.08	0.05	0.58	0.48
Max	-	-	-	34800	38940	40.80	12.90	66.48	73.90	0.48	1.13	1.67	1.24

BACKGROUND DATA SET - NON-MAGNETIC FRACTION

Sample Numbers			% of Total	Co-ordinates		ICP	ICP	XRF	ICP	ICP	ICP	XRF	ICP
Field No	Lab Seq	Lib No		East	North	SiO ₂	Al ₂ O ₃	Fe ₂ O ₃	Fe ₂ O ₃	MgO	CaO	TiO ₂	TiO ₂
BC 741	L08-00244	08-267	78.6	33747	39311	30.10	11.90	46.89	51.70	0.08	0.06	1.00	0.79
BC 742	L08-00302	08-268	80.0	34172	39314	28.40	11.60	46.89	47.10	0.08	0.05	0.98	0.75
BC 743	L08-00239	08-269	87.6	33545	38146	51.60	7.70	30.60	31.10	0.10	0.09	0.62	0.50
BC 744	L08-00303	08-270	69.6	34290	38110	27.10	8.91	51.90	52.90	0.09	0.06	1.09	0.84
Max	-	-	-	-	-	51.60	11.90	51.90	52.90	0.10	0.09	1.09	0.84
Min	-	-	-	-	-	27.10	7.70	30.60	31.10	0.08	0.05	0.62	0.50
G.Mean	-	-	-	-	-	33.07	9.86	43.23	44.74	0.09	0.06	0.90	0.71

FINE LAG - NON-MAGNETIC FRACTION

LINE 38940

Lib No	XRF Ag	INAA As	INAA Au	ICP Ba	ICP Be	XRF Bi	XRF Cd	INAA Ce	INAA Co	ICP Cr	INAA Cr	ICP Cu	XRF Cu	XRF Ga	XRF Ge	XRF In	INAA La	ICP Mn	XRF Mn
08-250	0	64	0.007	195	0	3	0	21.7	25.8	1440	1593	139	127	33	0	0	17.1	349	326
08-251	0	54	0.017	194	0	2	0	18.8	21.3	1462	1285	140	121	31	1	1	14.9	362	313
08-252	0	55	0.007	293	0	1	0	17.2	23.2	1382	1342	122	141	29	1	0	13.6	373	328
08-253	2	61	0.005	361	0	2	0	19.8	21.0	1405	1390	154	140	34	1	0	15.0	358	337
08-254	0	64	0.008	689	0	1	0	24.0	26.6	1276	1232	139	151	27	0	2	13.9	467	384
08-255	0	73	0.006	783	0	1	0	19.5	23.9	1060	968	260	210	24	0	0	14.6	731	635
08-256	0	85	0.025	1068	0	0	0	23.4	29.1	947	899	259	236	26	0	0	15.1	1001	897
08-257	4	148	0.050	1557	0	0	0	20.5	25.0	1031	909	270	206	27	1	0	14.1	977	864
08-258	0	322	0.487	1706	0	0	0	19.2	36.6	846	810	290	251	25	0	1	12.7	1869	1594
08-259	0	327	0.148	795	0	0	0	14.3	18.6	772	766	205	236	37	0	0	9.6	1132	1024
08-260	0	166	0.545	620	0	1	0	17.4	15.2	876	812	203	154	45	0	0	10.0	922	787
08-261	4	153	0.757	1428	0	1	1	20.2	19.3	798	776	173	160	38	2	0	11.2	853	720
08-262	1	139	0.091	272	0	1	0	11.5	13.7	894	877	109	112	36	4	0	7.6	744	613
08-263	0	145	0.123	36	0	2	2	13.1	13.2	1170	960	155	125	36	0	0	9.4	765	613
08-264	0	141	0.150	27	0	1	1	13.0	17.3	1188	1146	113	131	39	1	0	9.9	824	701
08-265	1	118	0.104	10	0	2	0	16.1	16.4	1221	1152	143	130	34	0	3	9.8	740	638
08-266	2	70	0.162	16	0	2	0	18.2	19.4	1310	1383	78	119	22	0	0	12.0	573	470
08-465	1	58	0.007	89	0	2	0	16.9	20.0	1463	1379	116	119	31	0	0	13.2	513	437
08-466	0	43	0.005	140	0	0	0	20.1	22.0	1187	1107	129	122	29	0	1	19.0	488	409
08-467	2	45	0.006	343	0	3	0	12.1	16.2	1048	965	121	107	31	1	0	10.2	395	327
08-469	0	34	0.165	280	0	0	0	11.3	14.5	766	732	133	144	21	1	1	8.0	325	280
Min	0	34	0.005	10	0	0	0	11.3	13.2	766	732	78	107	21	0	0	7.6	325	280
Max	4	327	0.757	1706	0	3	2	24.0	36.6	1463	1593	290	251	45	4	3	19.0	1869	1594

BACKGROUND DATA SET - NON-MAGNETIC FRACTION

Lib No	XRF Ag	INAA As	INAA Au	ICP Ba	ICP Be	XRF Bi	XRF Cd	INAA Ce	INAA Co	ICP Cr	INAA Cr	ICP Cu	XRF Cu	XRF Ga	XRF Ge	XRF In	INAA La	ICP Mn	XRF Mn
08-267	1	54	0.006	36	0	1	1	20.9	24.5	1445	1493	140	128	32	0	0	14.8	346	308
08-268	2	57	0.006	28	0	1	0	18.6	25.6	1597	1499	156	137	30	1	1	13.9	353	316
08-269	0	32	0.002	46	0	3	1	18.9	17.7	887	960	74	93	20	1	2	11.8	372	356
08-270	5	61	0.011	107	0	1	0	12.2	14.7	1126	1075	112	98	29	3	2	8.9	518	459
Max	5	61	0.011	107	0	3	1	20.9	25.6	1597	1499	156	137	32	3	2	14.8	518	459
Min	0	32	0.002	28	0	1	0	12.2	14.7	887	960	74	93	20	0	0	8.9	346	308
G.Mean	1	50	0.005	47	-	1	0	17.3	20.1	1232	1233	116	112	27	-	1	12.1	392	355

FINE LAG - NON-MAGNETIC FRACTION

LINE 38940

Lib No	INAA Mo	XRF Nb	ICP Ni	XRF Ni	XRF Pb	XRF Rb	INAA Sb	XRF Se	XRF Sn	XRF Sr	ICP V	XRF V	INAA W	XRF Y	XRF Zn	ICP Zr	XRF Zr
08-250	5.4	1	87	58	36	7	4.5	4	2	15	1083	1476	2.0	10	61	136	140
08-251	3.5	4	85	62	33	6	3.1	5	2	8	1015	1242	2.1	10	60	111	126
08-252	5.2	1	71	64	33	8	3.8	4	0	11	999	1342	1.2	11	67	116	139
08-253	2.6	4	83	61	39	4	4.6	5	3	17	1108	1539	1.9	12	74	123	136
08-254	2.4	5	69	51	38	5	3.8	6	1	20	1128	1459	3.8	13	86	118	123
08-255	4.8	4	93	57	43	4	2.8	6	0	32	1087	1365	2.3	15	101	106	106
08-256	2.2	3	71	58	35	5	3.2	6	1	25	1085	1416	3.3	14	127	92	98
08-257	3.3	0	80	44	44	6	3.6	5	1	51	1166	1470	2.6	14	112	90	114
08-258	2.3	7	56	45	44	6	4.8	10	1	82	1131	1420	3.4	12	98	98	105
08-259	5.1	5	43	31	37	7	3.5	11	2	43	1218	1716	2.9	10	79	121	114
08-260	2.1	8	69	37	31	4	2.8	7	3	26	1404	1825	8.6	10	83	142	135
08-261	5.8	5	62	30	34	10	2.4	4	1	18	1235	1640	4.0	10	91	115	139
08-262	3.7	5	45	32	47	6	2.5	4	1	7	1419	1992	6.6	9	66	128	126
08-263	7.3	3	63	36	45	6	2.4	6	4	3	1509	1870	6.7	5	67	134	130
08-264	2.4	5	52	40	40	4	2.9	6	0	7	1326	1798	8.1	11	69	120	126
08-265	5.8	3	63	42	44	6	2.8	7	0	2	1338	1797	4.5	7	72	137	125
08-266	3.4	4	45	53	31	3	2.5	5	1	5	934	1259	0.9	8	61	93	117
08-465	4.7	4	70	56	41	5	3.3	7	1	10	1097	1470	3.4	9	73	125	122
08-466	4.5	2	75	58	35	4	2.9	4	1	17	1055	1234	3.4	13	70	88	109
08-467	5.4	0	59	44	35	2	2.9	7	0	15	1230	1615	3.2	7	67	118	117
08-469	6.2	0	51	38	24	8	1.6	4	2	11	727	887	3.1	9	97	74	81
Min	2.1	0	43	30	24	2	1.6	4	0	2	727	887	0.9	5	60	74	81
Max	7.3	8	93	64	47	10	4.8	11	4	82	1509	1992	8.6	15	127	142	140

BACKGROUND DATA SET - NON-MAGNETIC FRACTION

Lib No	INAA Mo	XRF Nb	ICP Ni	XRF Ni	XRF Pb	XRF Rb	INAA Sb	XRF Se	XRF Sn	XRF Sr	ICP V	XRF V	INAA W	XRF Y	XRF Zn	ICP Zr	XRF Zr
08-267	2.4	4	100	71	33	8	3.7	5	1	7	987	1335	0.9	9	60	168	144
08-268	2.0	2	90	67	29	6	4.0	4	1	7	1065	1335	0.8	9	65	112	129
08-269	3.9	3	46	46	21	11	2.1	2	4	13	579	772	2.2	7	47	94	110
08-270	2.0	2	62	45	28	11	3.8	4	0	7	1097	1376	5.2	11	56	92	110
Max	3.9	4	100	71	33	11	4.0	5	4	13	1097	1376	5.2	11	65	168	144
Min	2.0	2	46	45	21	6	2.1	2	0	7	579	772	0.8	7	47	92	110
G.Mean	2.5	3	71	56	27	9	3.3	4	1	8	904	1173	1.7	9	57	113	122

FINE LAG - MAGNETIC FRACTION

LINE 38820

Magnetic Fraction

Field No	Sample Numbers			% of Total	Co-ordinates		ICP	ICP	XRF	ICP	ICP	ICP	XRF	ICP	
	Lab	Seq	Lib No		East	North	SiO ₂	Al ₂ O ₃	Fe ₂ O ₃	Fe ₂ O ₃	MgO	CaO	TiO ₂	TiO ₂	
BC 801	L08-00300	08-271	16.4	33600	38820	8.78	8.26	72.34	75.50	0.07	0.06	1.50	1.14		
BC 802	L08-00275	08-272	23.2	33650	38820	8.17	8.20	71.77	79.40	0.07	0.07	1.52	1.14		
BC 803	L08-00263	08-273	23.2	33700	38820	7.81	7.74	72.49	74.90	0.07	0.07	1.48	1.02		
BC 804	L08-00293	08-274	26.7	33750	38820	7.54	8.24	73.34	80.20	0.08	0.08	1.42	1.07		
BC 805	L08-00291	08-275	32.4	33800	38820	7.11	7.75	74.49	75.40	0.08	0.09	1.38	1.00		
BC 806	L08-00240	08-276	36.3	33850	38820	6.65	7.15	73.92	76.50	0.10	0.18	1.38	0.94		
BC 807	L08-00271	08-277	38.0	33900	38820	6.15	6.86	73.92	76.20	0.10	0.16	1.46	0.98		
BC 808	L08-00266	08-278	34.9	33925	38820	6.80	7.50	73.34	80.10	0.08	0.10	1.43	1.02		
BC 809	L08-00277	08-279	33.5	33950	38820	6.75	7.63	73.49	80.30	0.09	0.11	1.35	0.99		
BC 810	L08-00279	08-280	31.5	33975	38820	7.82	8.32	72.63	85.20	0.09	0.11	1.33	1.08		
BC 811	L08-00242	08-281	31.2	34000	38820	6.74	7.16	73.92	80.60	0.10	0.16	1.35	0.98		
BC 812	L08-00254	08-282	19.4	34025	38820	7.60	7.70	73.20	83.40	0.10	0.13	1.34	0.96		
BC 813	L08-00245	08-283	34.5	34050	38820	5.62	7.82	73.63	78.00	0.09	0.11	1.92	1.27		
BC 814	L08-00288	08-284	39.8	34075	38820	5.10	8.50	75.06	83.00	0.08	0.07	1.87	1.14		
BC 815	L08-00249	08-285	30.7	34100	38820	5.58	7.00	73.63	82.80	0.08	0.09	1.85	1.13		
BC 816	L08-00251	08-286	24.1	34150	38820	5.60	7.22	75.92	87.00	0.08	0.10	1.94	1.14		
BC 817	L08-00246	08-287	21.1	34200	38820	5.60	6.60	74.20	81.00	0.08	0.10	1.74	1.18		
BC 818	L08-00298	08-288	17.3	34250	38820	5.82	7.38	75.77	80.20	0.08	0.07	1.57	1.13		
BC 726	L08-00456	08-460	10.9	34350	38820	7.82	7.46	72.63	84.00	0.10	0.13	1.38	1.04		
BC 727	L08-00470	08-461	13.2	34450	38820	7.24	6.86	73.20	81.40	0.09	0.10	1.46	1.08		
BC 728	L08-00473	08-462	14.2	34550	38820	7.14	7.16	74.06	84.80	0.09	0.10	1.42	1.09		
BC 729	L08-00446	08-463	17.9	34650	38820	7.32	7.56	73.63	84.40	0.09	0.12	1.34	1.08		
BC 730	L08-00436	08-464	17.5	34750	38820	7.18	7.48	72.49	77.60	0.08	0.07	1.33	0.99		
	Min	-	-	-	33600	38820	5.10	6.60	71.77	74.90	0.07	0.06	1.33	0.94	
	Max	-	-	-	34750	38820	8.78	8.50	75.92	87.00	0.10	0.18	1.94	1.27	

FINE LAG - MAGNETIC FRACTION

LINE 38820

Lib No	XRF Ag	INAA As	INAA Au	ICP Ba	ICP Be	XRF Bi	XRF Cd	INAA Ce	INAA Co	ICP Cr	INAA Cr	ICP Cu	XRF Cu	XRF Ga	XRF Ge	XRF In	INAA La	ICP Mn	XRF Mn
08-271	0	70	0.005	9	0	3	0	23.0	13.2	1784	1662	62	45	45	4	1	12.9	442	362
08-272	0	67	0.006	0	0	1	0	19.1	12.0	1656	1546	59	42	52	0	1	12.1	424	348
08-273	0	69	0.008	0	0	1	0	17.2	10.9	1465	1473	50	45	46	0	0	10.8	384	331
08-274	4	72	0.007	11	0	0	0	14.7	11.4	1584	1427	67	40	50	0	0	10.2	422	339
08-275	0	69	0.135	192	0	3	0	17.0	10.1	1499	1338	67	48	50	0	0	10.2	402	338
08-276	0	66	0.007	384	0	2	1	21.2	7.5	1251	1331	54	36	45	0	1	10.4	391	341
08-277	0	70	0.005	1745	0	0	0	20.1	6.8	1284	1248	47	44	48	0	0	11.6	398	342
08-278	0	70	0.003	1387	0	1	2	17.4	7.2	1371	1321	40	34	45	0	0	9.3	375	296
08-279	3	73	0.006	1555	0	1	0	14.6	8.3	1394	1269	50	35	47	0	1	9.0	394	323
08-280	5	75	0.006	1292	0	2	0	14.5	12.2	1379	1220	108	41	41	3	0	10.0	479	363
08-281	0	76	0.002	1086	0	1	0	18.9	7.6	1092	1145	59	39	46	1	2	9.8	510	430
08-282	2	76	0.006	910	0	1	0	21.4	11.2	1210	1302	54	40	42	0	0	10.6	512	408
08-283	5	51	0.200	266	0	2	0	10.8	7.8	766	786	111	39	69	0	1	7.7	536	444
08-284	0	53	0.138	44	0	0	0	10.1	7.6	884	755	59	34	57	0	0	8.0	604	442
08-285	0	55	0.068	23	0	1	0	16.2	8.5	818	884	0	31	63	3	1	8.7	696	530
08-286	1	60	0.041	11	0	3	1	18.8	7.9	1032	970	54	35	57	0	0	9.0	824	651
08-287	0	62	0.034	43	0	0	0	20.1	8.6	1038	1067	144	32	60	1	2	9.1	880	714
08-288	0	72	0.022	22	0	1	2	24.5	10.0	1228	1195	56	34	49	0	1	11.4	890	715
08-460	0	83	0.007	81	0	1	0	17.5	13.2	1310	1456	67	38	49	3	2	11.1	616	489
08-461	0	80	0.007	0	0	3	1	16.8	12.7	1280	1409	50	38	51	0	0	9.5	576	469
08-462	0	71	0.006	7	0	0	0	18.2	9.5	1346	1265	37	34	57	0	0	8.4	606	467
08-463	0	64	0.007	144	0	5	0	19.2	10.8	1240	1328	74	42	46	0	0	11.1	530	435
08-464	1	59	0.007	37	0	2	0	15.6	9.0	1246	1175	18	38	43	0	0	10.4	660	427
Min	0	51	0.002	0	0	0	0	10.1	6.8	766	755	0	31	41	0	0	7.7	375	296
Max	5	83	0.200	1745	0	5	2	24.5	13.2	1784	1662	144	48	69	4	2	12.9	890	715

FINE LAG - MAGNETIC FRACTION

LINE 38820

Lib No	INAA Mo	XRF Nb	ICP Ni	XRF Ni	XRF Pb	XRF Rb	INAA Sb	XRF Se	XRF Sn	XRF Sr	ICP V	XRF V	INAA W	XRF Y	XRF Zn	ICP Zr	XRF Zr
08-271	3.4	4	74	39	49	8	8.6	7	0	2	1476	1863	4.3	9	24	197	179
08-272	5.7	7	65	39	52	6	8.1	7	1	1	1426	1870	2.4	12	23	212	180
08-273	2.4	5	52	32	51	6	7.7	5	0	4	1321	1877	1.2	9	22	179	170
08-274	3.0	5	71	31	49	6	8.2	6	6	4	1444	1873	2.2	12	28	168	159
08-275	9.4	3	79	31	53	6	8.0	6	2	5	1417	1872	2.6	12	29	165	158
08-276	8.4	0	50	29	52	8	7.7	6	1	16	1236	1834	5.7	10	28	185	162
08-277	5.7	1	49	24	51	6	7.2	4	1	33	1369	1930	3.9	10	23	181	160
08-278	2.4	1	41	26	52	5	8.5	6	1	21	1435	1912	3.7	10	28	178	160
08-279	9.8	0	52	30	49	3	8.2	7	1	30	1425	1890	4.4	11	23	184	150
08-280	8.6	2	58	27	59	5	7.9	4	3	17	1547	1893	5.0	9	28	199	149
08-281	2.2	5	38	33	51	4	7.4	6	1	21	1272	1896	3.2	9	31	174	149
08-282	4.3	0	50	30	53	3	8.6	7	2	13	1398	1975	4.0	10	37	141	146
08-283	1.3	6	74	2	56	4	3.3	4	3	3	1434	2250	8.1	6	23	238	151
08-284	4.6	0	37	11	54	5	2.8	4	2	2	1732	2301	7.3	6	25	156	143
08-285	8.1	4	0	3	51	4	3.1	5	3	1	1484	2241	4.4	10	18	98	139
08-286	5.3	4	28	14	49	5	3.1	6	1	3	1594	2280	8.7	7	23	161	151
08-287	7.6	1	96	7	48	5	3.0	11	1	3	1526	2310	7.9	8	30	254	142
08-288	13.8	3	44	18	50	4	3.8	4	0	6	1644	2263	6.7	12	26	127	140
08-460	6.0	3	54	27	45	8	5.8	7	2	4	1448	2024	4.1	10	37	163	136
08-461	6.0	2	36	22	51	7	5.5	6	1	5	1546	2073	4.0	8	30	110	144
08-462	5.2	3	28	18	55	3	4.6	9	0	6	1646	2165	4.1	10	28	116	138
08-463	5.0	1	49	21	60	5	5.6	3	2	7	1450	2030	4.1	7	27	175	144
08-464	5.9	3	20	17	52	3	4.5	4	2	2	1498	2014	4.0	9	32	143	131
Min	1.3	0	0	2	45	3	2.8	3	0	1	1236	1834	1.2	6	18	98	131
Max	13.8	7	96	39	60	8	8.6	11	6	33	1732	2310	8.7	12	37	254	180

FINE LAG - MAGNETIC FRACTION

LINE 38940

Sample Numbers			% of Total	Co-ordinates		ICP SiO ₂	ICP Al ₂ O ₃	XRF Fe ₂ O ₃	ICP Fe ₂ O ₃	ICP MgO	ICP CaO	XRF TiO ₂	ICP TiO ₂
Field No	Lab Seq	Lib No		East	North								
BC 821	L08-00312	08-289	26.5	33650	38940	7.79	7.85	73.92	78.30	0.09	0.10	1.55	1.14
BC 822	L08-00243	08-290	20.3	33700	38940	8.82	7.66	71.63	78.80	0.10	0.11	1.54	1.11
BC 823	L08-00247	08-291	22.5	33750	38940	8.68	8.08	72.20	83.20	0.10	0.12	1.54	1.16
BC 824	L08-00314	08-292	26.6	33800	38940	7.74	8.22	73.34	86.40	0.11	0.13	1.59	1.27
BC 825	L08-00315	08-293	27.2	33850	38940	7.90	8.14	72.63	85.80	0.12	0.13	1.46	1.18
BC 826	L08-00270	08-294	22.1	33900	38940	7.22	7.23	74.20	76.10	0.10	0.12	1.48	1.01
BC 827	L08-00282	08-295	22.7	33925	38940	7.24	7.30	72.63	80.20	0.12	0.14	1.35	0.98
BC 828	L08-00309	08-296	27.6	33950	38940	6.78	7.54	73.63	79.00	0.15	0.23	1.43	1.04
BC 829	L08-00256	08-297	23.9	33975	38940	7.52	7.36	74.06	86.60	1.98	0.46	1.41	1.04
BC 830	L08-00269	08-298	9.4	34000	38940	7.08	7.25	72.91	74.10	0.19	0.37	1.33	0.90
BC 831	L08-00304	08-299	12.3	34025	38940	6.62	7.42	73.63	74.10	0.13	0.16	1.44	1.01
BC 832	L08-00313	08-300	16.2	34050	38940	7.02	7.79	72.91	78.70	0.10	0.08	1.55	1.17
BC 833	L08-00306	08-301	14.7	34100	38940	6.32	7.02	75.06	79.00	0.09	0.07	1.49	1.05
BC 834	L08-00297	08-302	17.0	34150	38940	6.52	7.82	73.63	83.80	0.09	0.07	1.48	1.14
BC 835	L08-00287	08-303	17.5	34200	38940	6.73	7.34	75.06	78.10	0.07	0.07	1.46	1.07
BC 836	L08-00232	08-304	19.8	34250	38940	5.77	6.47	73.77	72.20	0.06	0.06	1.39	0.91
BC 837	L08-00267	08-305	15.0	34300	38940	8.66	8.08	71.06	81.10	0.08	0.08	1.46	1.12
BC 721	L08-00455	08-455	21.0	34400	38940	8.28	8.16	72.63	85.00	0.10	0.15	1.31	1.01
BC 722	L08-00441	08-456	15.3	34500	38940	8.93	8.18	71.34	73.50	0.09	0.12	1.32	0.91
BC 723	L08-00444	08-457	26.6	34600	38940	7.26	7.46	73.20	81.60	0.11	0.14	1.19	0.86
BC 725	L08-00445	08-459	15.5	34800	38940	8.28	6.94	74.34	83.20	0.10	0.13	1.33	0.97
Min			-	33650	38940	5.77	6.47	71.06	72.20	0.06	0.06	1.19	0.86
Max			-	34800	38940	8.93	8.22	75.06	86.60	1.98	0.46	1.59	1.27

BACKGROUND DATA SET - MAGNETIC FRACTION

Sample Numbers			% of Total	Co-ordinates		ICP SiO ₂	ICP Al ₂ O ₃	XRF Fe ₂ O ₃	ICP Fe ₂ O ₃	ICP MgO	ICP CaO	XRF TiO ₂	ICP TiO ₂
Field No	Lab Seq	Lib No		East	North								
BC 841	L08-00260	08-306	21.4	33747	39311	9.52	8.64	72.20	84.00	0.09	0.10	1.51	1.14
BC 842	L08-00274	08-307	20.0	34172	39314	8.85	8.34	71.77	76.30	0.07	0.08	1.39	1.01
BC 843	L08-00253	08-308	12.4	33545	38146	8.82	7.99	71.63	77.10	0.08	0.08	1.58	1.12
BC 844	L08-00284	08-309	30.4	34290	38110	5.82	6.66	74.34	79.00	0.08	0.08	1.75	1.19
Max			-	-	-	9.52	8.64	74.34	84.00	0.09	0.10	1.75	1.19
Min			-	-	-	5.82	6.66	71.63	76.30	0.07	0.08	1.39	1.01
G.Mean			-	-	-	8.11	7.87	72.48	79.04	0.08	0.09	1.55	1.11

FINE LAG - MAGNETIC FRACTION

LINE 38940

Lib No	XRF Ag	INAA As	INAA Au	ICP Ba	ICP Be	XRF Bi	XRF Cd	INAA Ce	INAA Co	ICP Cr	INAA Cr	ICP Cu	XRF Cu	XRF Ga	XRF Ge	XRF In	INAA La	ICP Mn	XRF Mn
08-289	3	61	0.003	96	0	2	1	20.9	8.9	1589	1519	48	48	48	0	2	10.3	342	295
08-290	0	70	0.017	120	0	1	0	20.3	12.8	1422	1493	88	47	45	0	0	10.8	378	322
08-291	1	65	0.011	199	0	3	1	21.6	11.0	1540	1624	0	39	49	0	2	11.0	360	288
08-292	0	68	0.002	310	0	1	0	18.6	9.5	1586	1463	41	42	49	0	0	12.3	386	309
08-293	0	67	0.002	666	0	0	0	19.0	9.4	1516	1396	47	38	47	0	1	11.9	394	309
08-294	0	72	0.005	909	0	2	3	22.7	9.6	1368	1429	50	42	46	2	0	12.7	434	373
08-295	0	83	0.005	1576	0	0	1	30.2	10.6	1374	1439	70	35	46	0	0	18.5	472	390
08-296	0	75	0.007	1982	0	1	0	21.6	9.7	1502	1364	40	46	43	2	0	13.7	588	472
08-297	0	73	0.053	2376	0	2	0	22.0	8.9	1406	1342	35	30	48	0	0	12.3	630	501
08-298	3	114	0.004	1712	0	0	0	21.3	11.3	1234	1444	75	60	57	2	1	13.0	755	669
08-299	0	88	0.026	1249	0	2	0	17.4	7.7	1313	1316	60	46	54	0	0	11.4	565	474
08-300	2	82	0.341	1575	0	1	0	13.8	9.8	1134	1092	53	43	55	0	0	8.4	537	436
08-301	3	90	0.049	430	0	2	0	13.7	9.5	1232	1220	56	30	49	0	2	8.5	538	413
08-302	4	87	0.033	23	0	3	0	16.5	12.9	1284	1185	56	28	54	0	0	9.9	578	428
08-303	0	83	0.031	6	0	0	0	13.7	10.2	1309	1114	66	46	50	0	3	9.0	686	562
08-304	0	75	0.007	0	0	2	1	17.9	8.9	1123	1215	34	38	51	2	1	8.3	544	475
08-305	0	68	0.002	0	0	2	0	15.4	11.1	1441	1346	38	37	46	0	1	9.6	575	435
08-455	0	71	0.007	72	0	1	0	24.7	12.2	1420	1424	67	37	47	0	0	13.8	518	424
08-456	1	56	0.007	121	0	2	0	24.2	11.7	1328	1363	54	35	44	4	1	16.3	535	457
08-457	1	55	0.007	185	0	2	0	15.2	9.4	1200	1172	58	42	44	0	0	9.6	430	366
08-459	1	61	0.007	294	0	3	2	21.7	11.4	1262	1333	294	43	46	0	0	11.0	436	365
Min	0	55	0.002	0	0	0	0	13.7	7.7	1123	1092	0	28	43	0	0	8.3	342	288
Max	4	114	0.341	2376	0	3	3	30.2	12.9	1589	1624	294	60	57	4	3	18.5	755	669

BACKGROUND DATA SET - MAGNETIC FRACTION

Lib No	XRF Ag	INAA As	INAA Au	ICP Ba	ICP Be	XRF Bi	XRF Cd	INAA Ce	INAA Co	ICP Cr	INAA Cr	ICP Cu	XRF Cu	XRF Ga	XRF Ge	XRF In	INAA La	ICP Mn	XRF Mn
08-306	0	65	0.002	14	0	0	1	21.7	10.4	1638	1538	34	52	49	1	1	11.8	430	344
08-307	0	64	0.006	5	0	0	2	18.8	9.8	1538	1417	60	57	52	1	0	10.6	373	321
08-308	0	66	0.005	0	0	3	3	25.1	11.8	1633	1809	56	50	45	0	3	12.4	366	316
08-309	0	58	0.006	49	0	2	0	15.7	9.1	1258	1250	62	40	60	3	0	9.3	532	449
Max	0	66	0.006	49	0	3	3	25.1	11.8	1638	1809	62	57	60	3	3	12.4	532	449
Min	0	58	0.002	0	0	0	0	15.7	9.1	1258	1250	34	40	45	0	0	9.3	366	316
G.Mean	0	63	0.004	-	-	0	1	20.0	10.2	1508	1490	52	49	51	-	0	11.0	420	354

FINE LAG - MAGNETIC FRACTION

LINE 38940

Lib No	INAA Mo	XRF Nb	ICP Ni	XRF Ni	XRF Pb	XRF Rb	INAA Sb	XRF Se	XRF Sn	XRF Sr	ICP V	XRF V	INAA W	XRF Y	XRF Zn	ICP Zr	XRF Zr
08-289	3.2	4	58	37	56	7	7.7	4	4	7	1477	1928	4.4	10	27	196	176
08-290	2.2	10	88	33	49	9	7.9	4	0	6	1246	1828	3.2	8	30	224	171
08-291	4.4	2	22	25	52	7	7.7	5	4	4	1326	1884	1.1	15	20	174	173
08-292	2.0	6	59	33	51	1	7.5	5	2	12	1542	1934	1.0	11	20	200	169
08-293	2.3	5	60	38	57	6	8.0	5	0	20	1536	1918	1.0	13	22	173	166
08-294	7.7	2	54	30	54	4	7.9	5	1	21	1359	1891	2.9	11	33	184	166
08-295	6.5	4	64	23	51	4	8.7	7	1	26	1382	1849	3.5	13	29	163	156
08-296	3.6	3	58	32	54	3	8.4	4	3	47	1472	1910	6.4	13	32	135	156
08-297	2.7	4	38	25	54	4	7.9	4	0	82	1404	1922	4.3	13	30	148	162
08-298	4.1	6	53	38	57	6	7.9	5	0	49	1404	2010	4.0	9	32	161	149
08-299	4.1	4	53	23	47	5	6.8	6	5	22	1588	2139	4.9	9	28	156	149
08-300	5.5	3	54	26	41	6	5.7	6	2	19	1606	2117	7.2	7	27	169	149
08-301	3.8	3	49	28	56	4	5.8	8	3	4	1558	2049	6.5	12	27	124	148
08-302	3.6	1	54	20	48	5	5.5	6	0	6	1684	2122	4.5	10	25	143	143
08-303	8.2	5	51	25	45	4	5.0	6	3	6	1602	2131	5.5	7	28	160	143
08-304	5.2	2	36	22	60	5	5.2	6	4	2	1444	2186	6.1	8	26	130	137
08-305	2.3	4	47	27	50	3	5.5	6	3	2	1580	2018	3.6	8	28	165	148
08-455	6.5	0	63	35	65	7	7.3	6	0	12	1408	1916	4.8	10	30	186	150
08-456	6.3	5	56	38	58	9	6.4	10	0	11	1249	1796	3.5	13	30	152	151
08-457	6.1	5	47	21	60	5	4.6	6	0	14	1386	1994	3.5	6	29	148	132
08-459	8.9	1	55	33	63	4	4.0	4	0	10	1370	1949	4.0	10	38	152	138
Min	2.0	0	22	20	41	1	4.0	4	0	2	1246	1796	1.0	6	20	124	132
Max	8.9	10	88	38	65	9	8.7	10	5	82	1684	2186	7.2	15	38	224	176

BACKGROUND DATA SET - MAGNETIC FRACTION

Lib No	INAA Mo	XRF Nb	ICP Ni	XRF Ni	XRF Pb	XRF Rb	INAA Sb	XRF Se	XRF Sn	XRF Sr	ICP V	XRF V	INAA W	XRF Y	XRF Zn	ICP Zr	XRF Zr
08-306	2.4	6	45	38	49	8	8.4	7	1	4	1374	1882	1.1	9	21	168	175
08-307	8.8	5	65	33	53	7	8.7	5	2	3	1338	1793	1.9	11	25	188	163
08-308	6.7	2	59	34	64	3	9.2	5	2	3	1313	1860	2.4	13	28	195	175
08-309	5.1	4	56	20	50	6	5.9	6	3	3	1480	2048	2.6	12	18	146	142
Max	8.8	6	65	38	64	8	9.2	7	3	4	1480	2048	2.6	13	28	195	175
Min	2.4	2	45	20	49	3	5.9	5	1	3	1313	1793	1.1	9	18	146	142
G.Mean	5.2	4	56	30	54	6	7.9	6	2	3	1375	1893	1.9	11	23	173	163

STANDARDS

Sample Numbers			% of Total	Co-ordinates		ICP	ICP	XRF	ICP	ICP	ICP	XRF	ICP
Field No	Lab Seq	Lib No		East	North	SiO ₂	Al ₂ O ₃	Fe ₂ O ₃	Fe ₂ O ₃	MgO	CaO	TiO ₂	TiO ₂
STD 9	L08-00310	08-310	-	-	-	14.00	7.78	65.05	69.60	0.17	0.13	0.71	0.54
STD 9	L08-00233	08-311	-	-	-	13.30	7.16	63.48	65.80	0.15	0.12	0.69	0.48
STD 9	L08-00234	08-312	-	-	-	13.50	7.30	64.62	67.00	0.15	0.12	0.70	0.50
STD 9	L08-00294	08-313	-	-	-	13.60	7.66	64.19	66.70	0.16	0.12	0.70	0.53
STD 9	L08-00259	08-314	-	-	-	14.10	7.90	63.91	72.50	0.16	0.14	0.69	0.53
STD 9	L08-00295	08-315	-	-	-	14.00	7.93	64.34	68.60	0.16	0.13	0.70	0.55
STD 9	L08-00437	08-475	-	-	-	14.30	7.49	63.19	63.90	0.16	0.13	0.70	0.53
STD 9	L08-00457	08-476	-	-	-	13.70	7.64	64.34	69.10	0.16	0.13	0.70	0.52
STD 9	L08-00459	08-448	-	-	-	14.00	7.71	64.48	69.80	0.16	0.13	0.70	0.53
STD 9	L08-00465	08-468	-	-	-	13.70	7.72	64.34	69.80	0.16	0.13	0.69	0.53
STD 9	L08-00442	08-458	-	-	-	14.00	7.69	64.91	70.00	0.16	0.13	0.69	0.52
STD 9	L08-00230	08-229	-	-	-	12.90	7.22	64.34	64.90	0.15	0.11	0.69	0.49
STD 9	L08-00202	08-230	-	-	-	13.40	7.28	63.91	69.10	0.15	0.13	0.70	0.50
STD 9	L08-00203	08-231	-	-	-	13.50	7.29	64.34	68.80	0.15	0.13	0.71	0.50
Mean	-	-	-	-	-	13.71	7.56	64.24	68.26	0.16	0.13	0.70	0.52
2s	-	-	-	-	-	0.76	0.52	1.00	4.63	0.01	0.01	0.01	0.04
Pre Val	-	-	-	-	-	14.14	7.48	72.92	72.92	0.10	0.10	0.70	0.70

STANDARDS

Lib No	XRF Ag	INAA As	INAA Au	ICP Ba	ICP Be	XRF Bi	XRF Cd	INAA Ce	INAA Co	ICP Cr	INAA Cr	ICP Cu	XRF Cu	XRF Ga	XRF Ge	XRF In	INAA La	ICP Mn	XRF Mn
08-310	2	436	0.085	244	0	2	1	17.2	17.4	491	447	165	149	24	1	1	11.5	1823	1578
08-311	6	426	0.065	241	0	0	0	17.4	18.6	467	469	151	138	28	0	0	11.4	1777	1556
08-312	0	425	0.134	246	0	3	0	20.1	18.5	476	469	135	141	22	0	0	11.4	1834	1513
08-313	1	449	0.130	251	0	0	0	19.2	17.8	519	466	166	146	20	1	2	12.0	1745	1542
08-314	0	433	0.092	262	0	2	0	22.1	19.3	499	474	130	131	28	0	1	11.5	1798	1547
08-315	1	448	0.062	261	0	2	0	15.9	17.3	539	463	170	133	30	5	0	11.7	1833	1542
08-475	0	443	0.084	241	0	0	0	16.9	17.3	505	474	152	141	24	0	1	11.8	2532	1526
08-476	0	447	0.109	252	0	2	0	17.8	19.6	484	475	139	138	26	0	2	12.2	1806	1536
08-448	0	444	0.089	257	0	1	0	15.9	19.0	492	480	141	137	27	1	1	11.9	1852	1534
08-468	1	436	0.071	213	0	0	2	16.6	18.5	493	467	151	140	26	3	0	11.6	1765	1551
08-458	0	436	0.049	254	0	1	0	17.3	18.2	493	464	139	147	22	2	3	11.9	1821	1526
08-229	2	406	0.075	233	0	1	0	18.0	17.1	439	447	108	139	25	2	3	10.8	1694	1536
08-230	7	438	0.179	240	0	1	0	20.0	19.3	458	484	207	135	25	0	2	12.1	1732	1527
08-231	1	442	0.062	239	0	1	2	17.5	19.6	440	490	209	139	21	5	0	12.0	1702	1567
Mean	2	436	0.092	245	0	1	0	18.0	18.4	485	469	155	140	25	1	1	11.7	1837	1542
2s	4	23	0.071	26	0	2	1	3.5	1.8	56	24	56	10	6	4	2	0.7	413	35
Pre Val	1	437	0.088	270	-	1	1	18.0	18.0	469	469	141	141	25	1	0	12.0	1557	1557

STANDARDS

Lib No	INAA Mo	XRF Nb	ICP Ni	XRF Ni	XRF Pb	XRF Rb	INAA Sb	XRF Se	XRF Sn	XRF Sr	ICP V	XRF V	INAA W	XRF Y	XRF Zn	ICP Zr	XRF Zr
08-310	5.9	2	51	34	60	4	0.5	2	0	12	850	968	6.9	14	301	85	88
08-311	0.9	2	57	31	59	5	0.4	0	0	15	790	955	10.4	13	294	90	87
08-312	7.7	2	43	22	59	4	0.7	1	0	13	807	958	8.2	12	298	77	99
08-313	6.2	2	54	22	59	7	0.5	4	3	13	834	960	15.7	10	299	83	91
08-314	5.3	3	42	32	52	5	0.5	6	2	14	795	950	8.1	13	295	85	88
08-315	5.5	0	64	23	56	4	0.4	3	0	11	863	964	9.1	12	297	88	86
08-475	5.7	2	43	28	53	5	1.3	5	0	15	727	941	6.7	11	295	110	86
08-476	6.0	4	48	28	57	4	0.6	3	0	13	754	962	13.0	13	300	93	86
08-448	5.2	1	47	29	53	6	0.6	5	1	11	765	954	8.1	14	297	88	89
08-468	5.2	0	47	29	58	6	0.6	4	1	11	816	953	3.9	13	294	77	91
08-458	5.9	0	47	26	54	7	1.2	2	0	6	766	936	9.9	13	301	88	87
08-229	7.4	1	27	33	61	4	1.5	2	2	12	753	961	11.5	13	293	64	87
08-230	4.9	4	67	28	56	5	0.6	3	0	11	856	940	2.2	13	296	120	91
08-231	5.6	2	91	31	54	6	0.5	4	1	12	838	946	2.3	13	295	107	90
Mean	5.5	2	52	28	57	5	0.7	3	1	12	801	953	8.3	13	297	90	89
2s	3.1	3	30	8	6	2	0.7	3	2	4	87	19	7.7	2	5	29	7
Pre Val	5.2	2	28	28	57	5	0.6	5	2	12	948	948	7.9	13	297	89	89

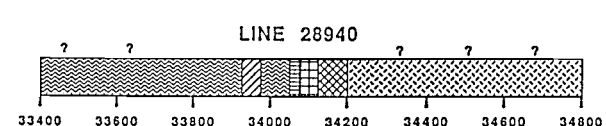
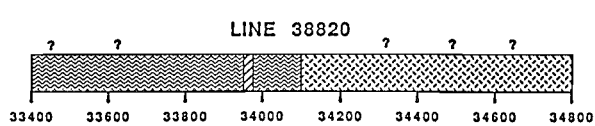
APPENDIX 3

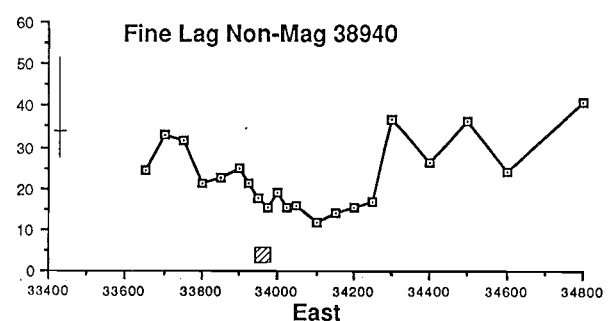
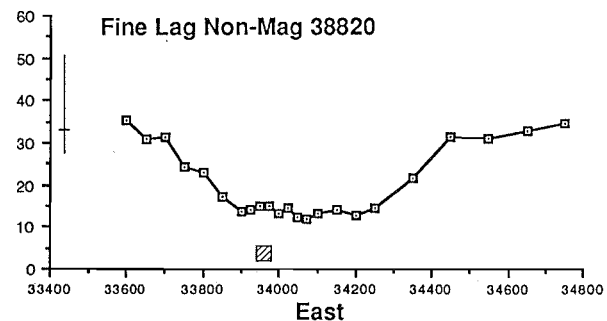
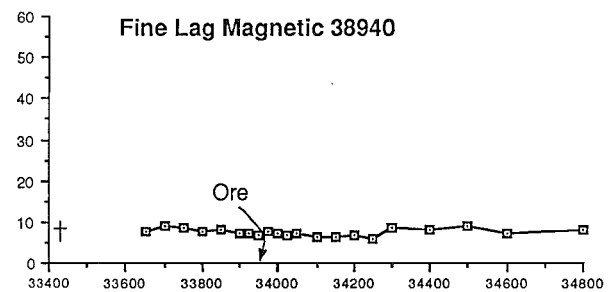
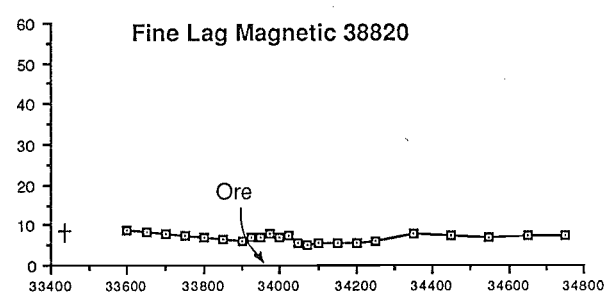
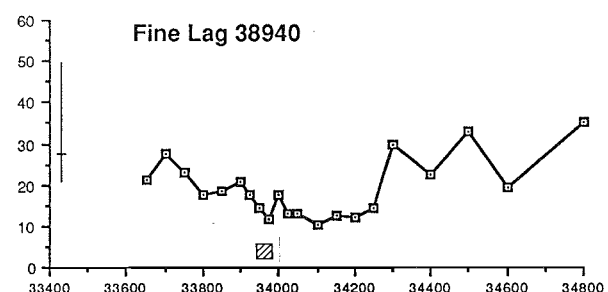
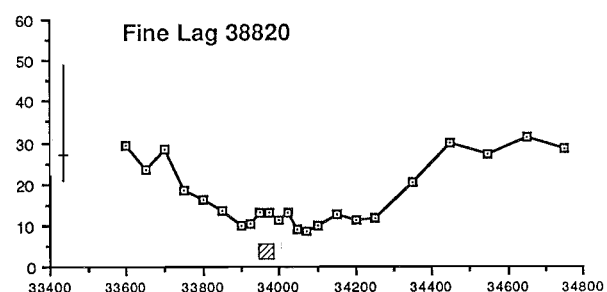
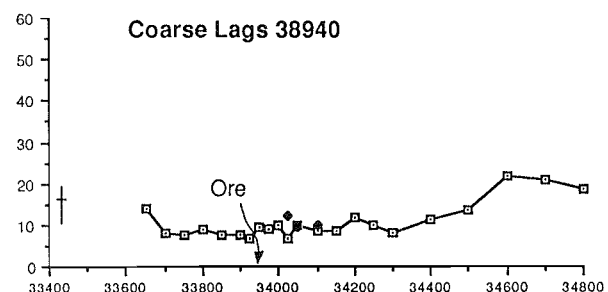
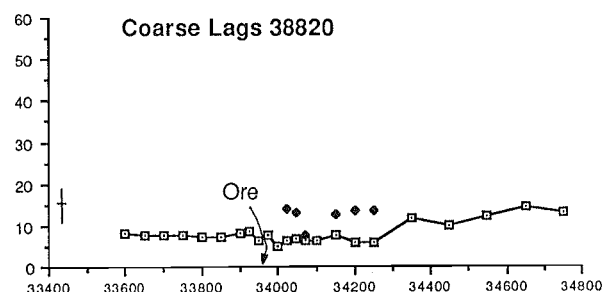
Graphed Geochemistry

- Lines represent black ferruginous lag
- Diamonds represent Khaki Lag
- Range and geometric mean of background data
- Ore

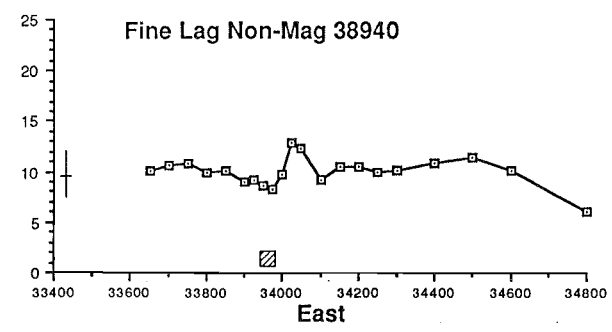
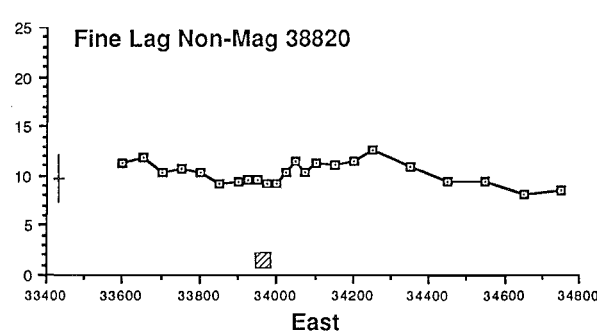
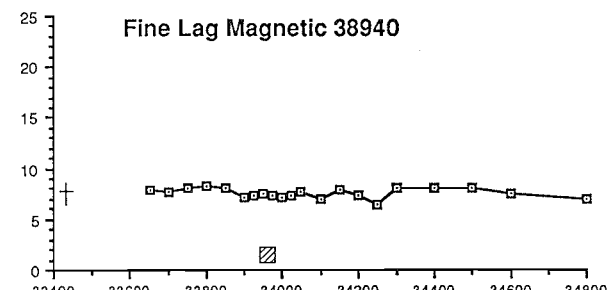
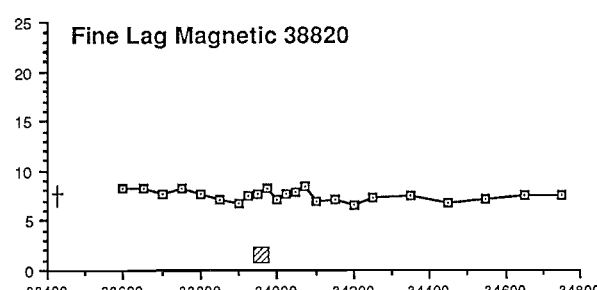
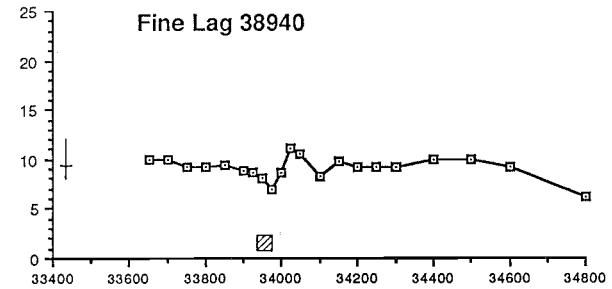
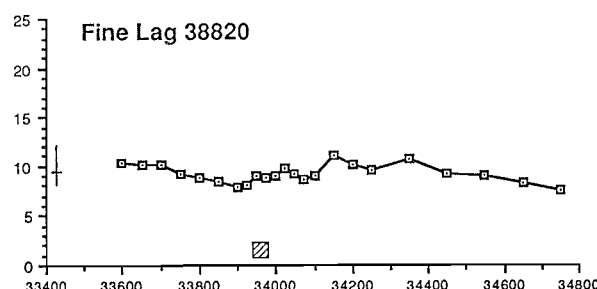
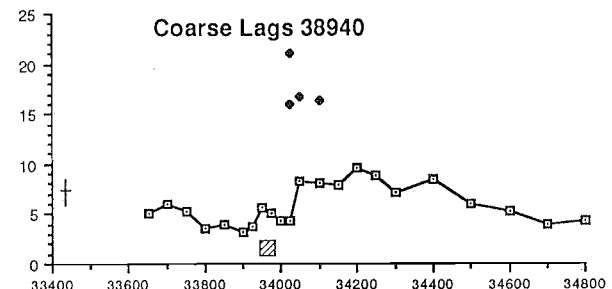
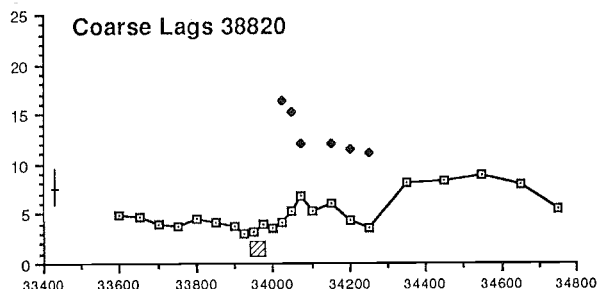
PERMIAN GLACIALS GRANITOID DOLERITE

ULTRAMAFIC SCHISTS BLACK SHALE METABASALT

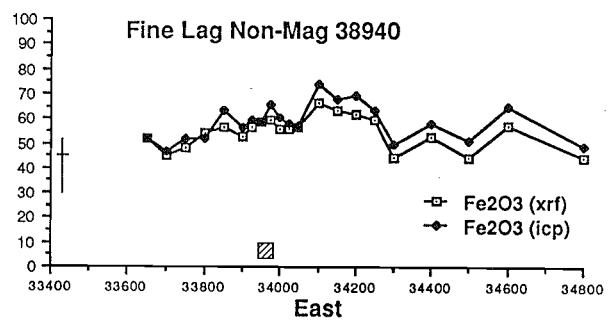
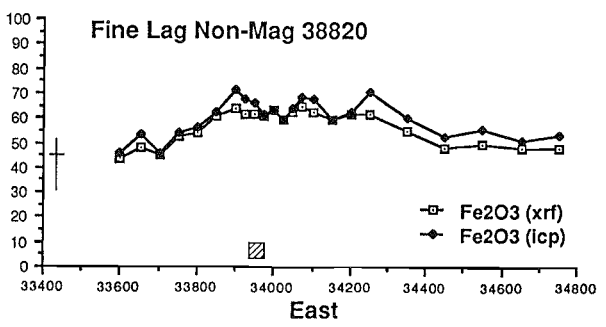
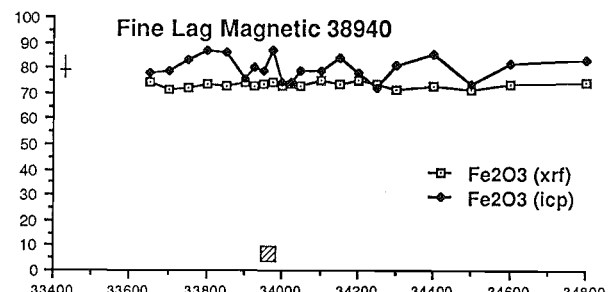
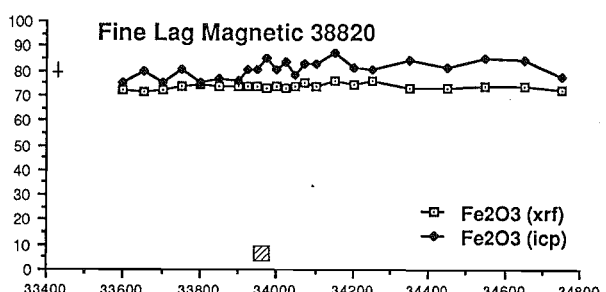
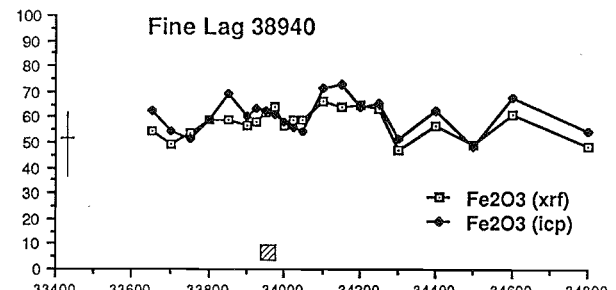
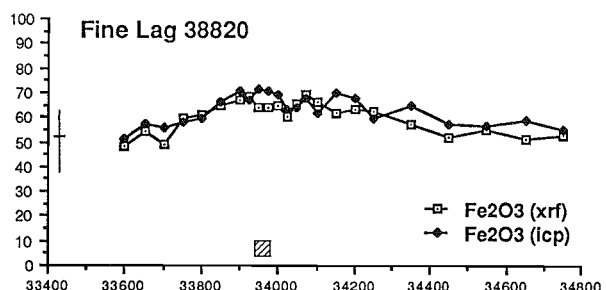
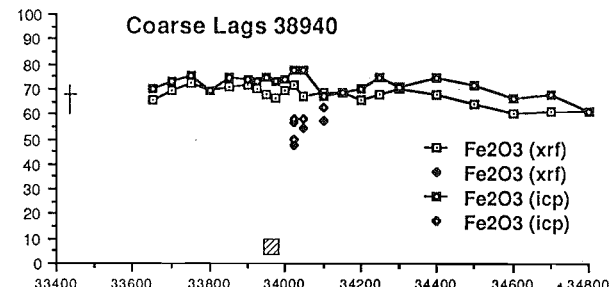
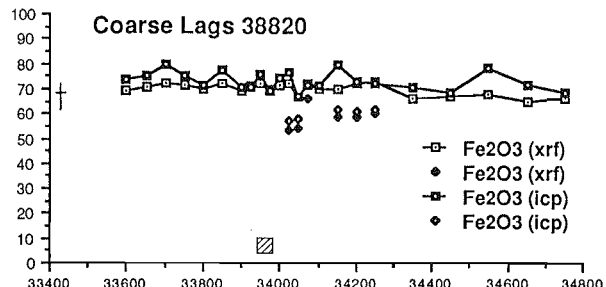




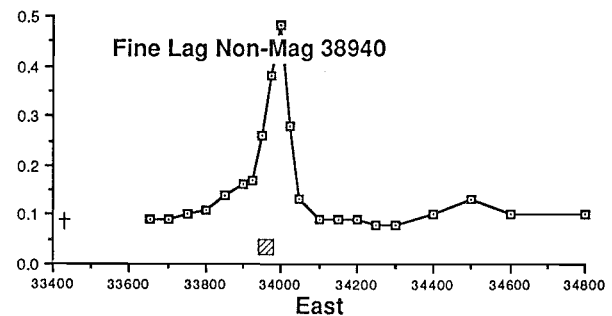
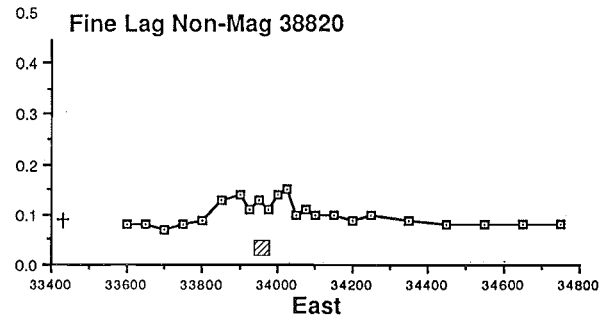
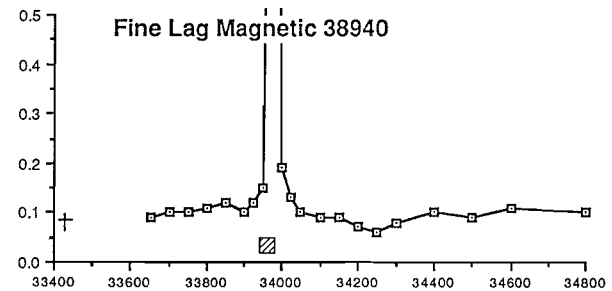
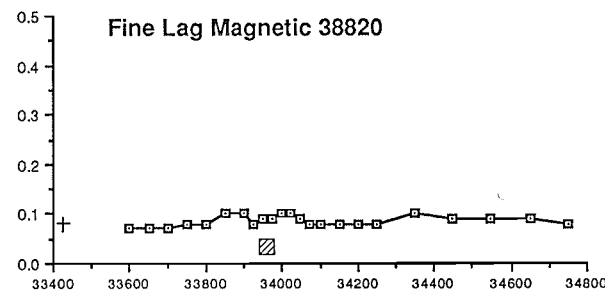
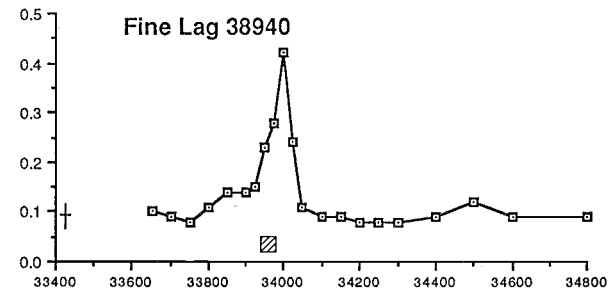
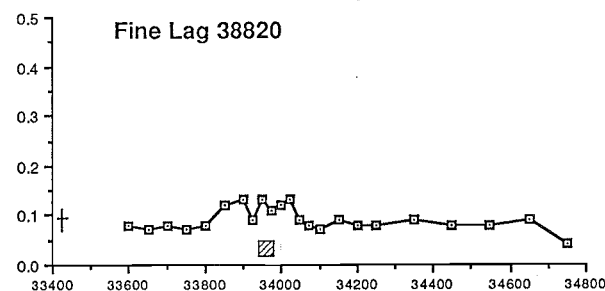
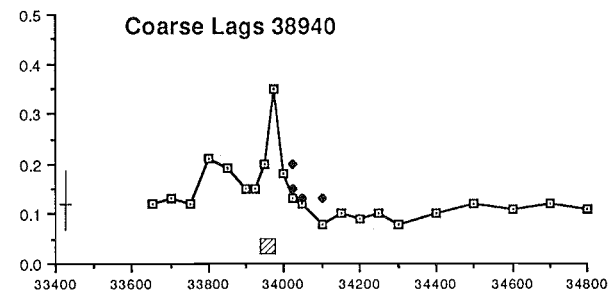
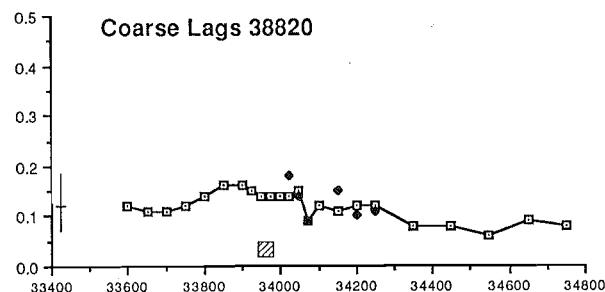
Al_2O_3 (%)



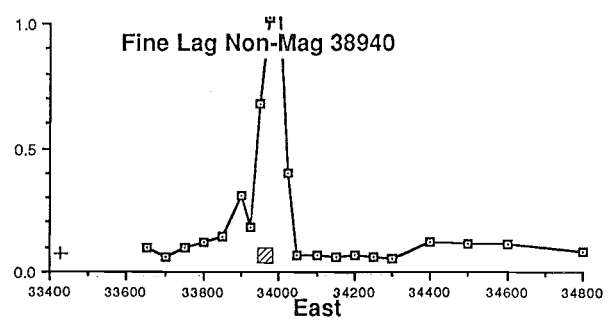
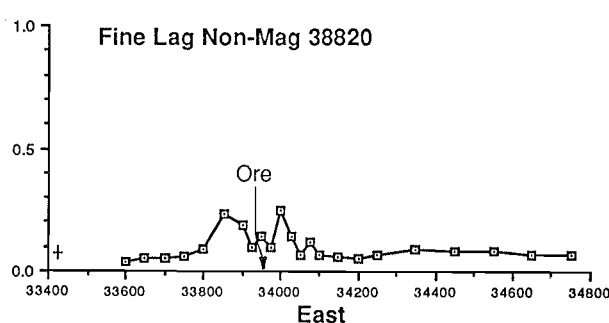
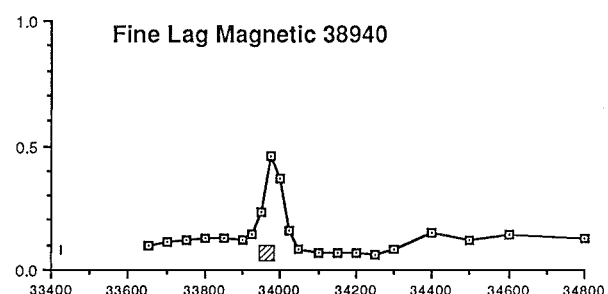
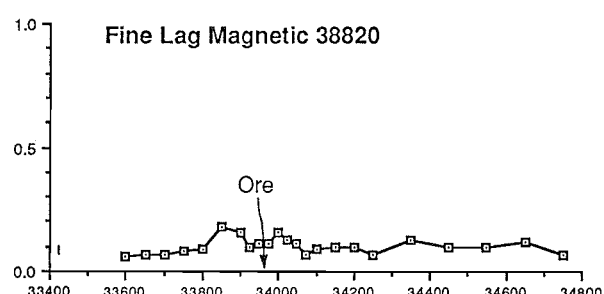
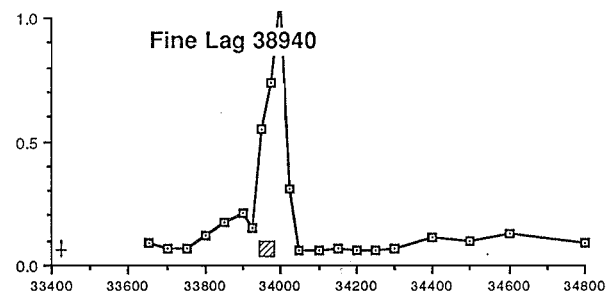
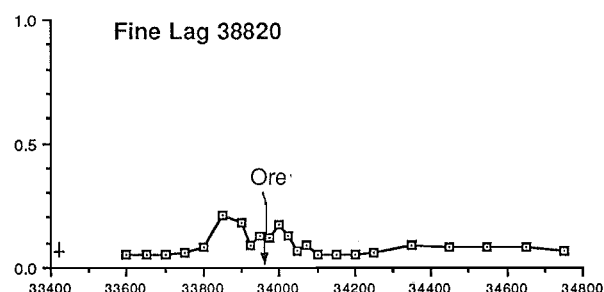
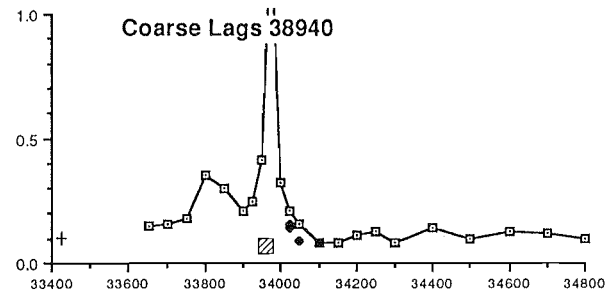
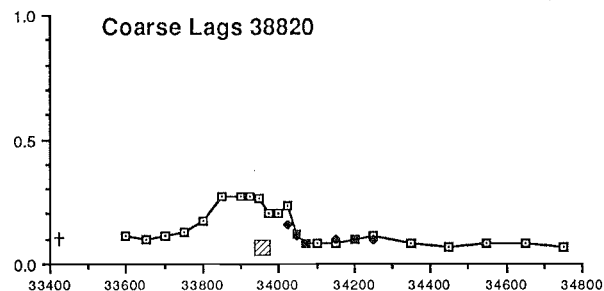
Fe_2O_3 (%)



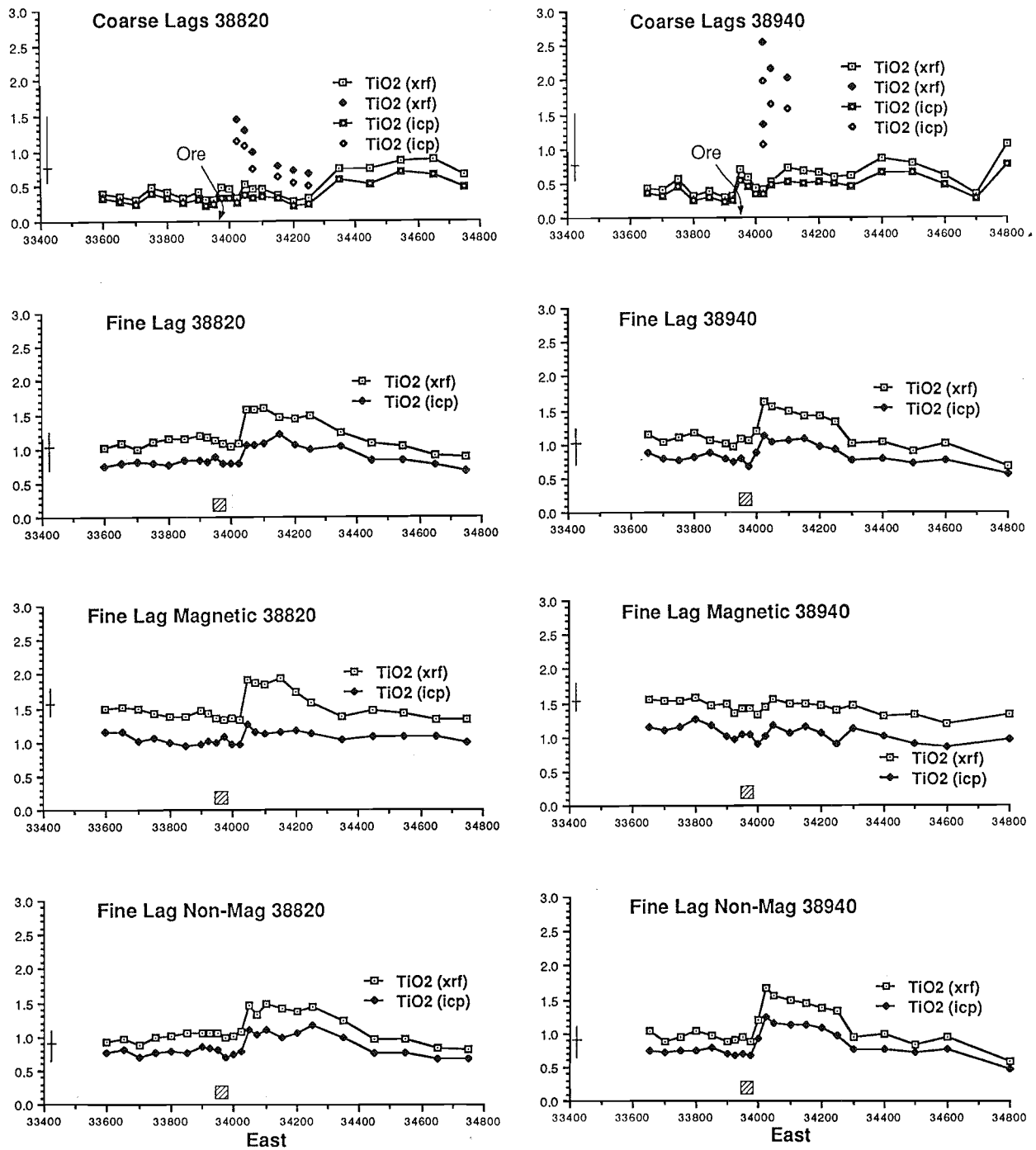
MgO (%)

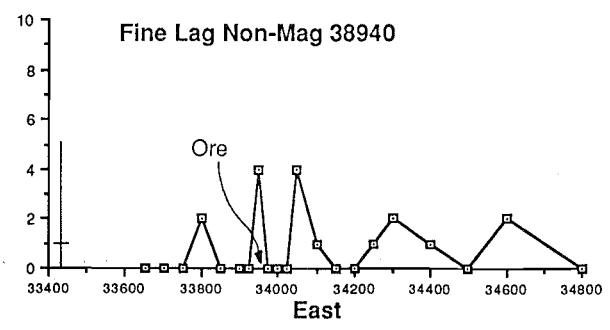
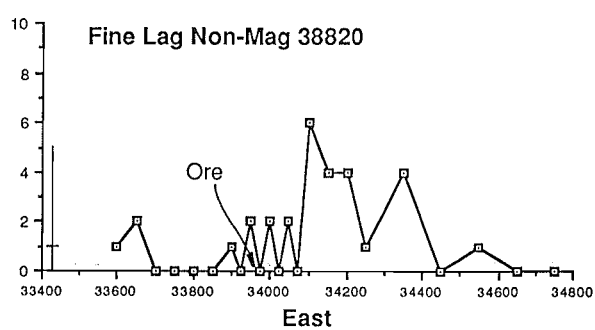
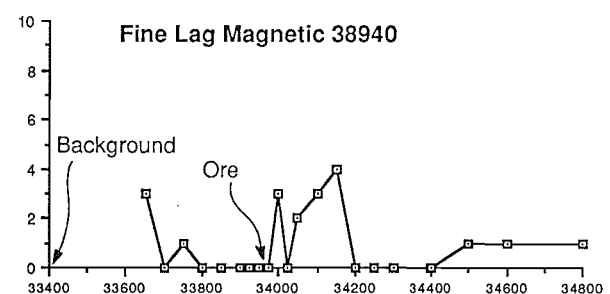
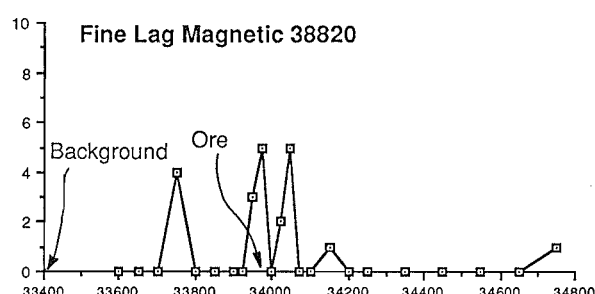
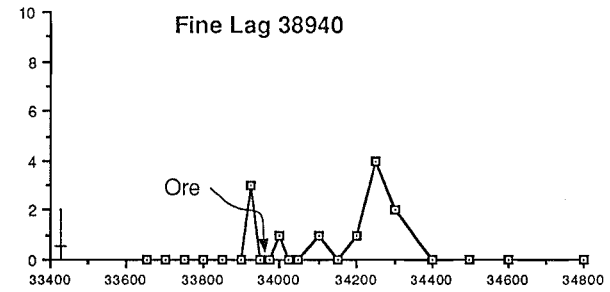
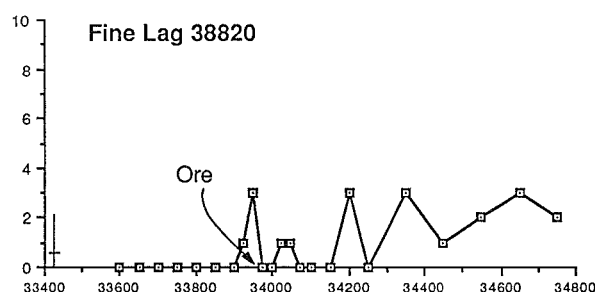
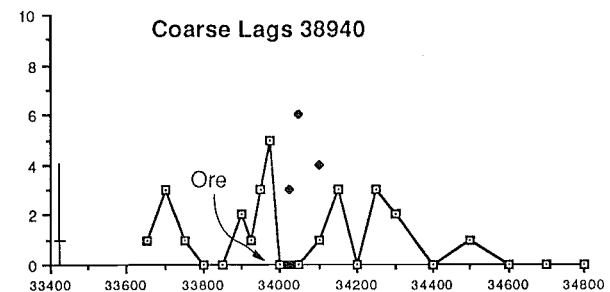
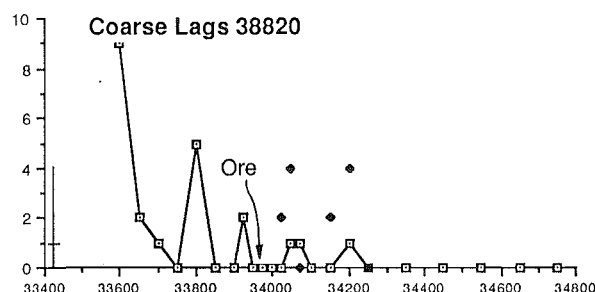


CaO (%)

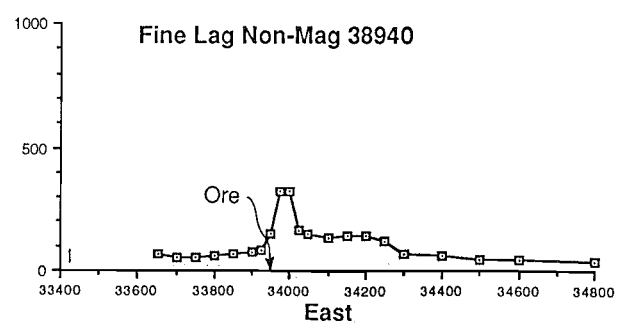
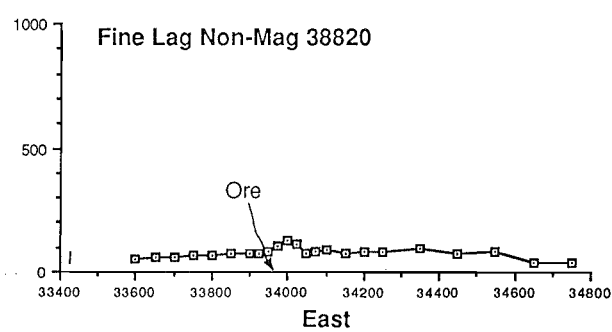
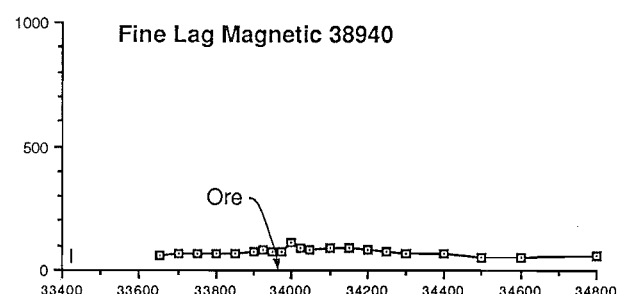
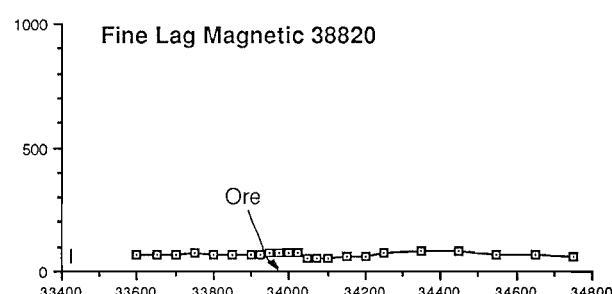
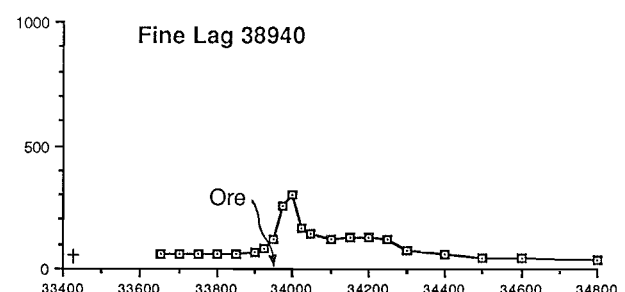
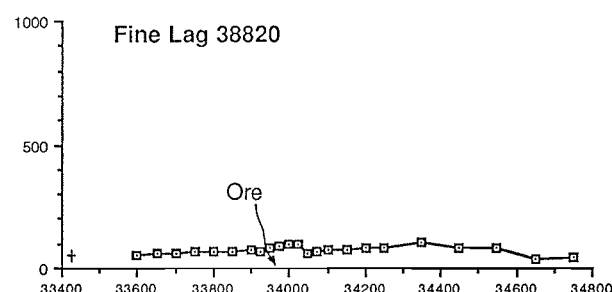
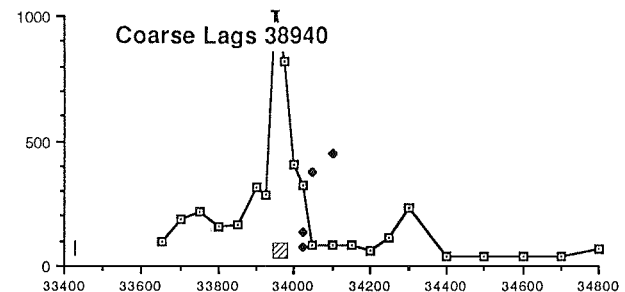
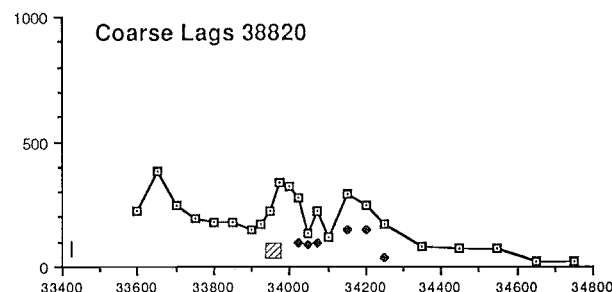


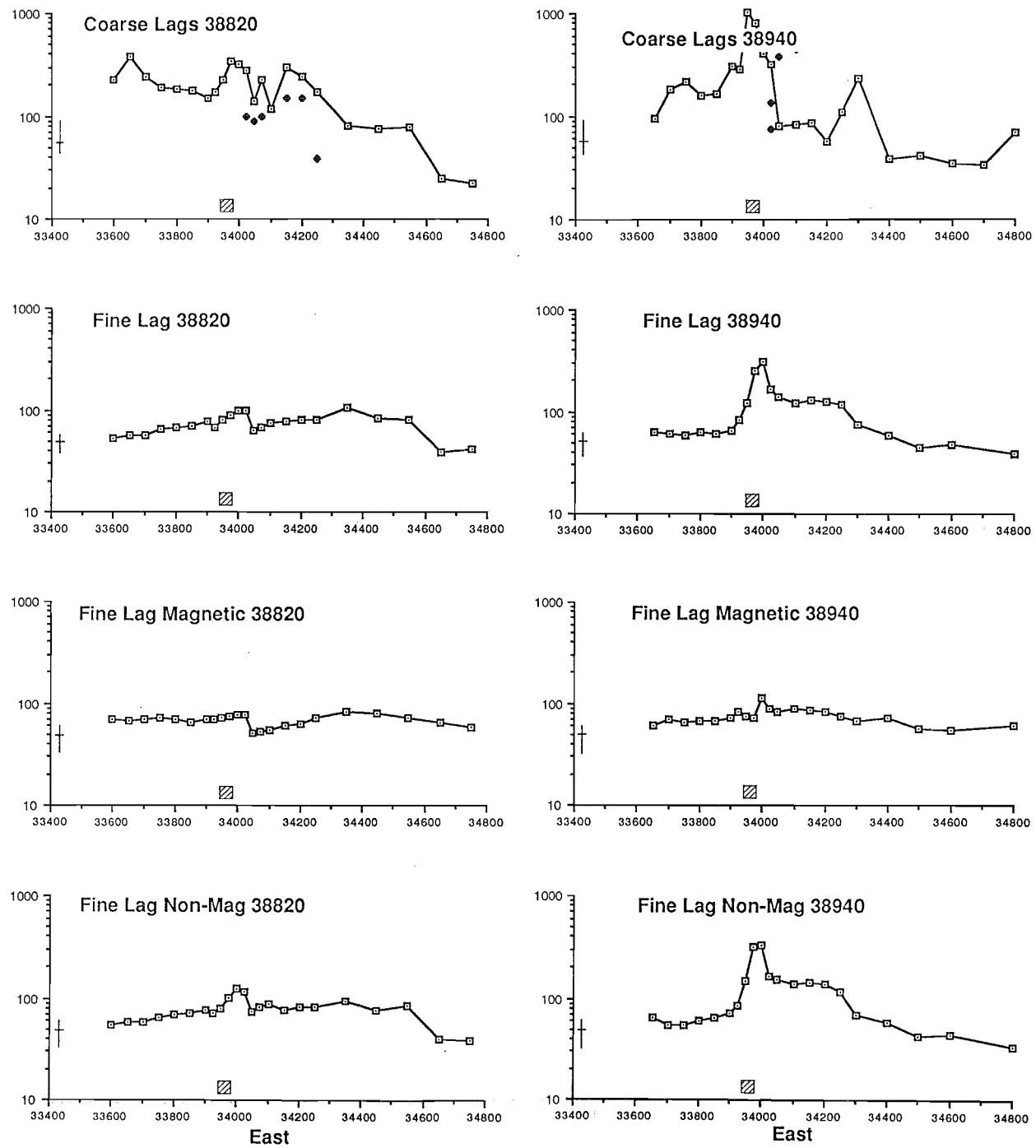
TiO_2 (%)



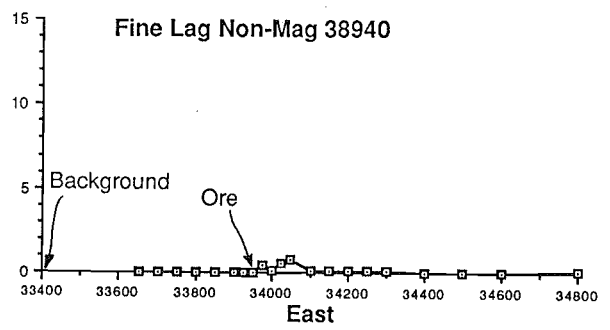
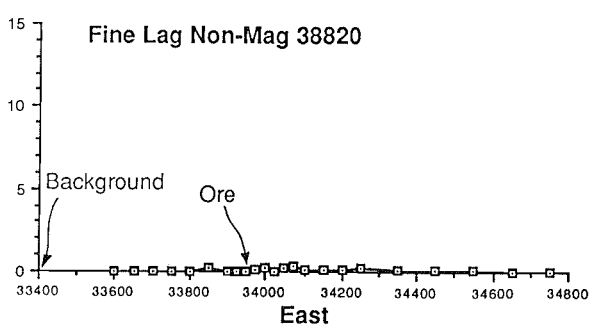
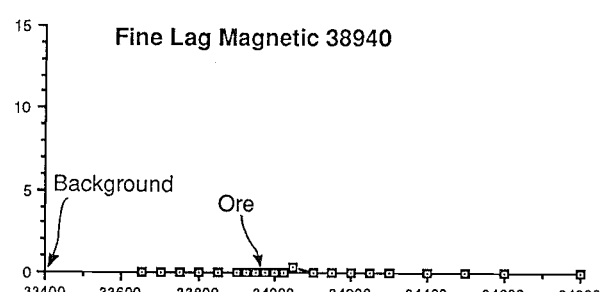
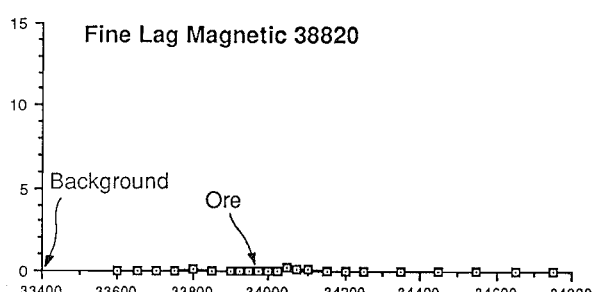
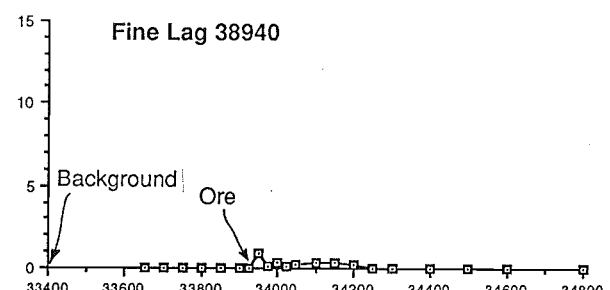
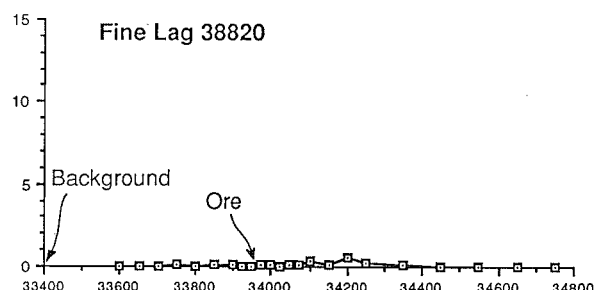
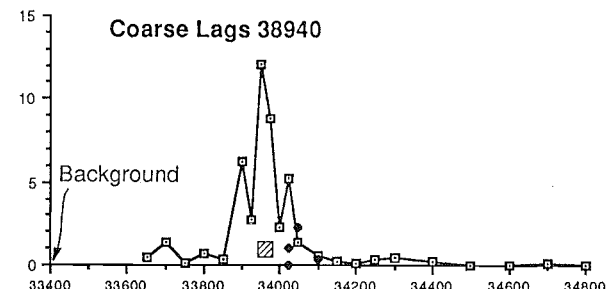
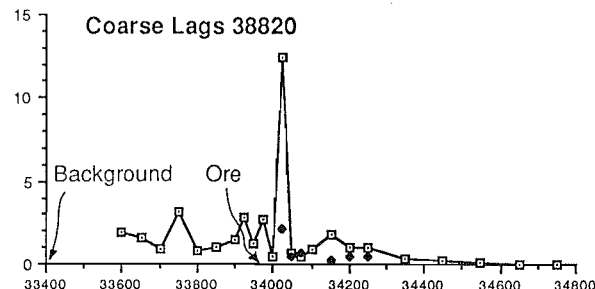


As (ppm)
(0-1000)

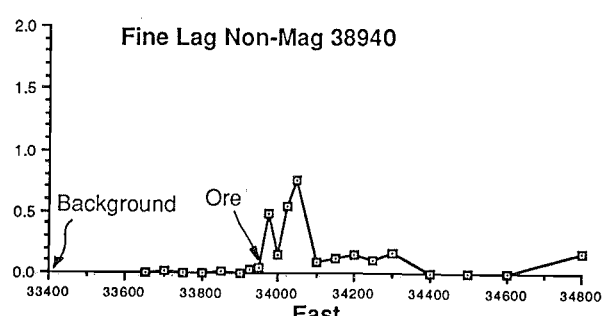
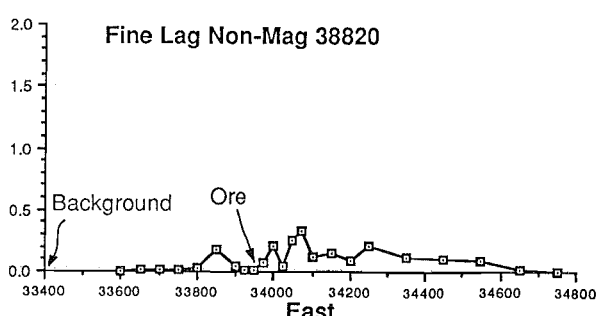
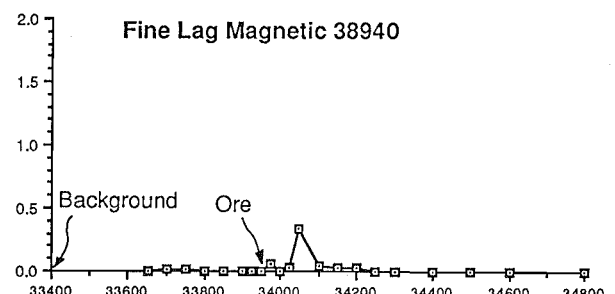
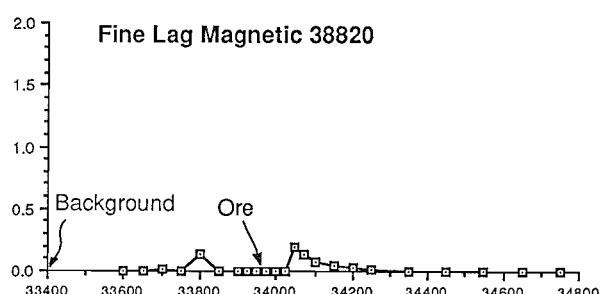
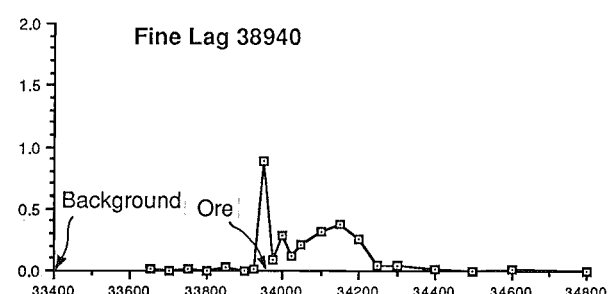
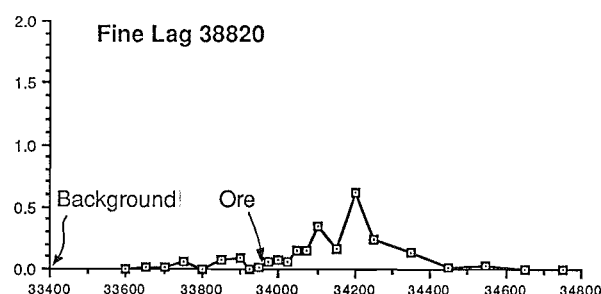
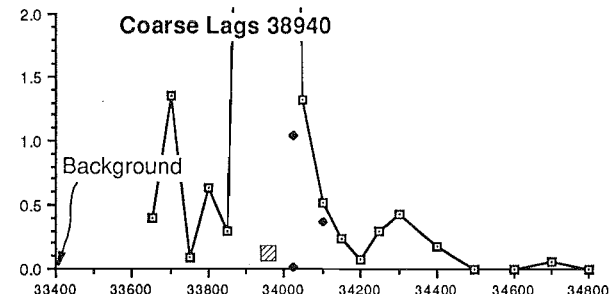
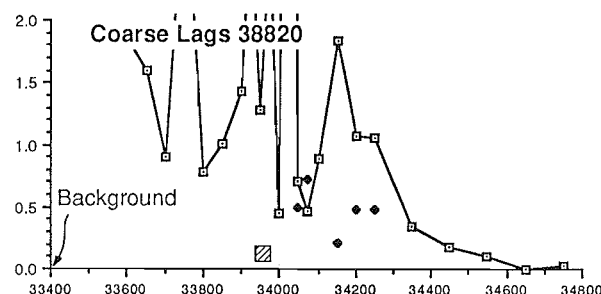




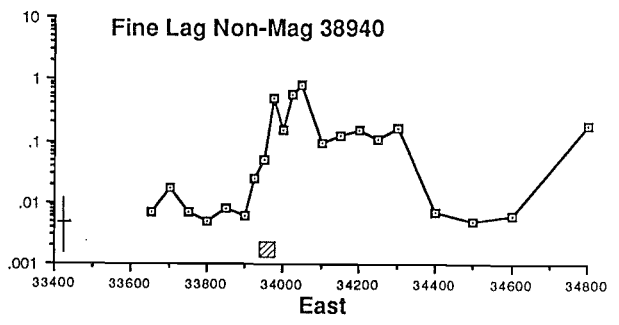
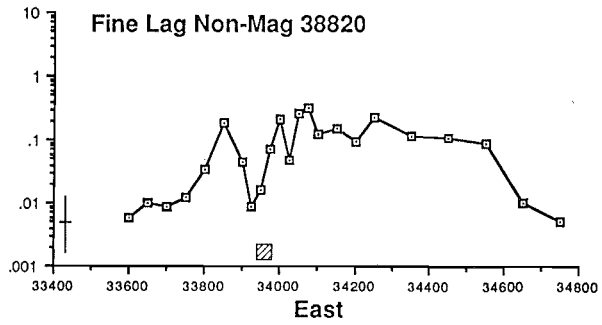
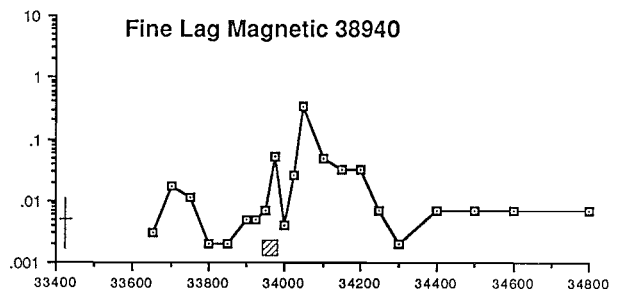
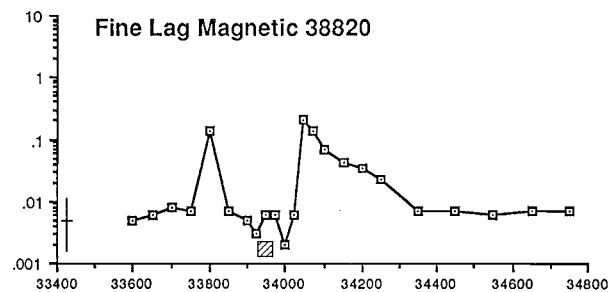
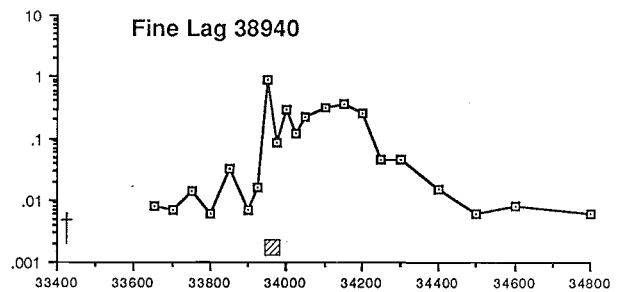
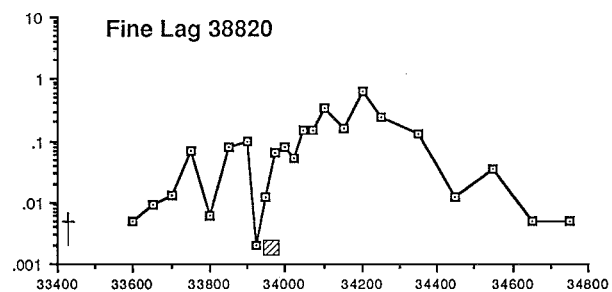
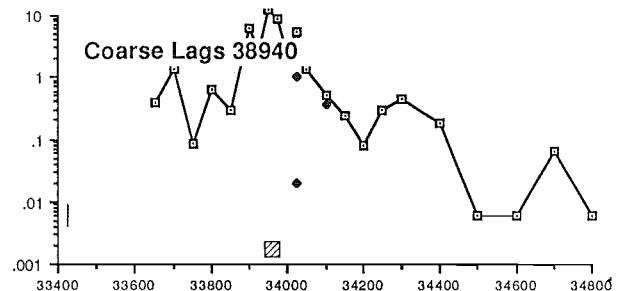
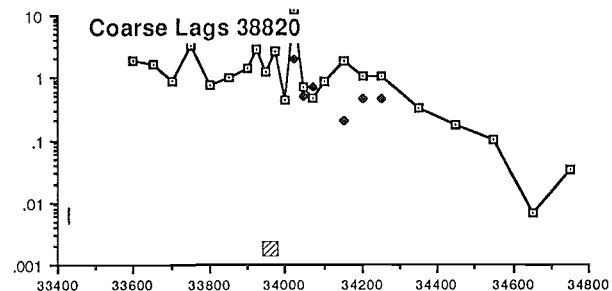
Au (ppm)
(0-15)



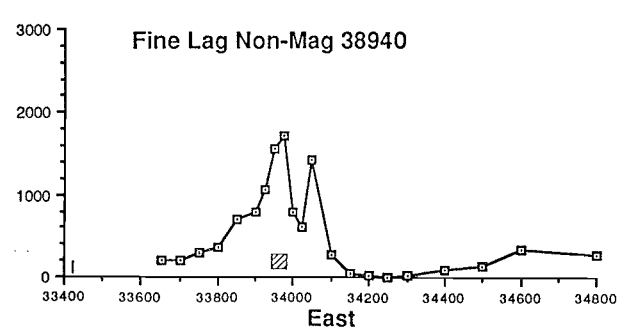
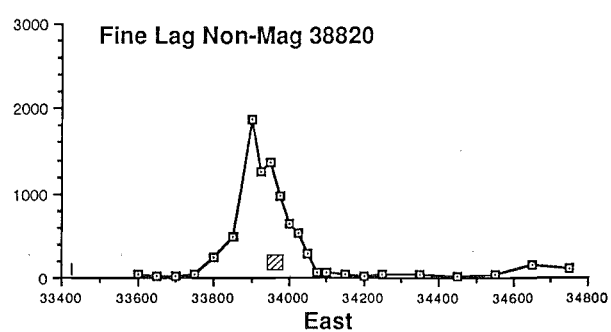
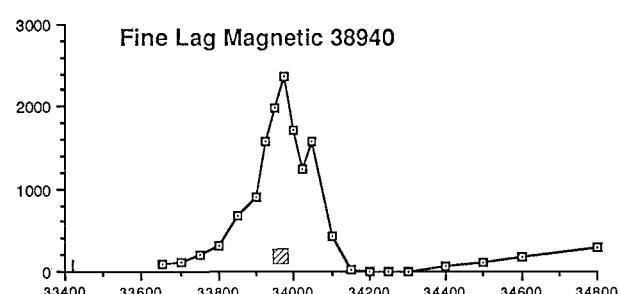
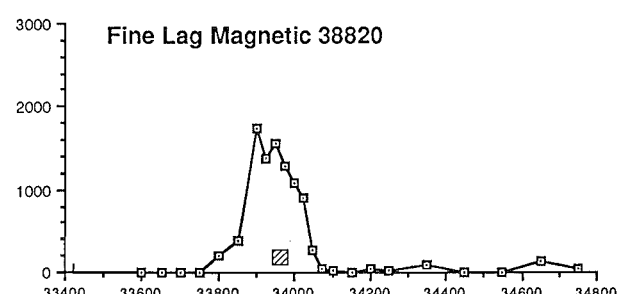
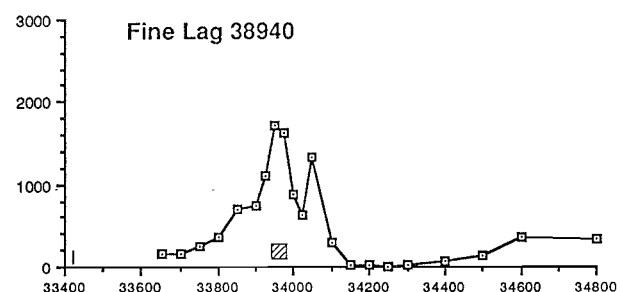
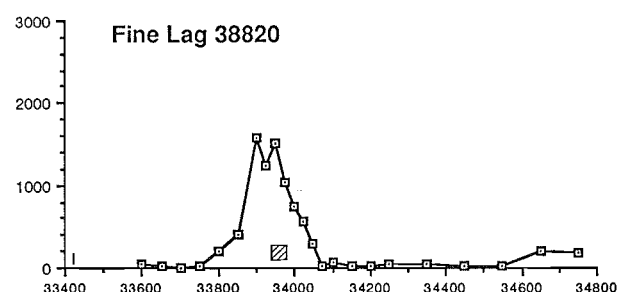
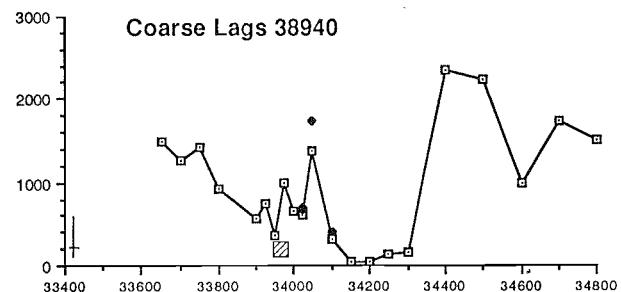
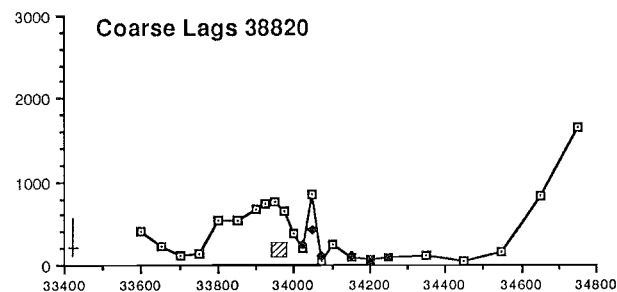
Au (ppm)
(0-2)

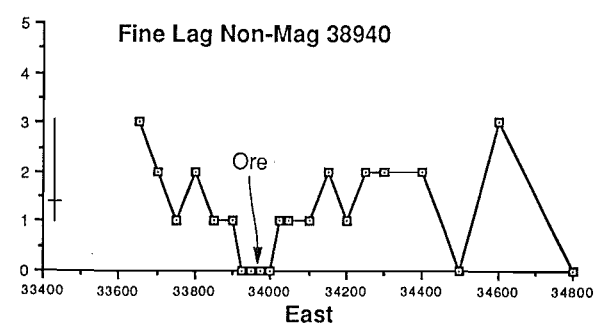
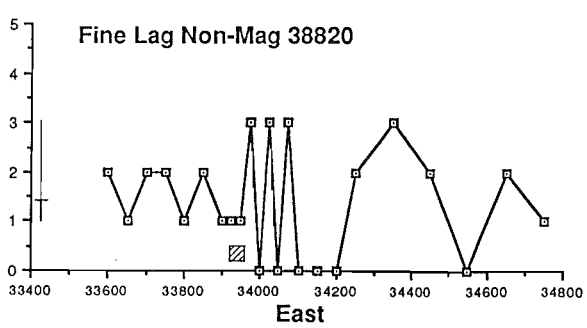
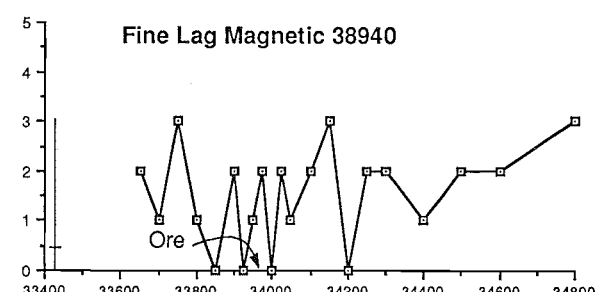
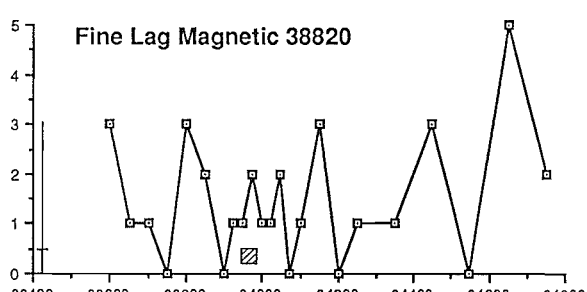
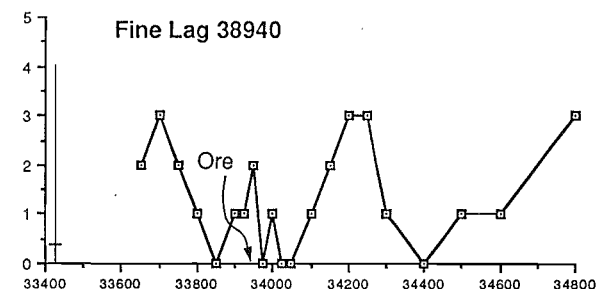
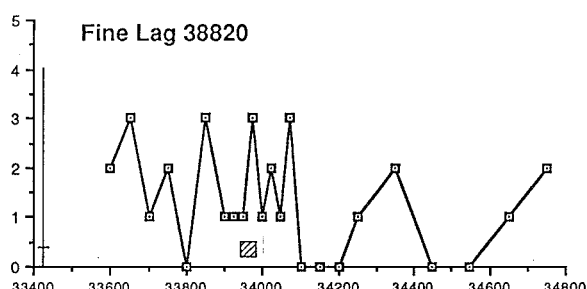
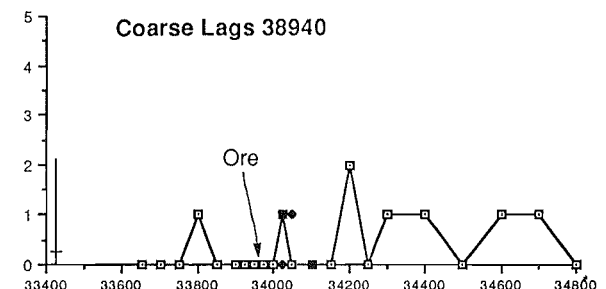
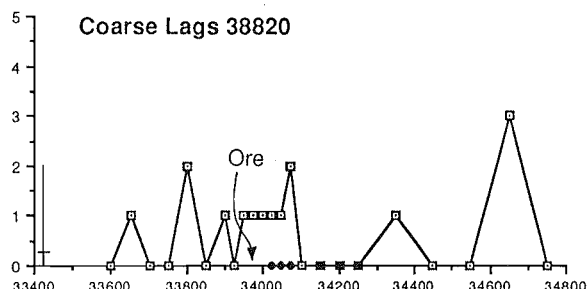


Au (ppm)
(Log)

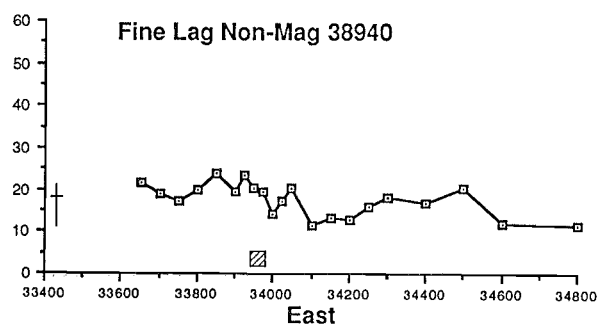
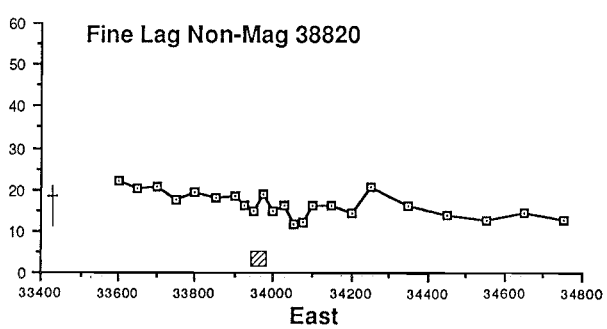
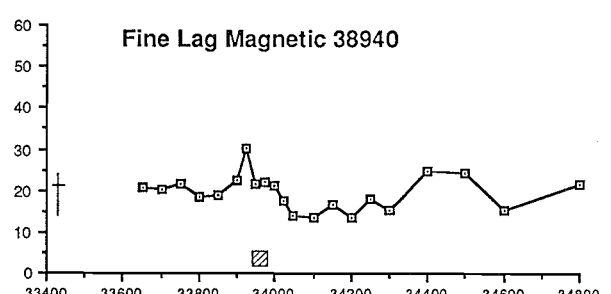
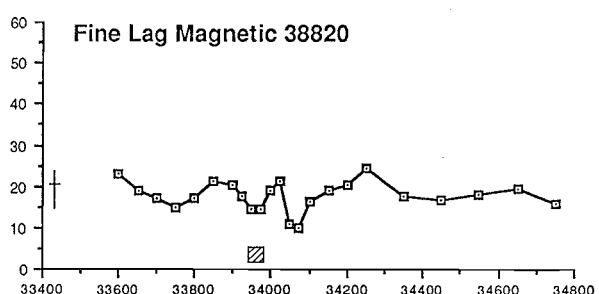
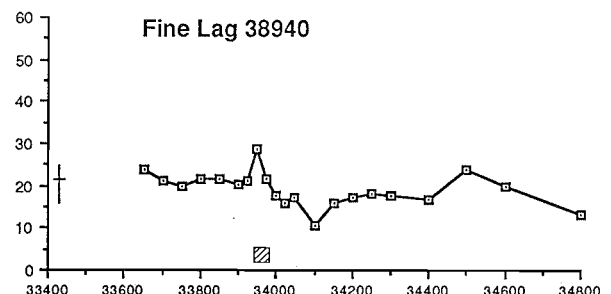
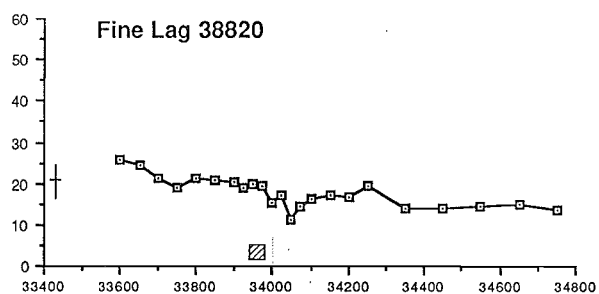
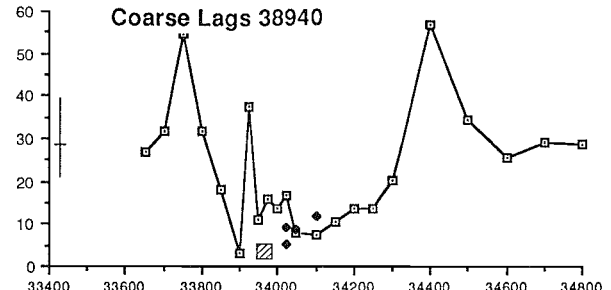
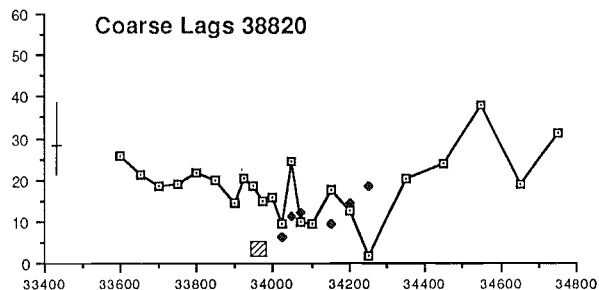


Ba (ppm)

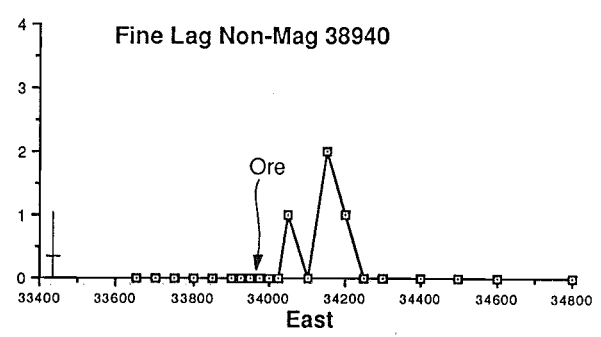
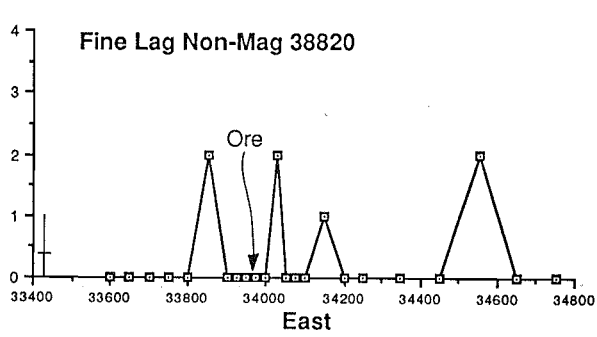
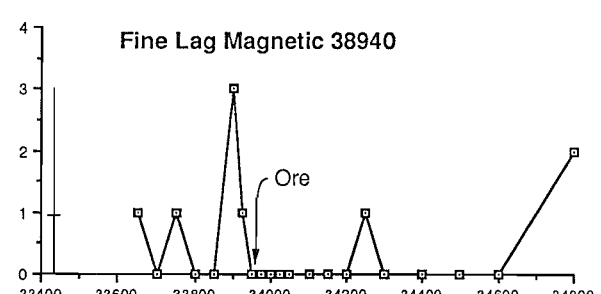
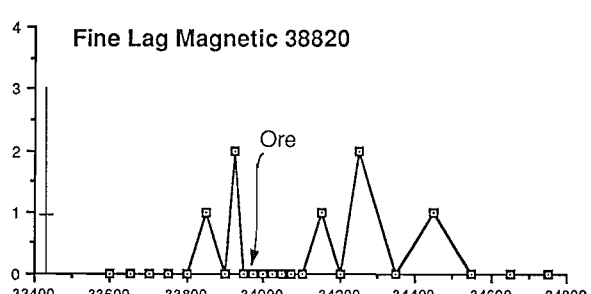
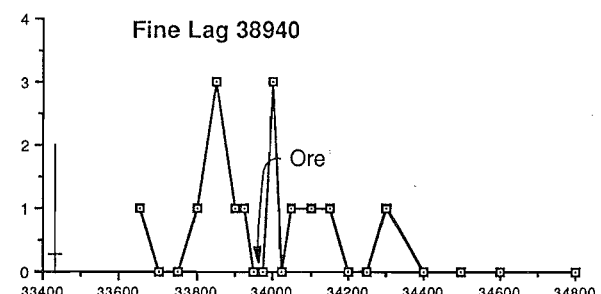
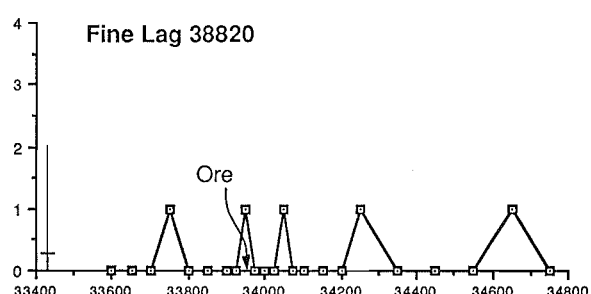
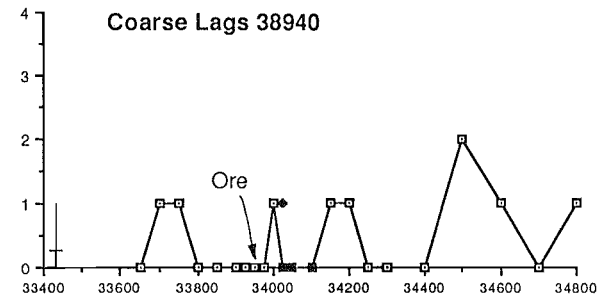
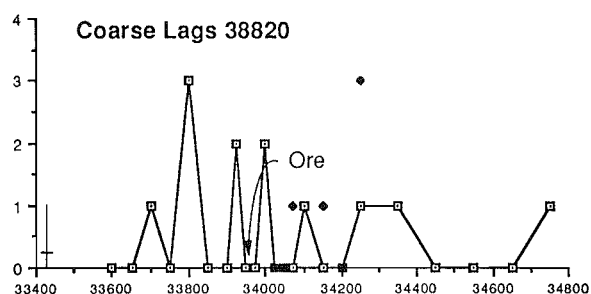




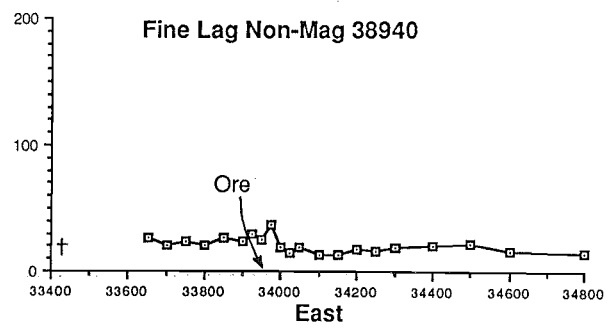
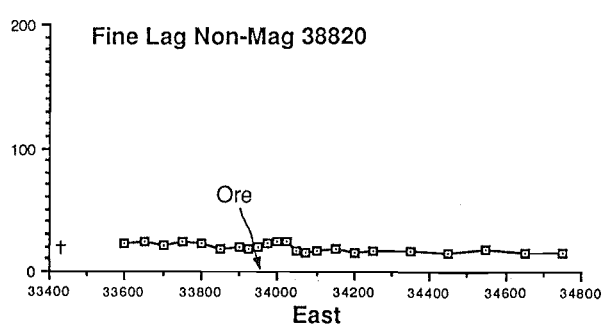
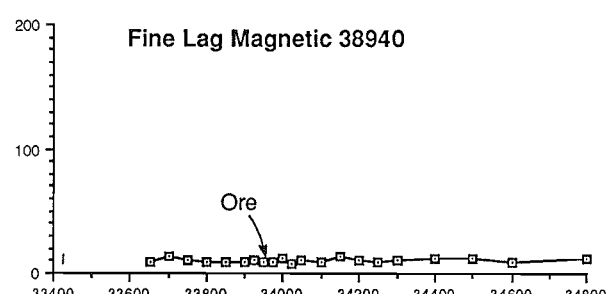
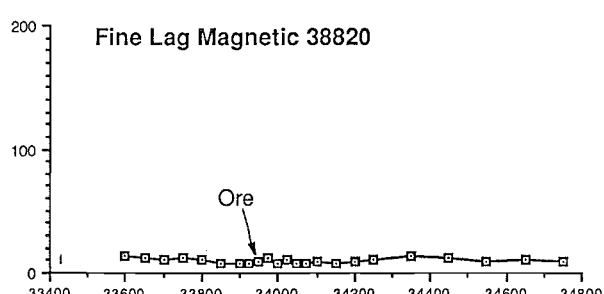
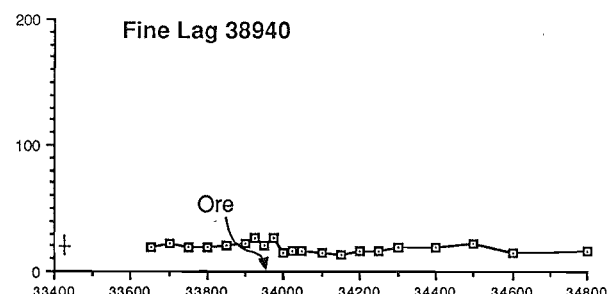
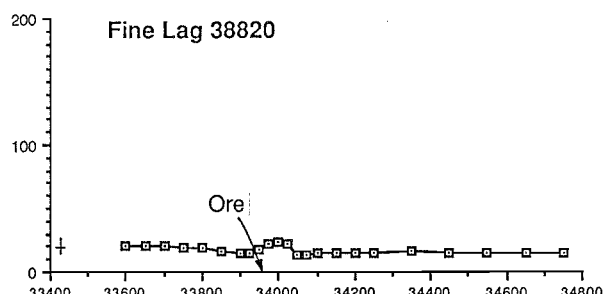
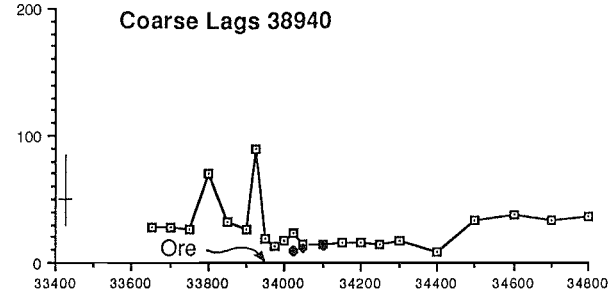
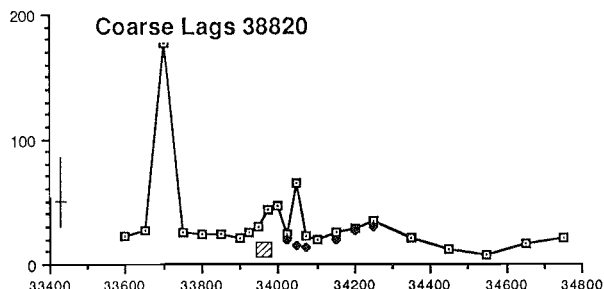
Ce (ppm)

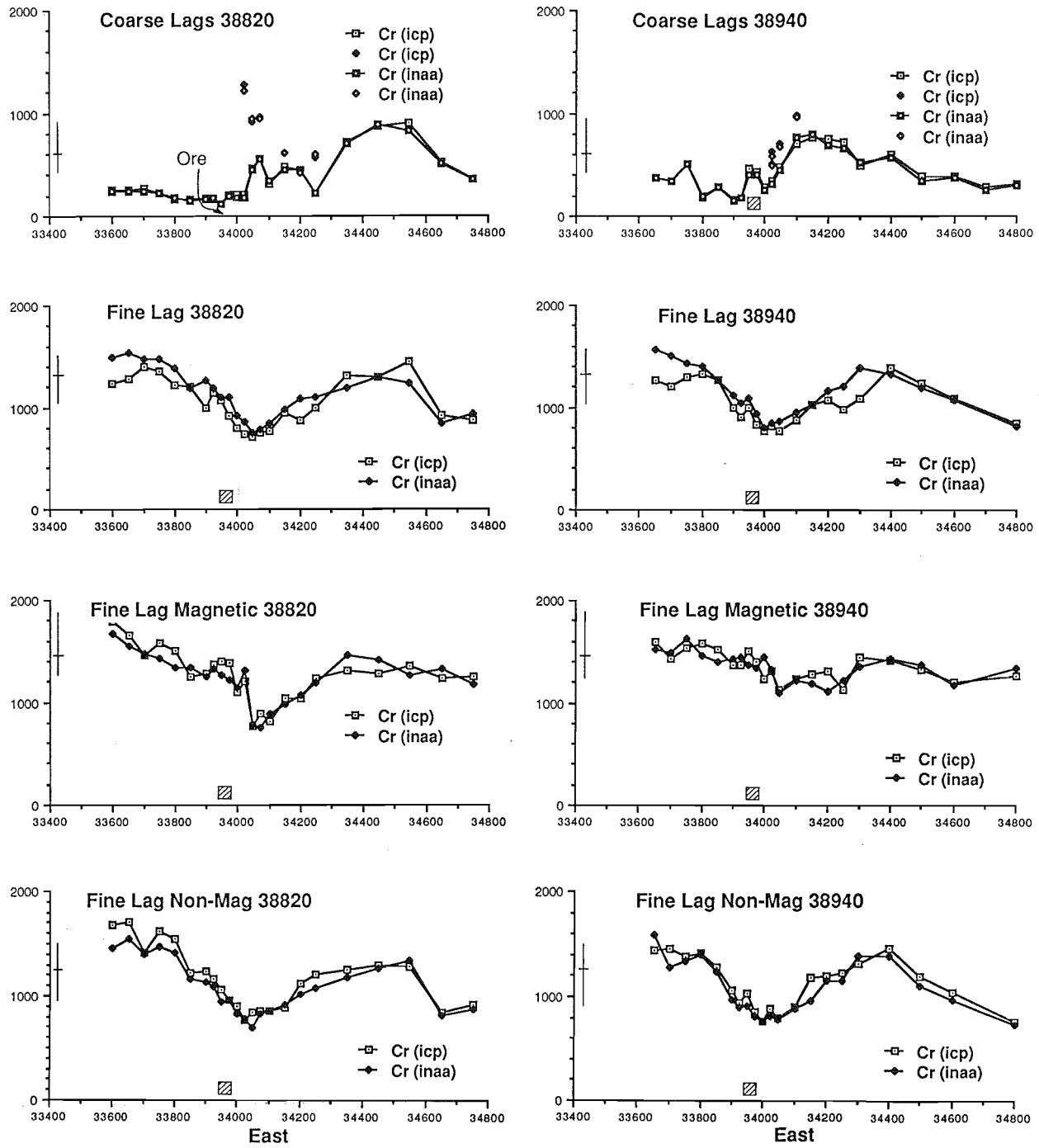


Cd (ppm)

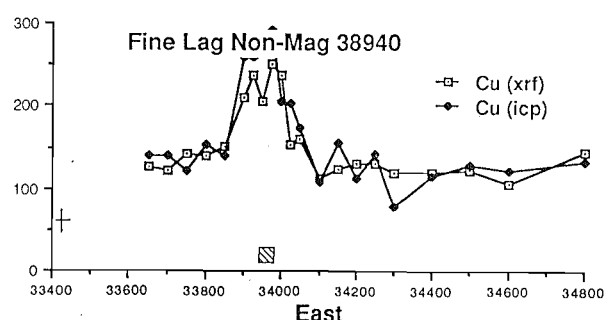
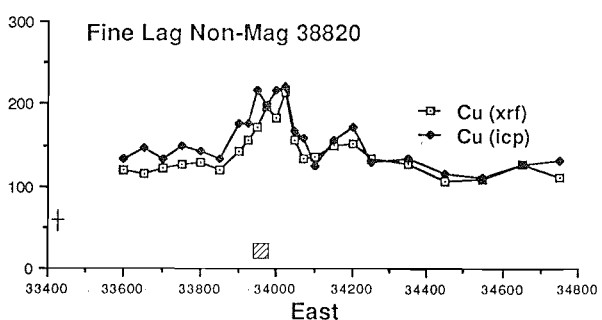
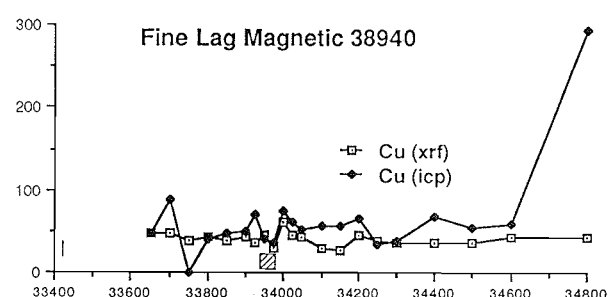
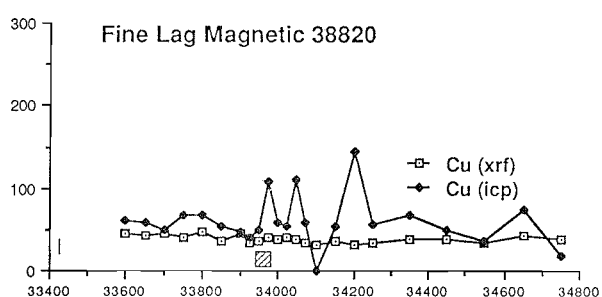
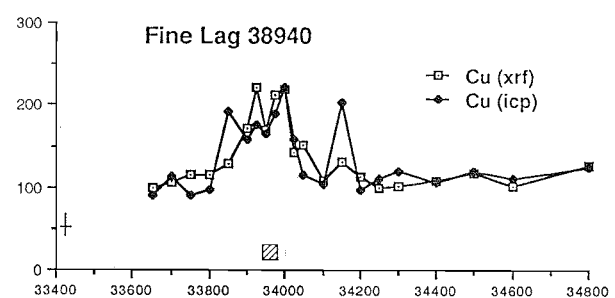
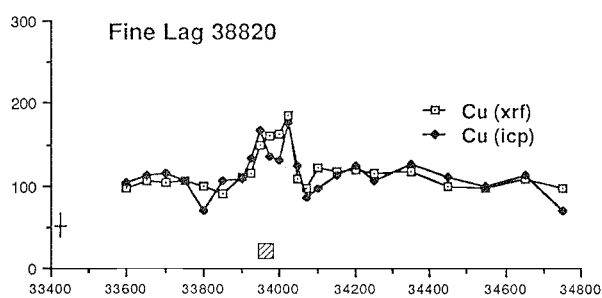
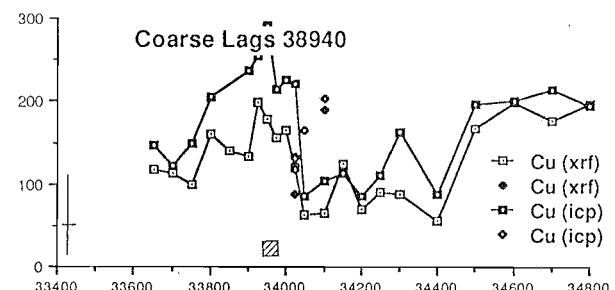
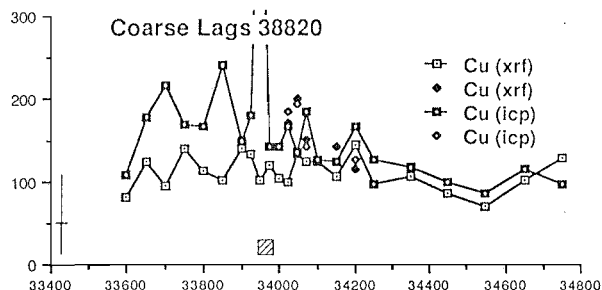


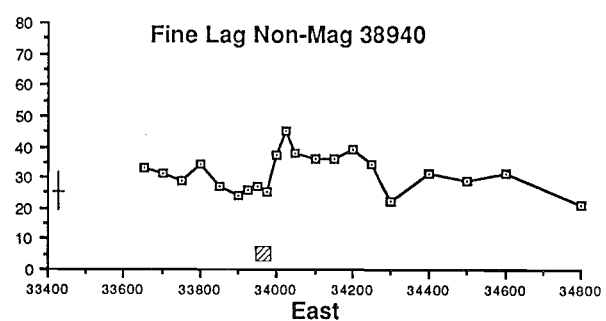
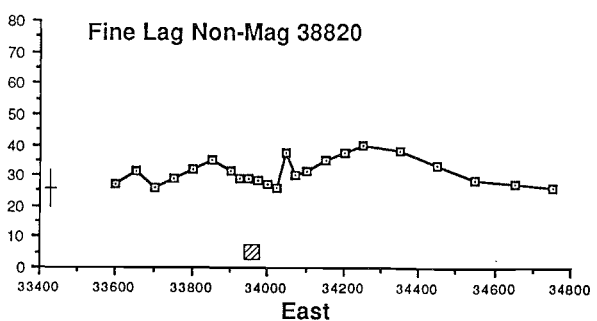
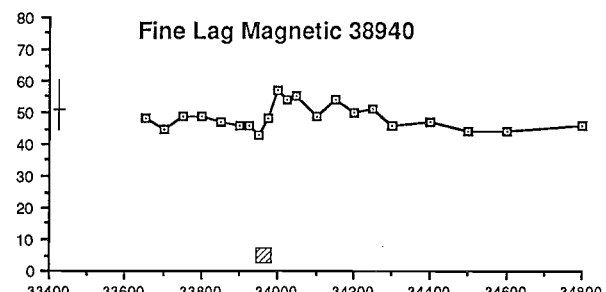
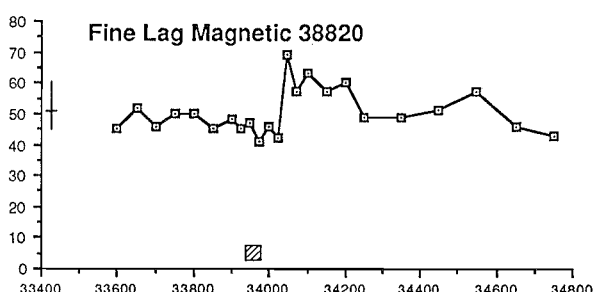
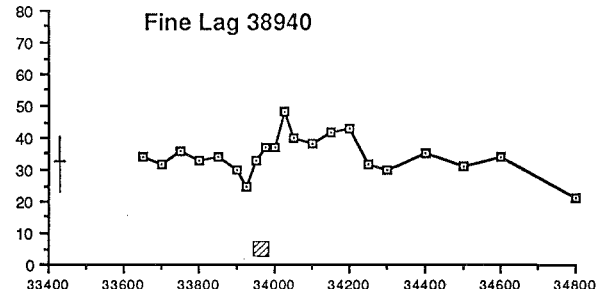
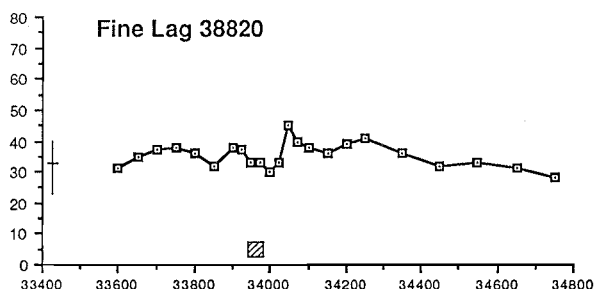
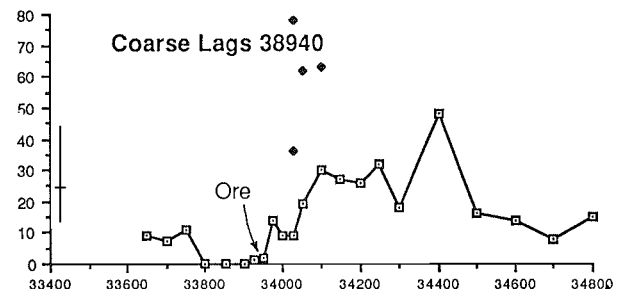
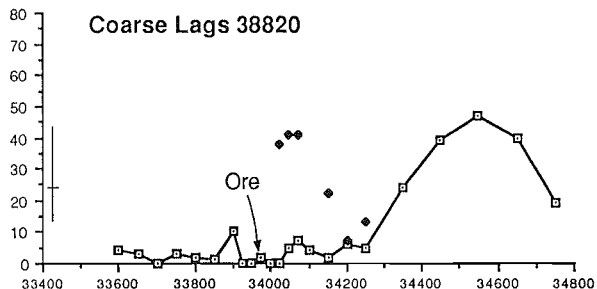
Co (ppm)

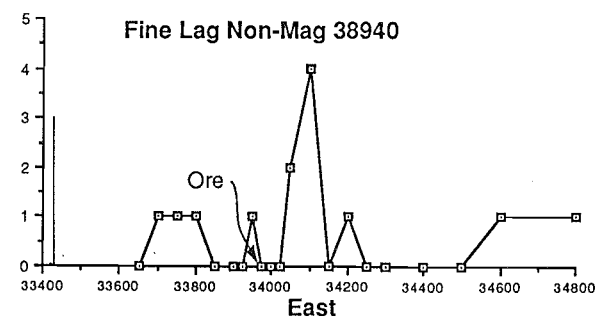
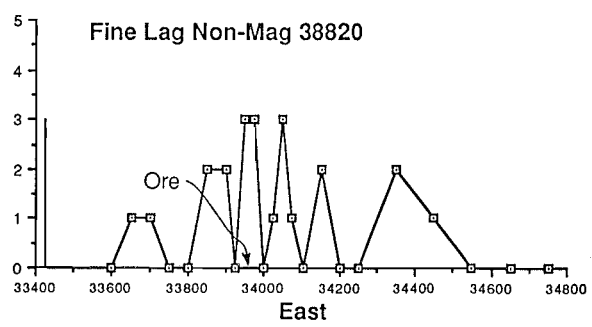
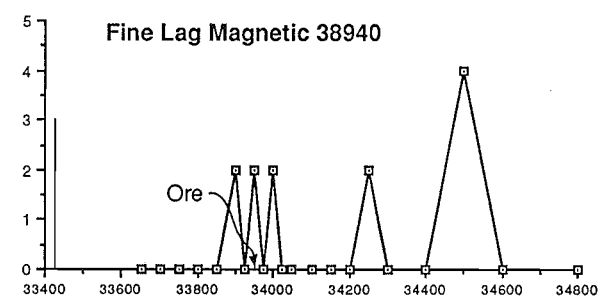
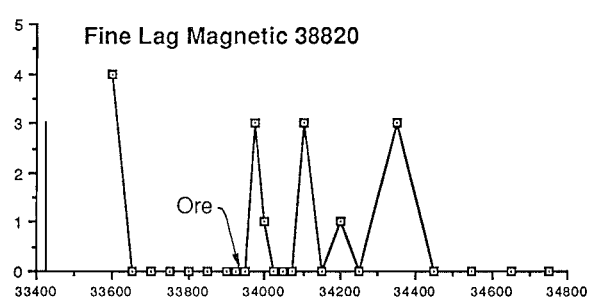
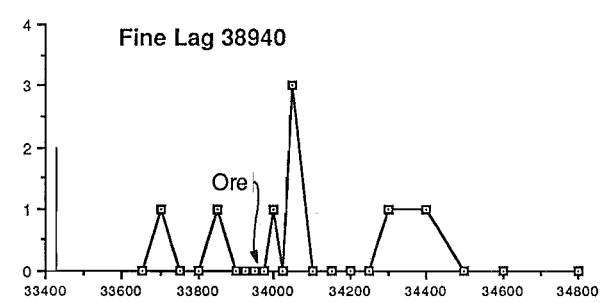
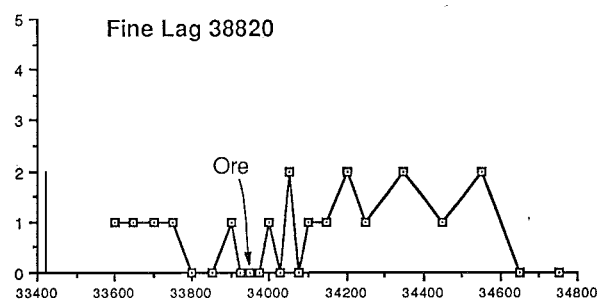
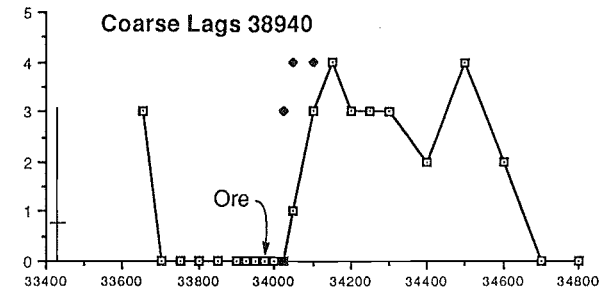
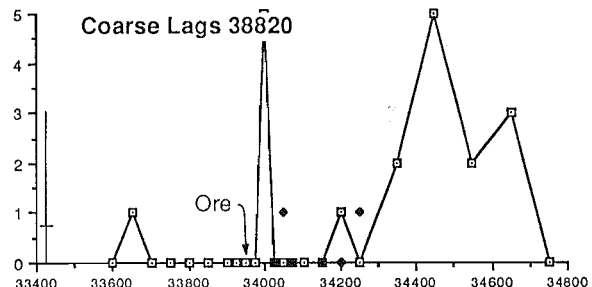




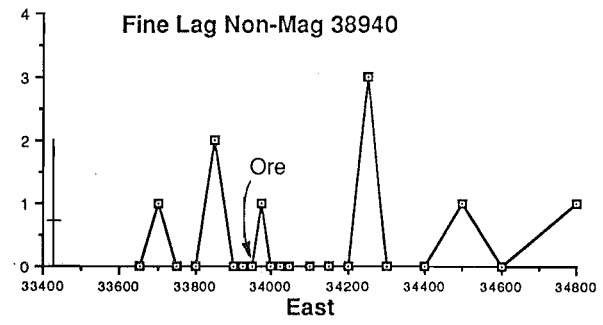
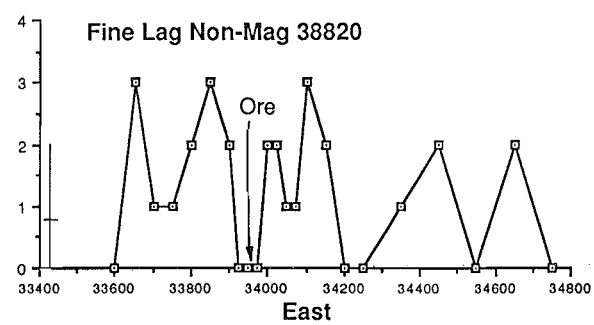
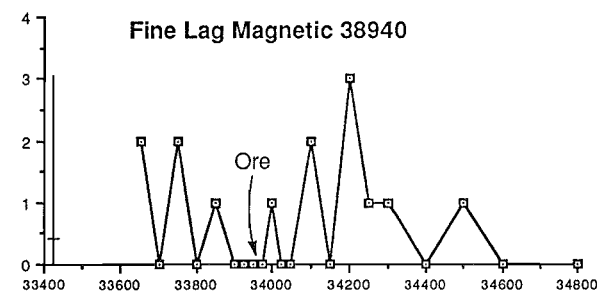
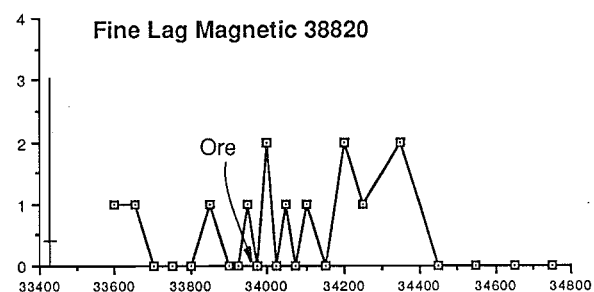
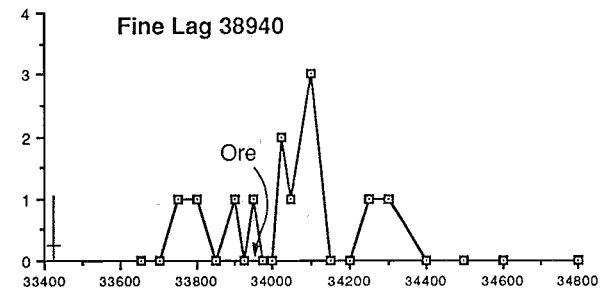
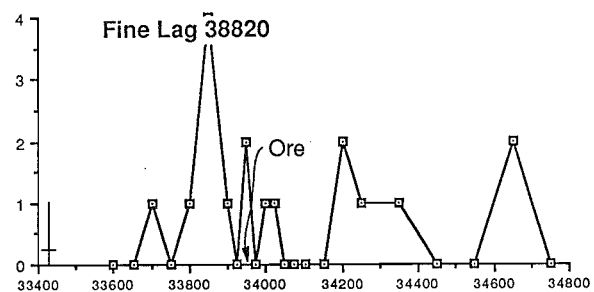
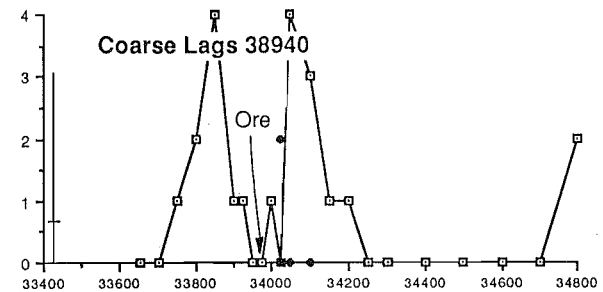
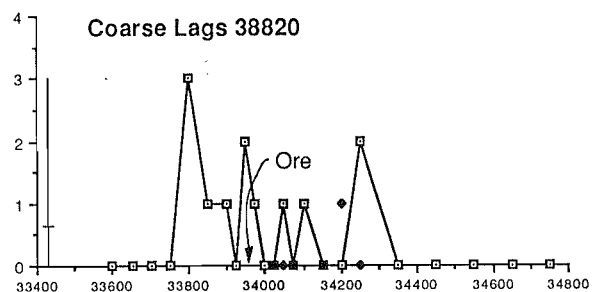
Cu (ppm)

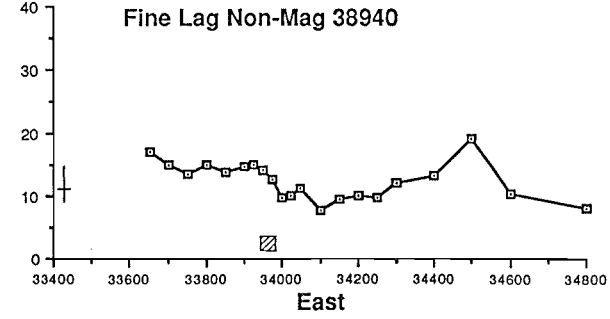
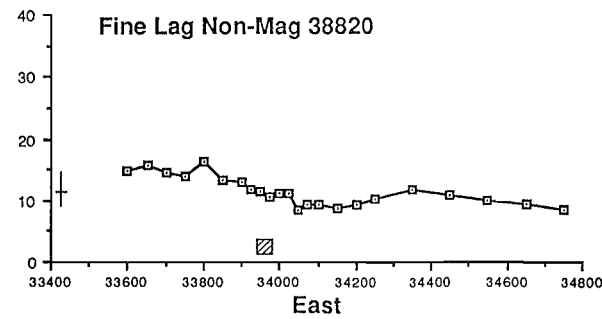
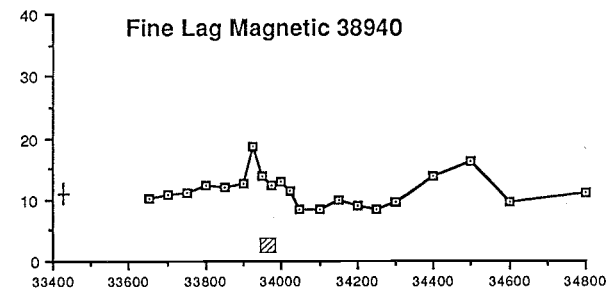
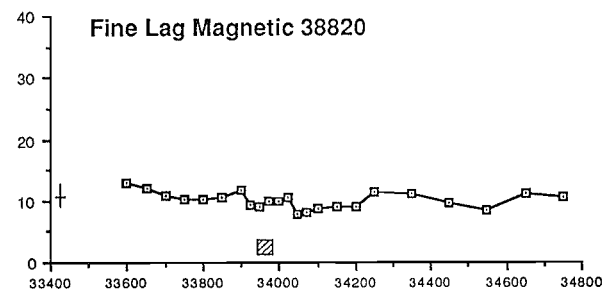
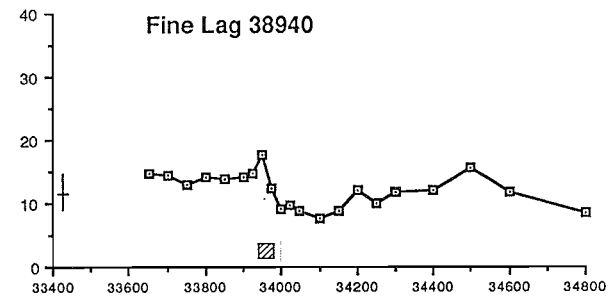
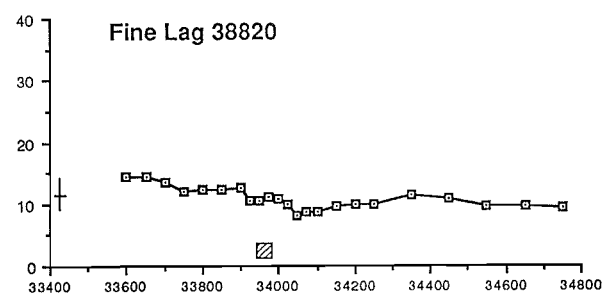
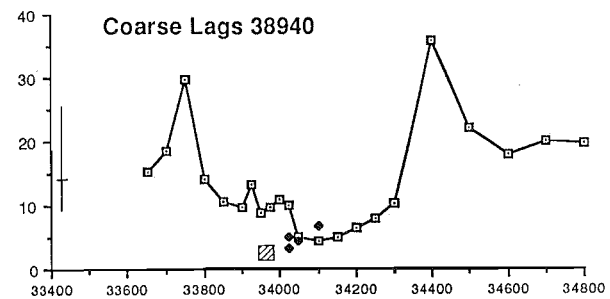
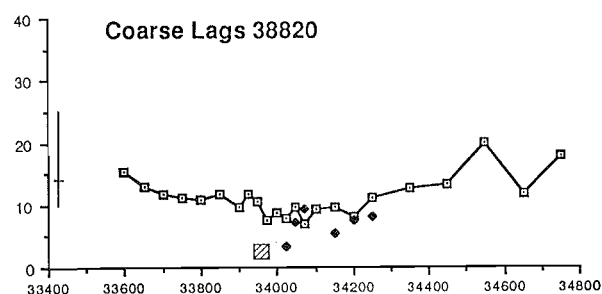




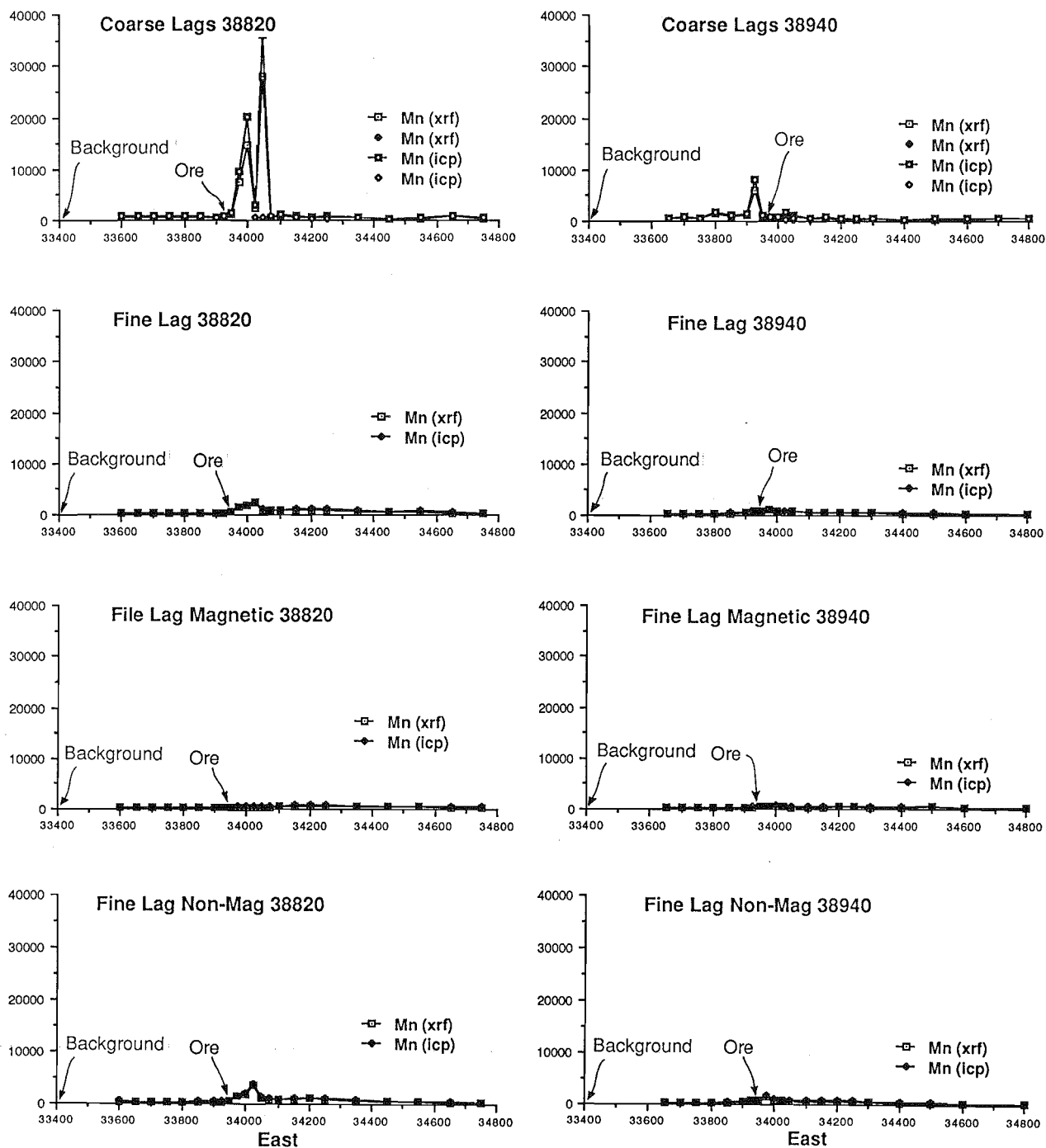


In (ppm)

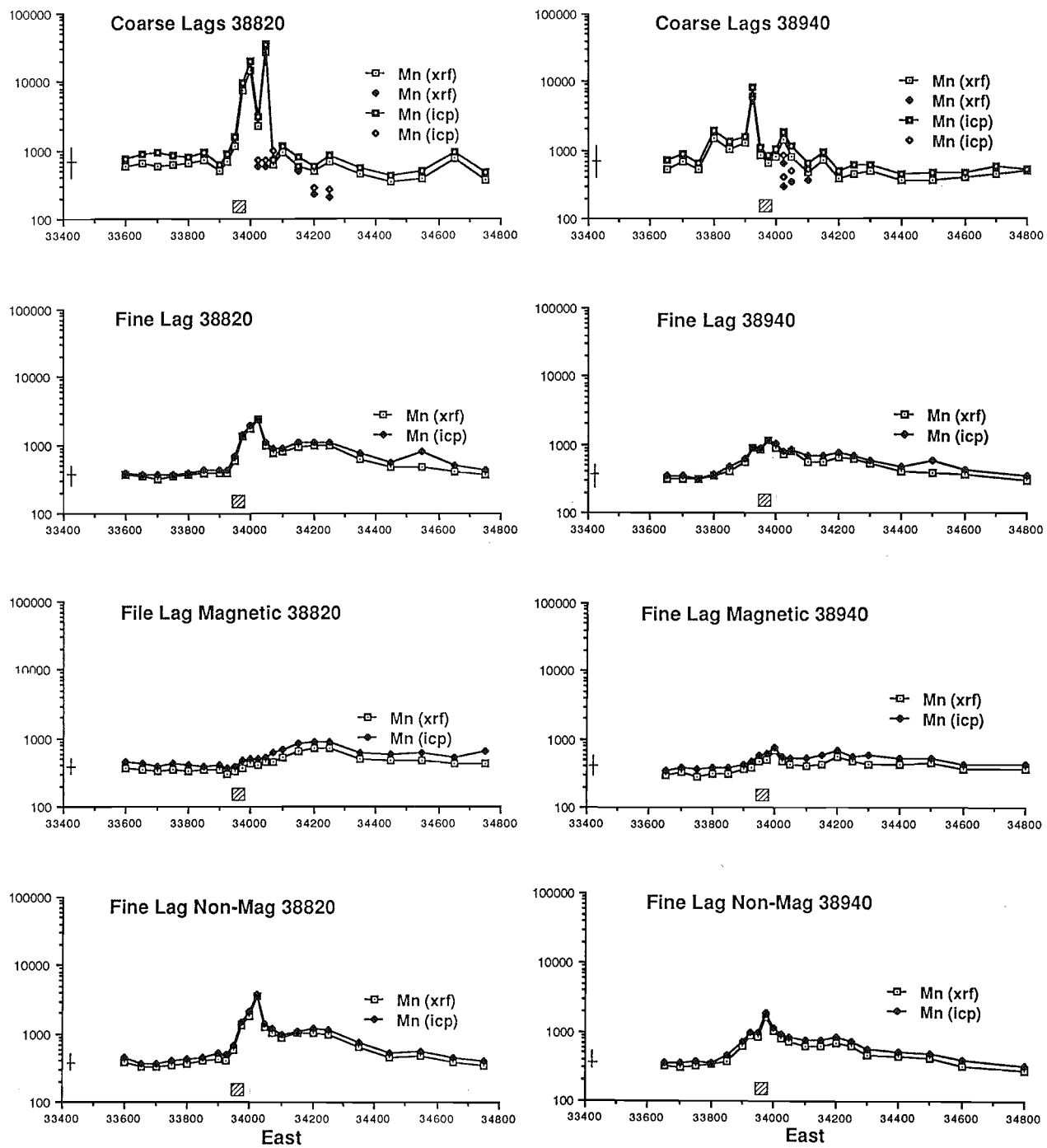




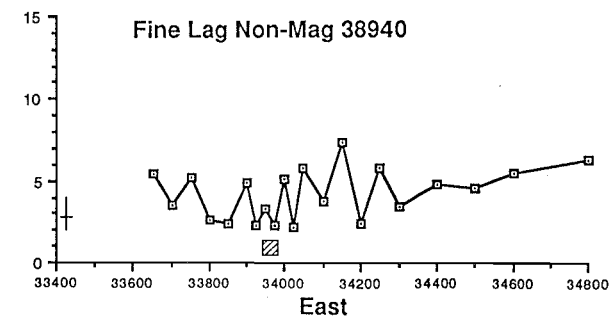
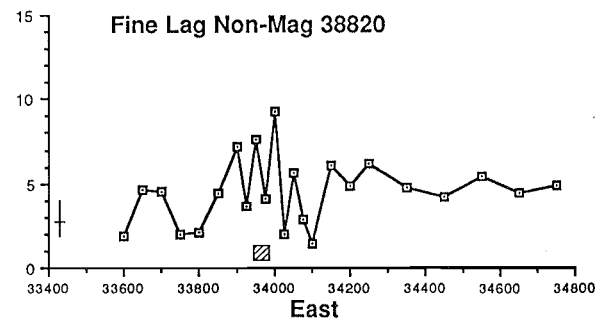
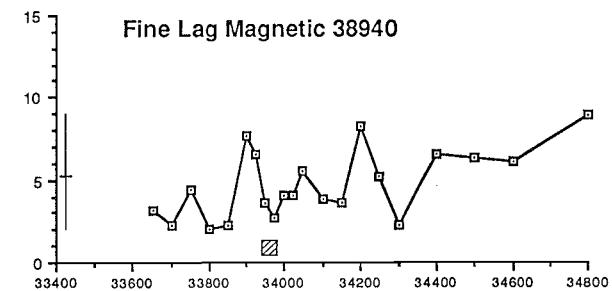
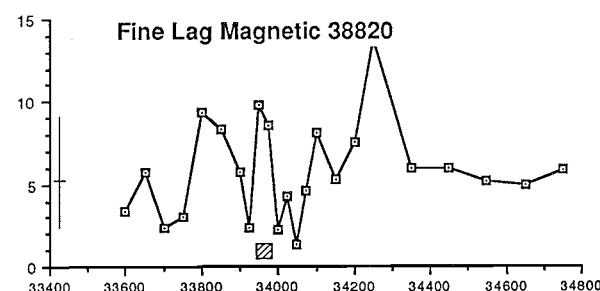
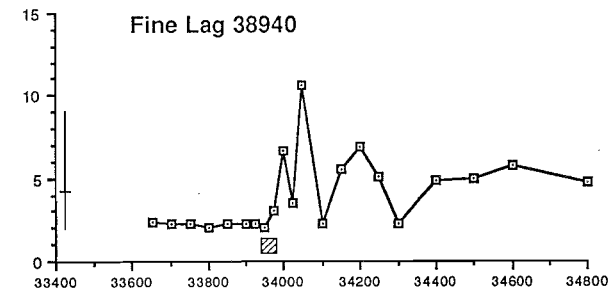
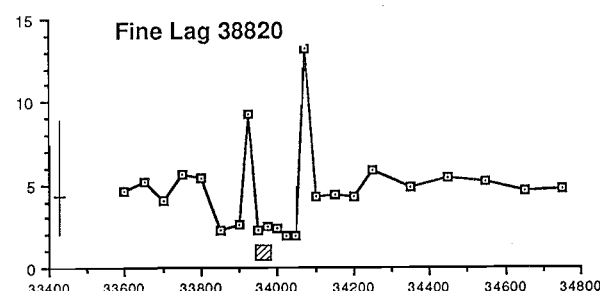
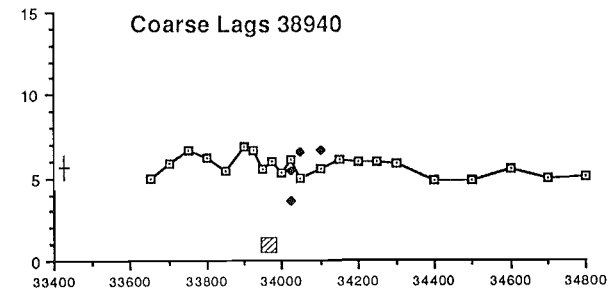
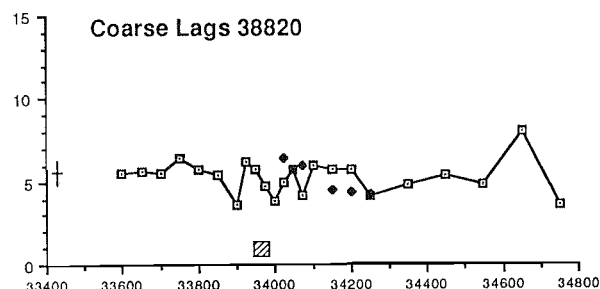
Mn (ppm)
(0-40000)

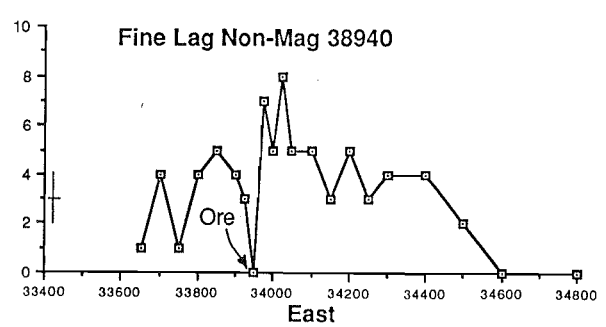
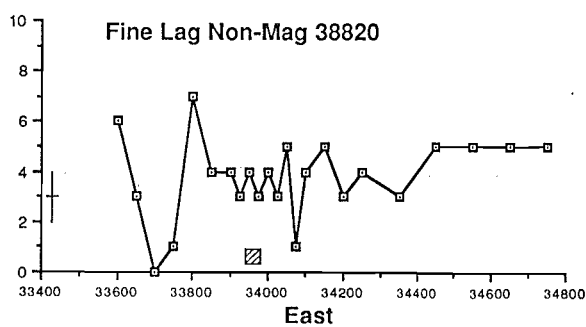
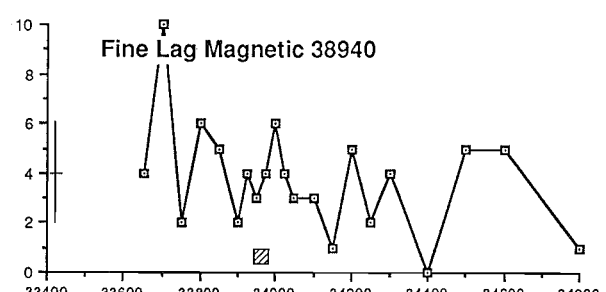
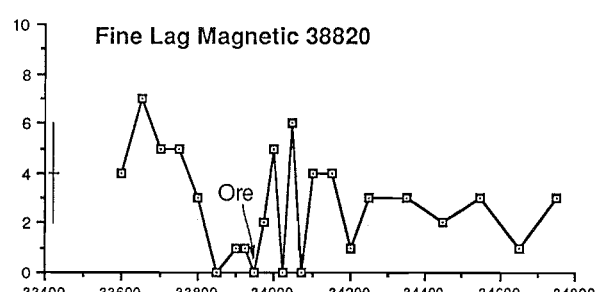
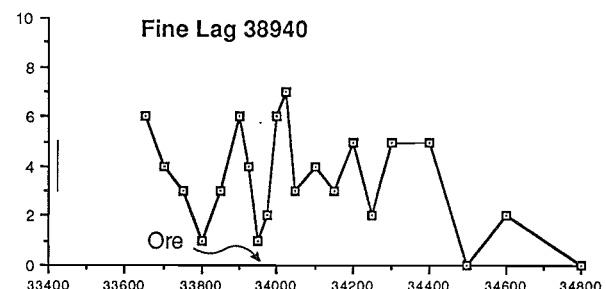
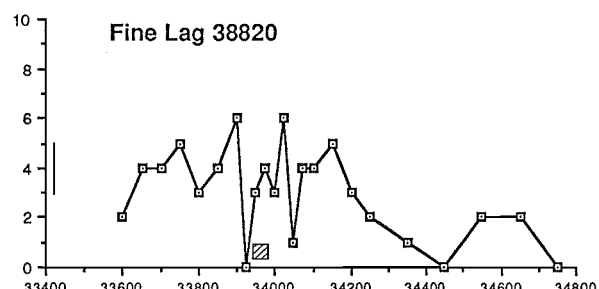
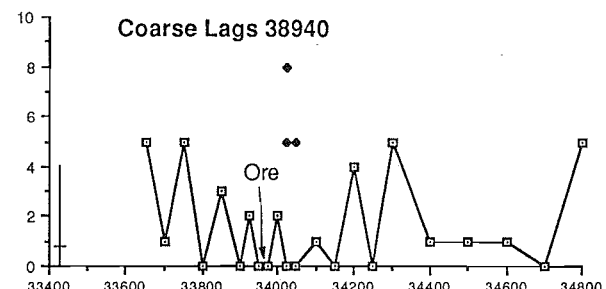
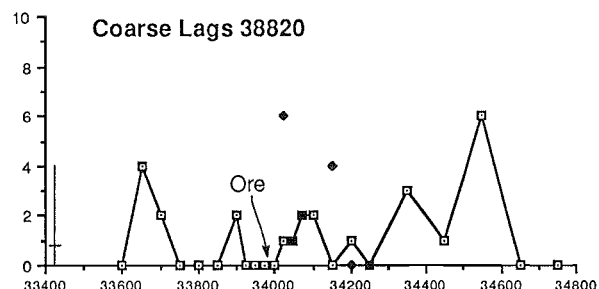


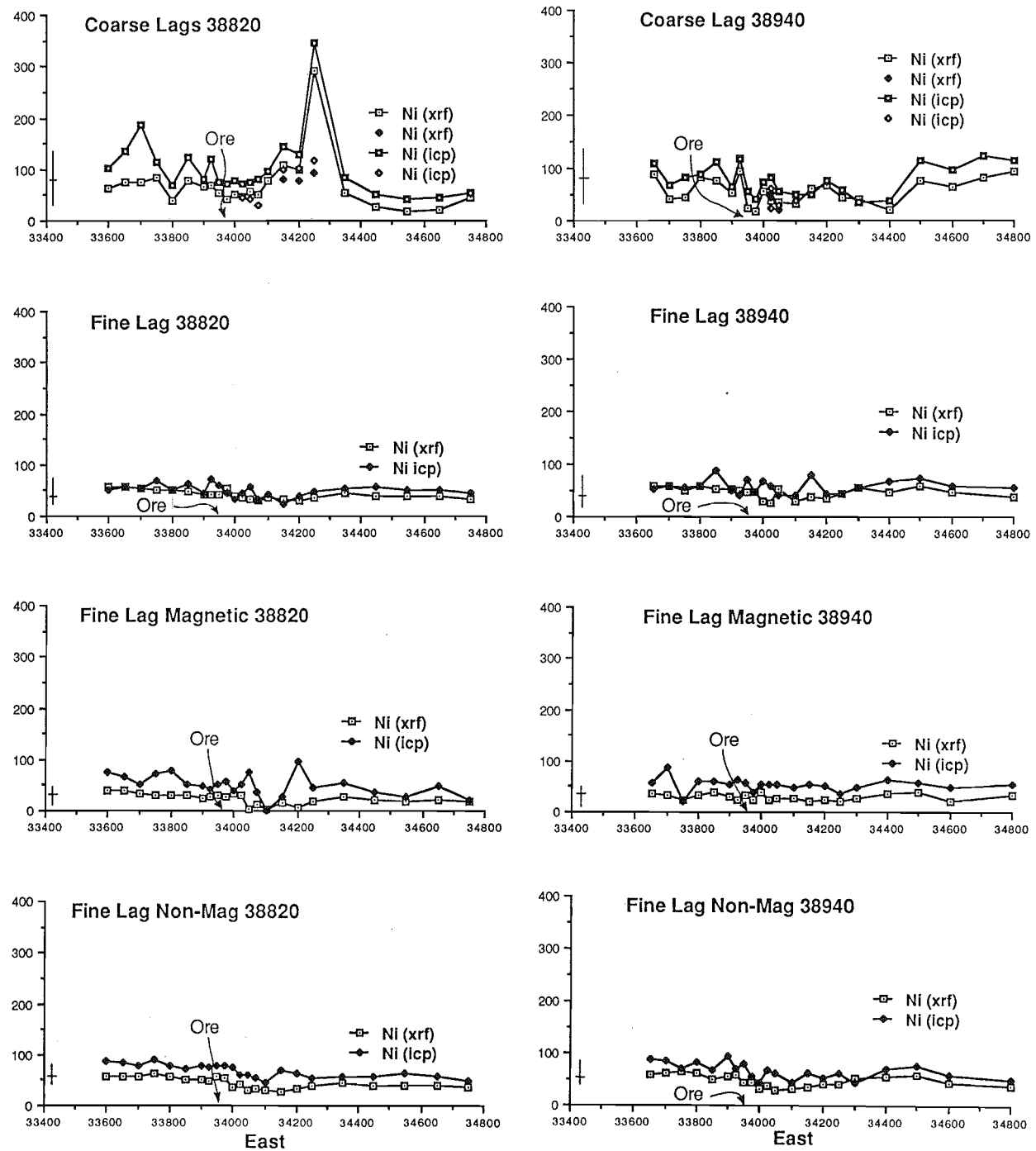
Mn (ppm)
(Log)



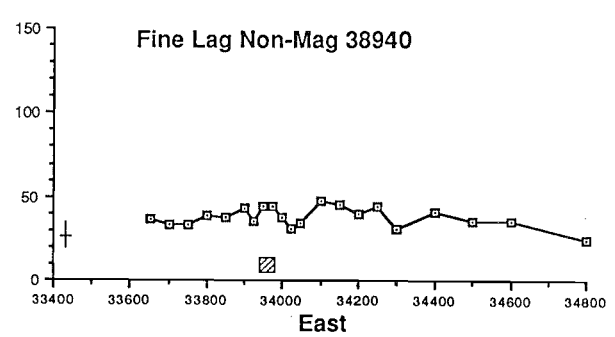
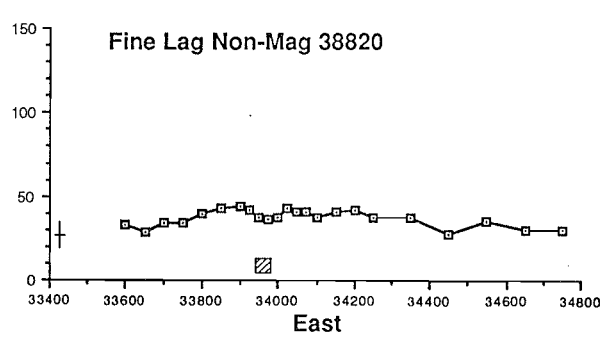
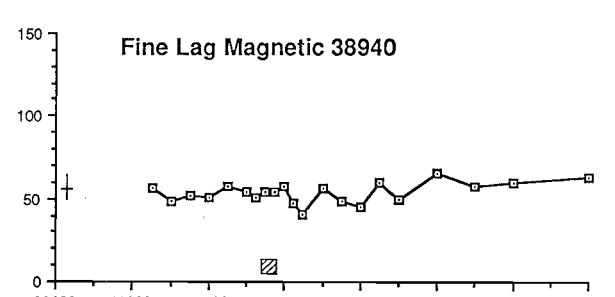
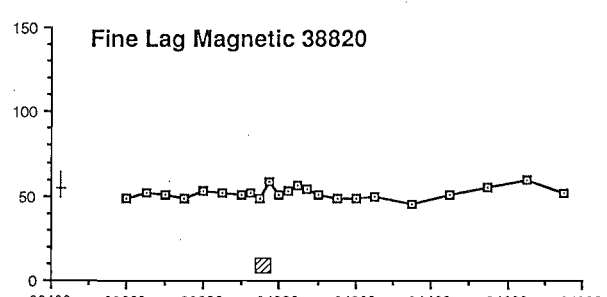
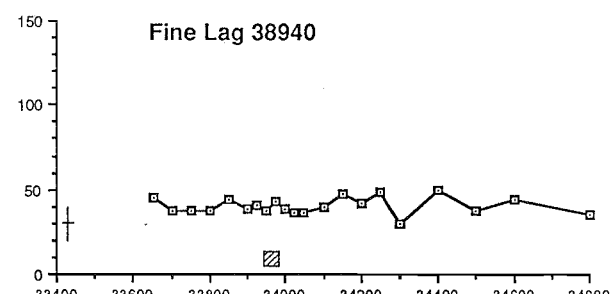
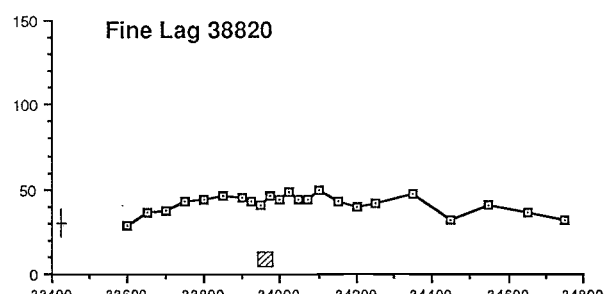
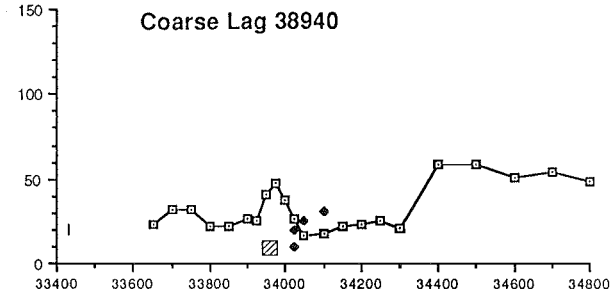
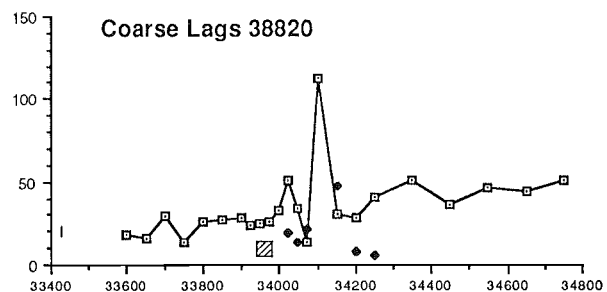
Mo (ppm)

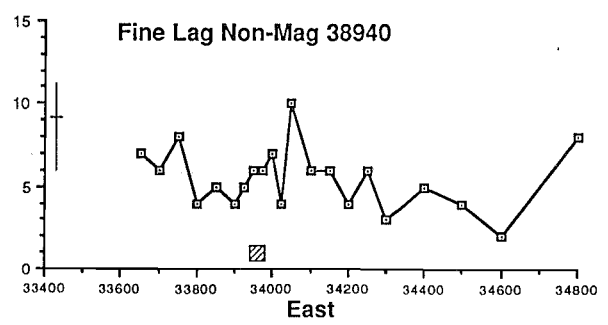
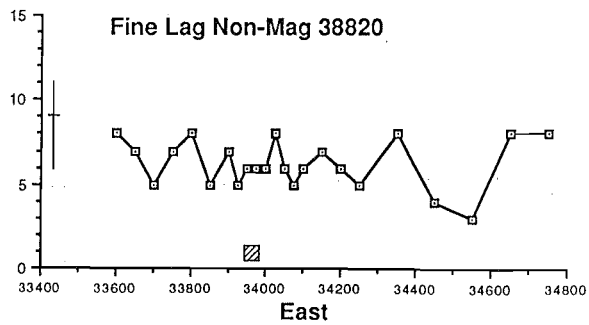
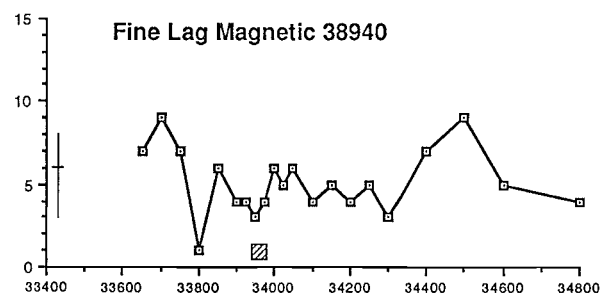
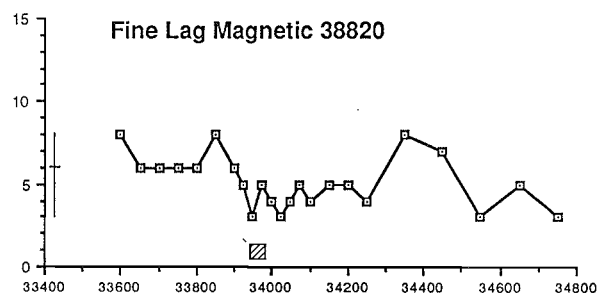
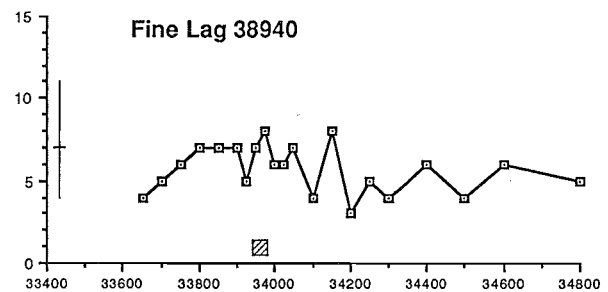
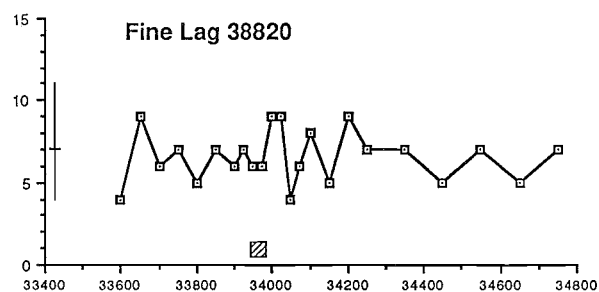
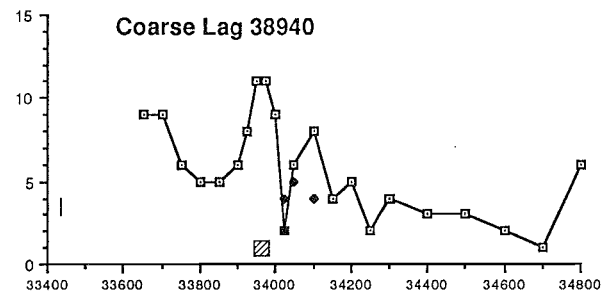
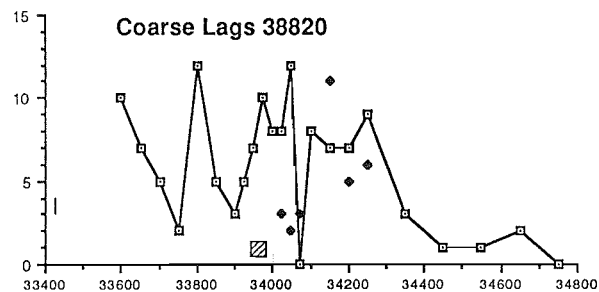




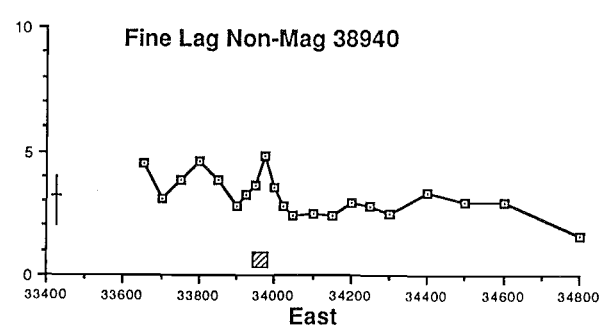
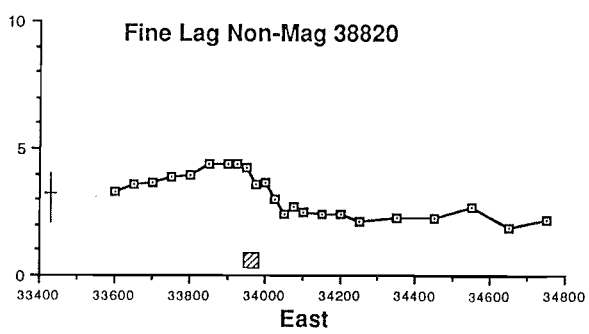
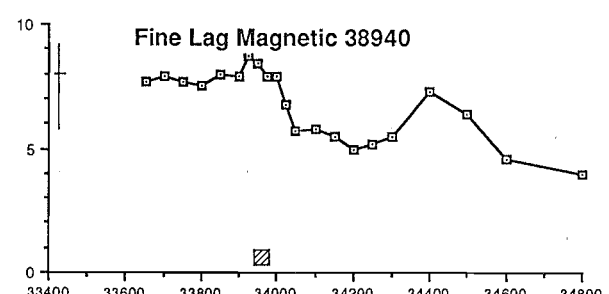
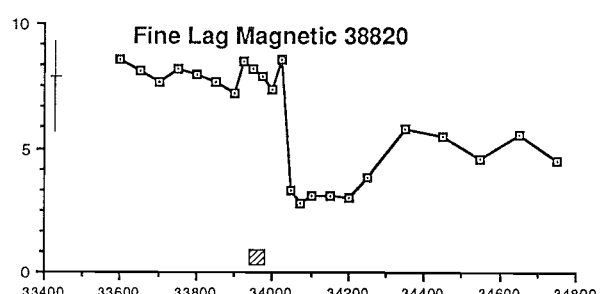
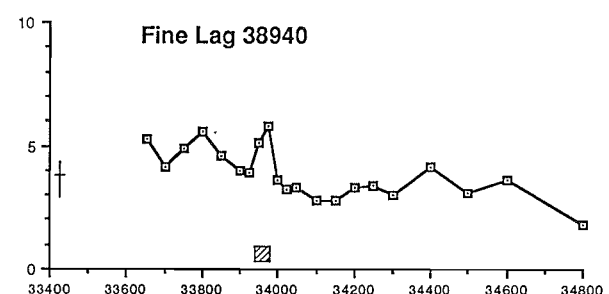
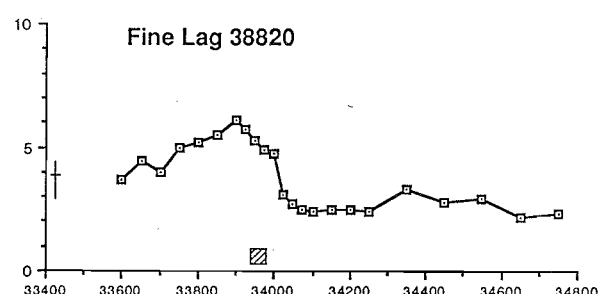
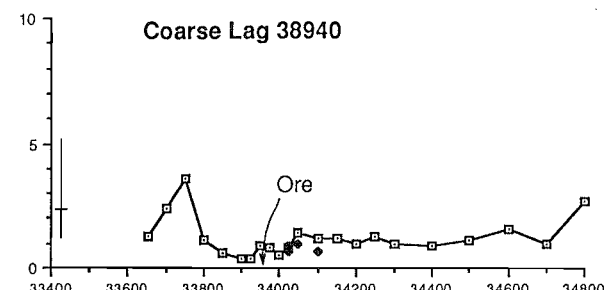
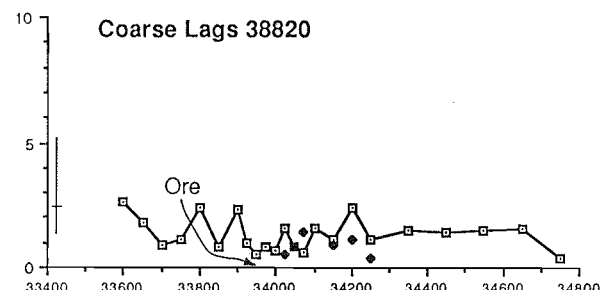


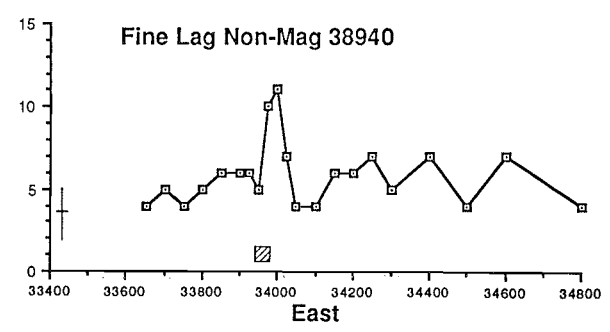
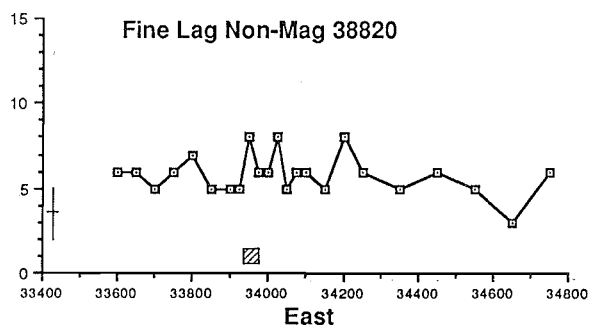
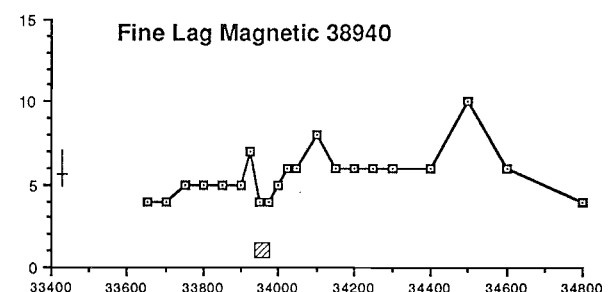
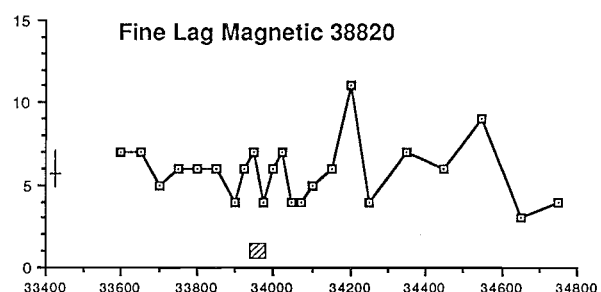
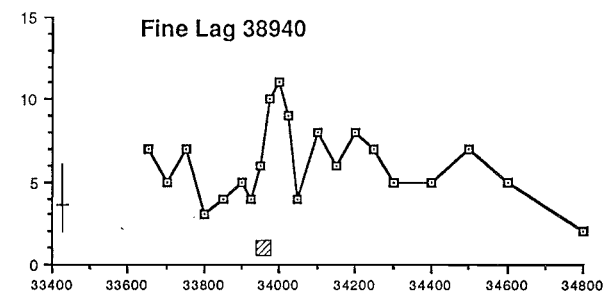
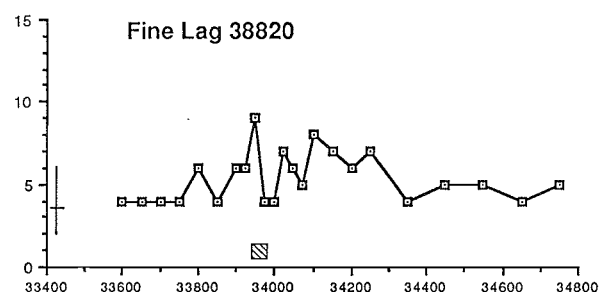
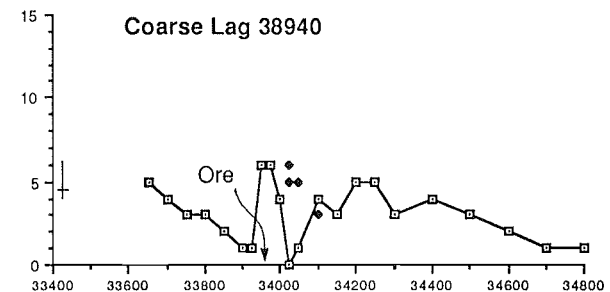
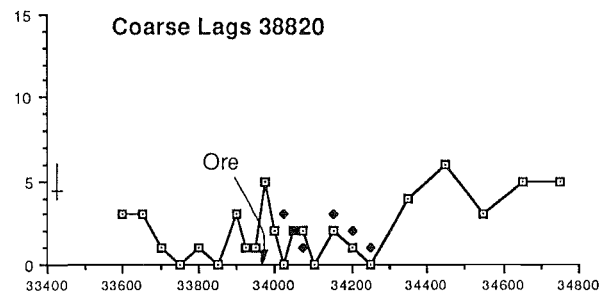
Pb (ppm)

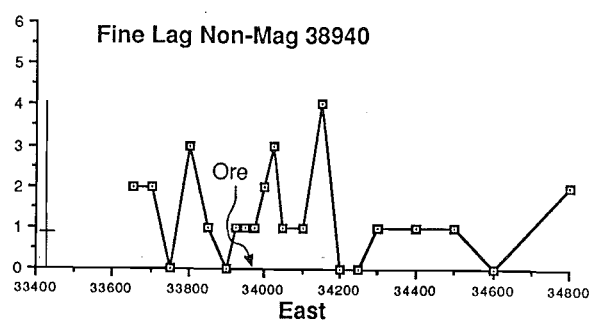
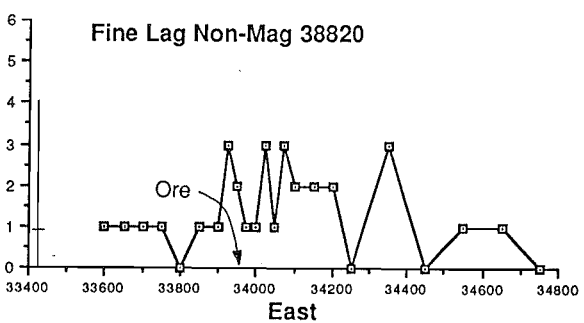
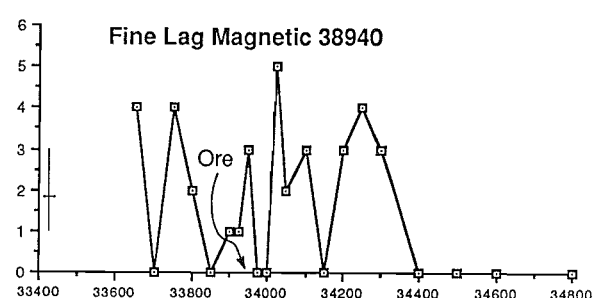
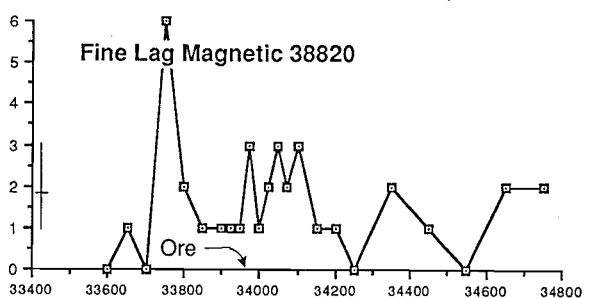
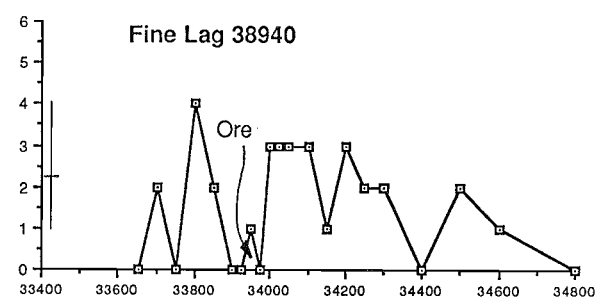
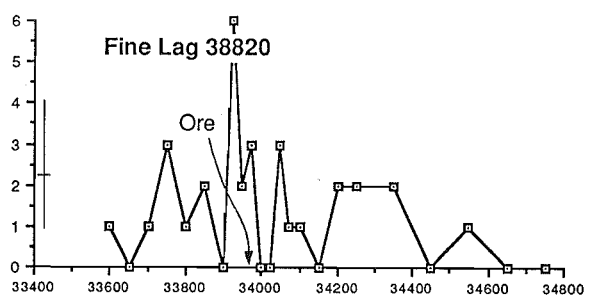
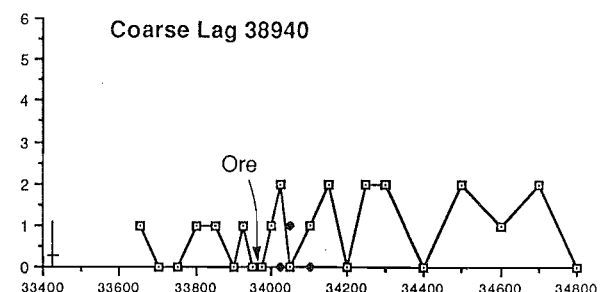
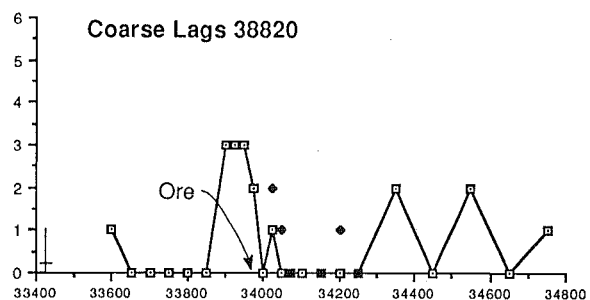




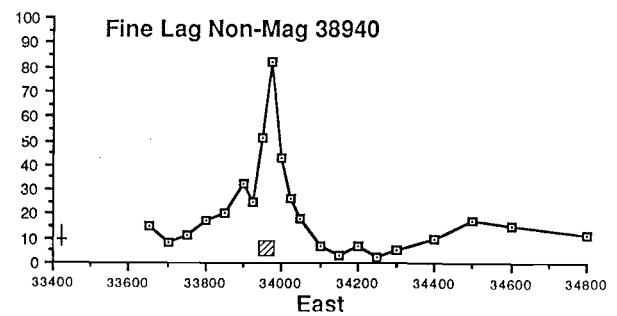
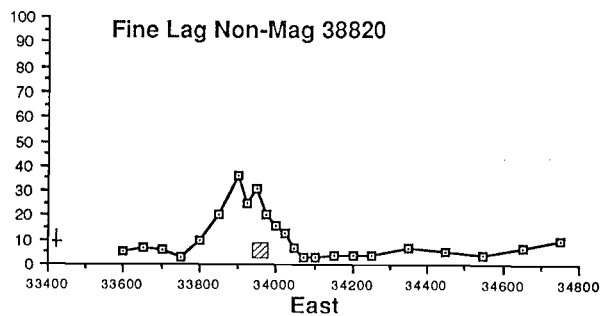
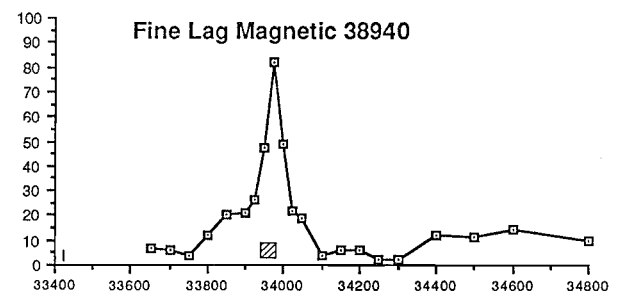
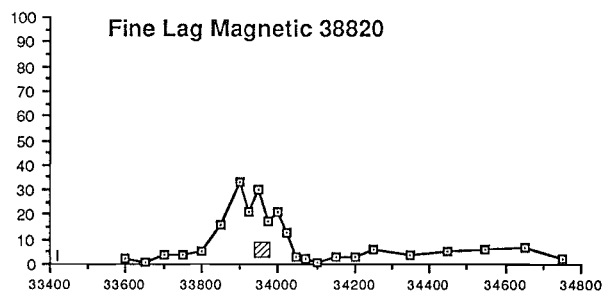
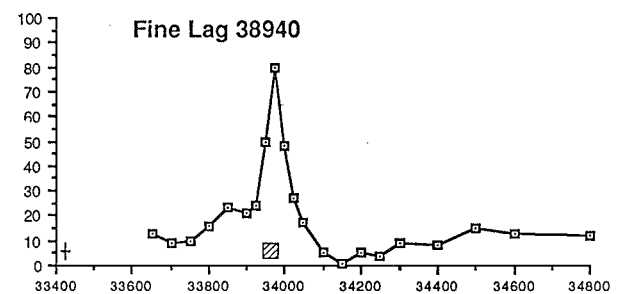
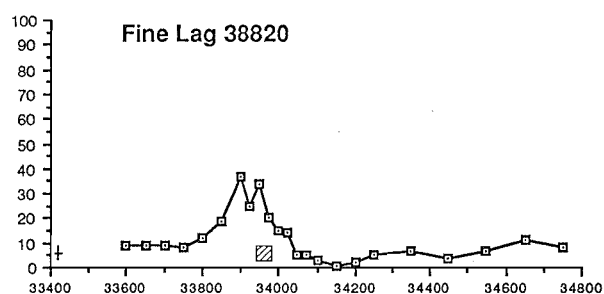
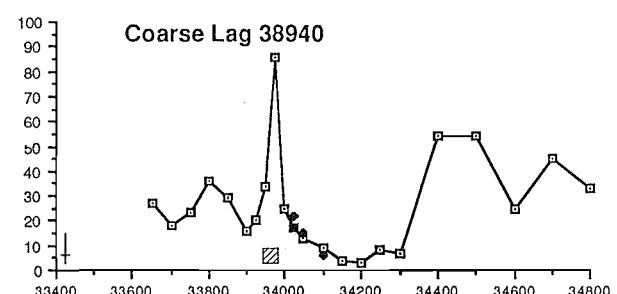
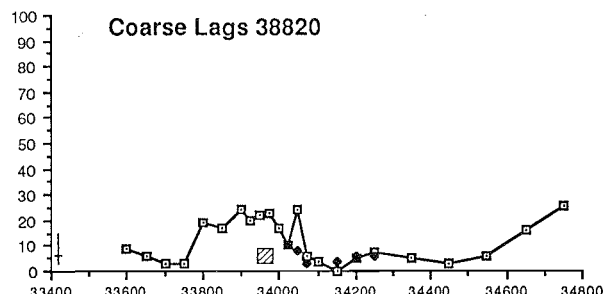
Sb (ppm)

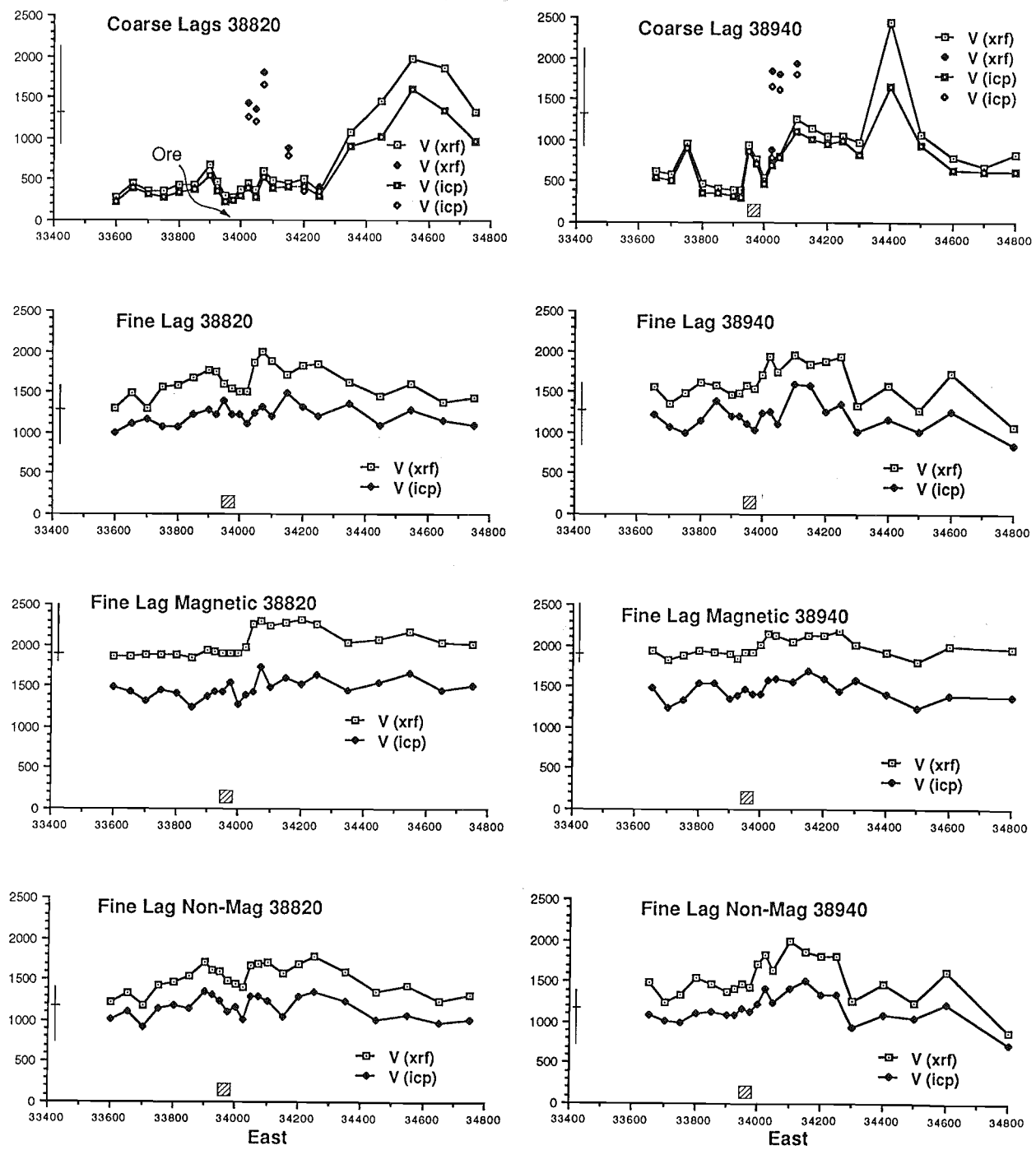




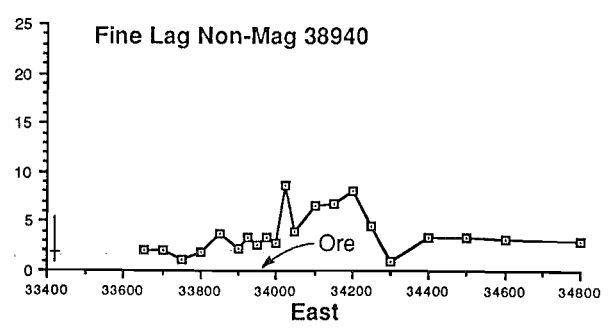
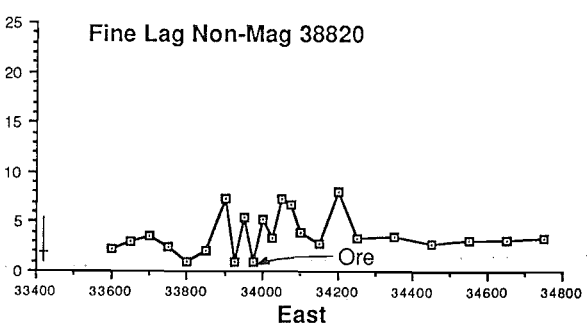
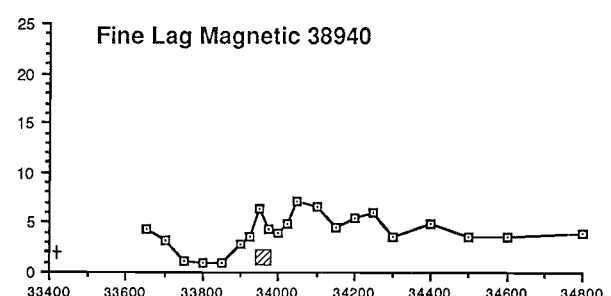
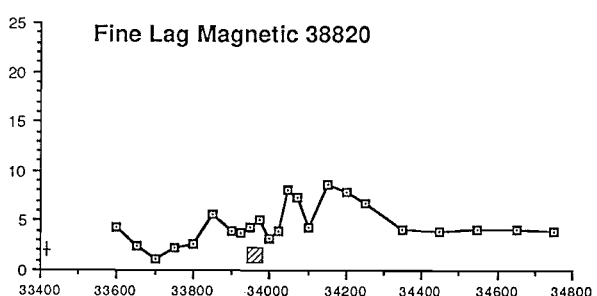
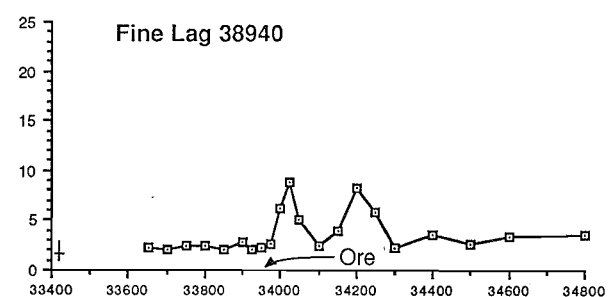
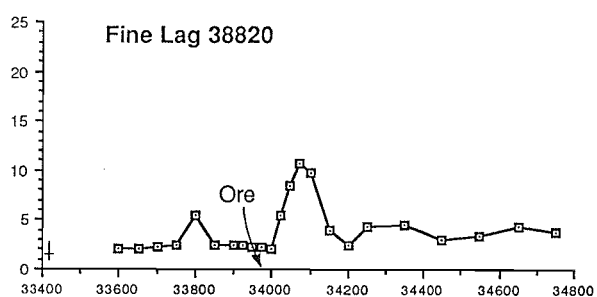
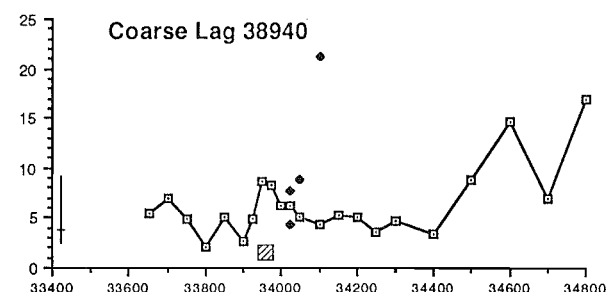
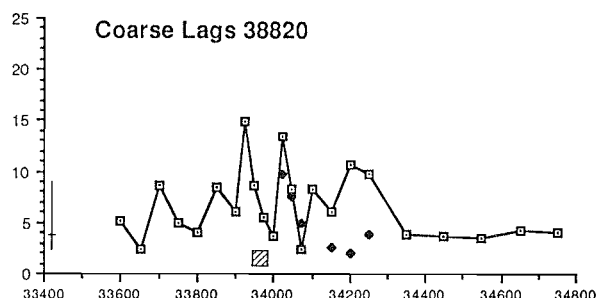


Sr (ppm)

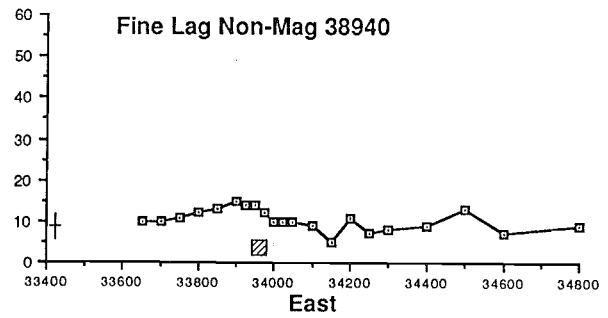
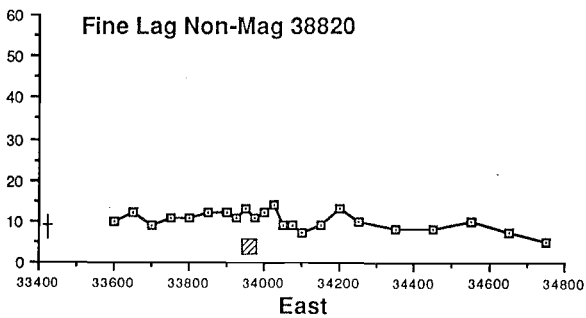
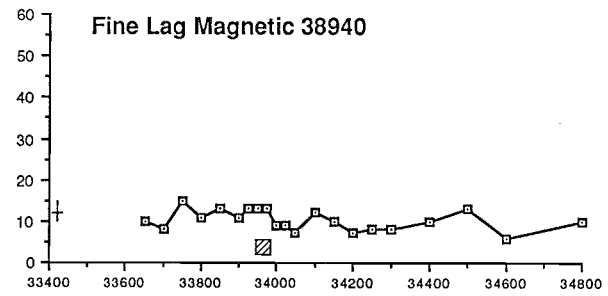
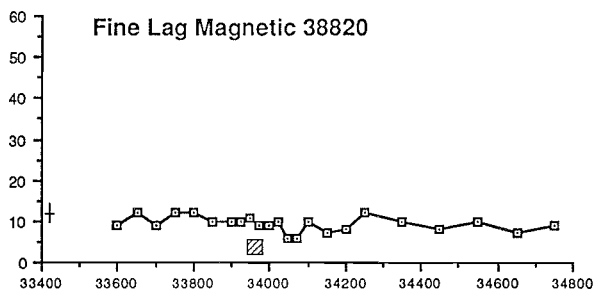
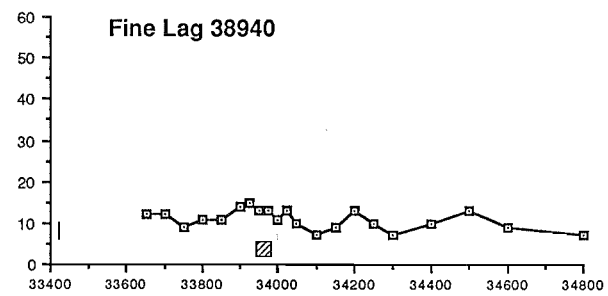
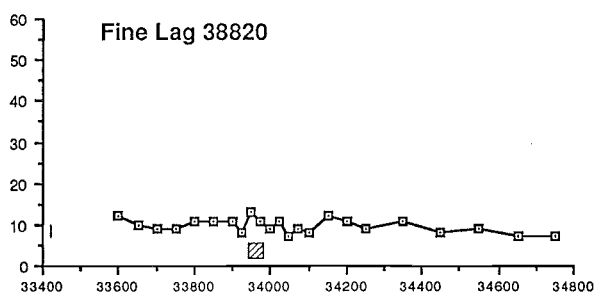
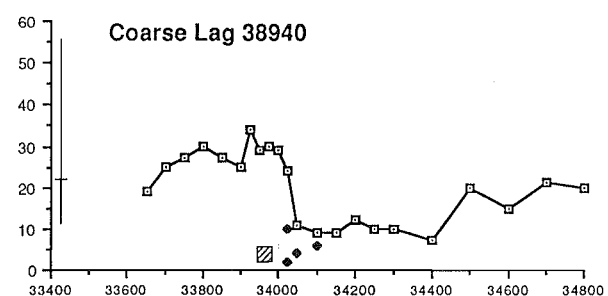
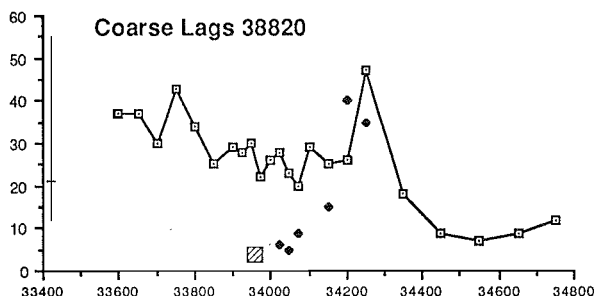




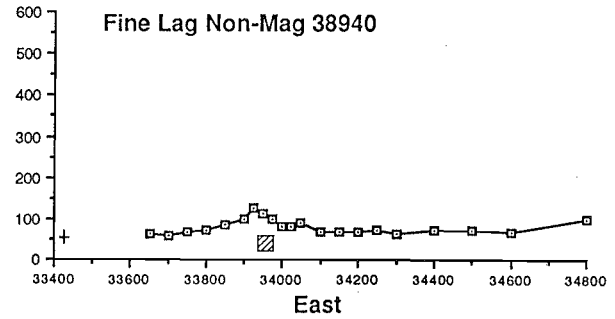
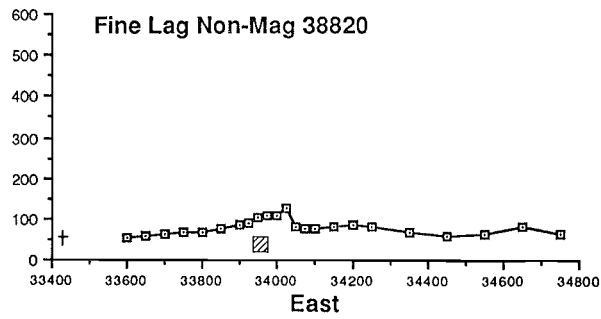
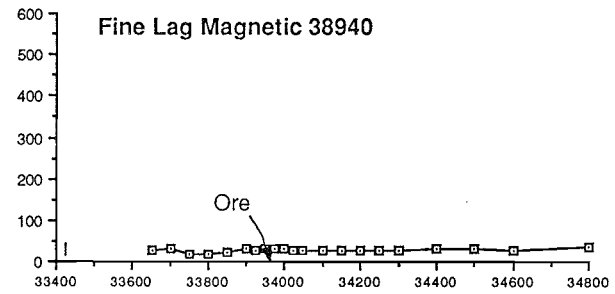
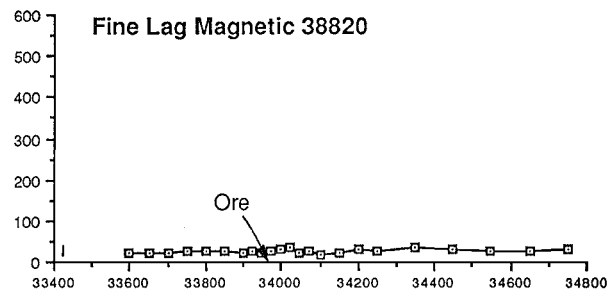
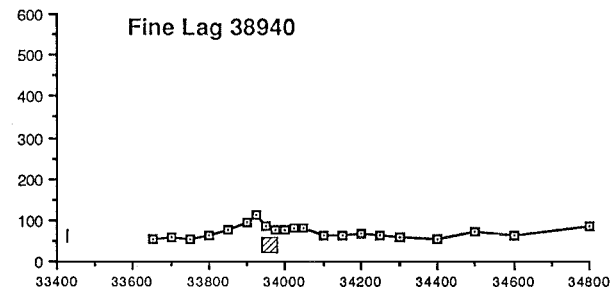
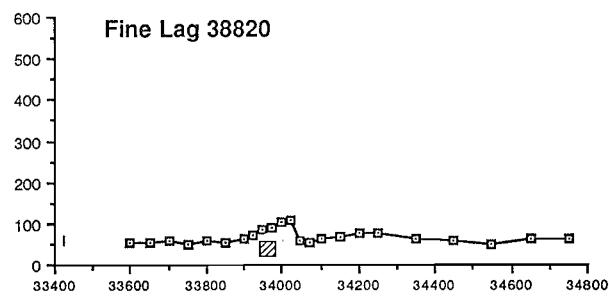
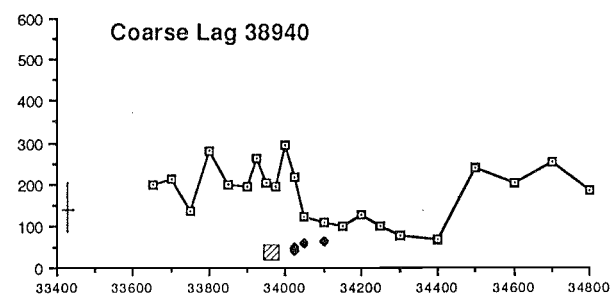
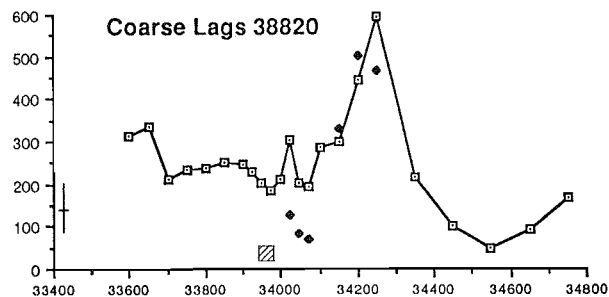
W (ppm)

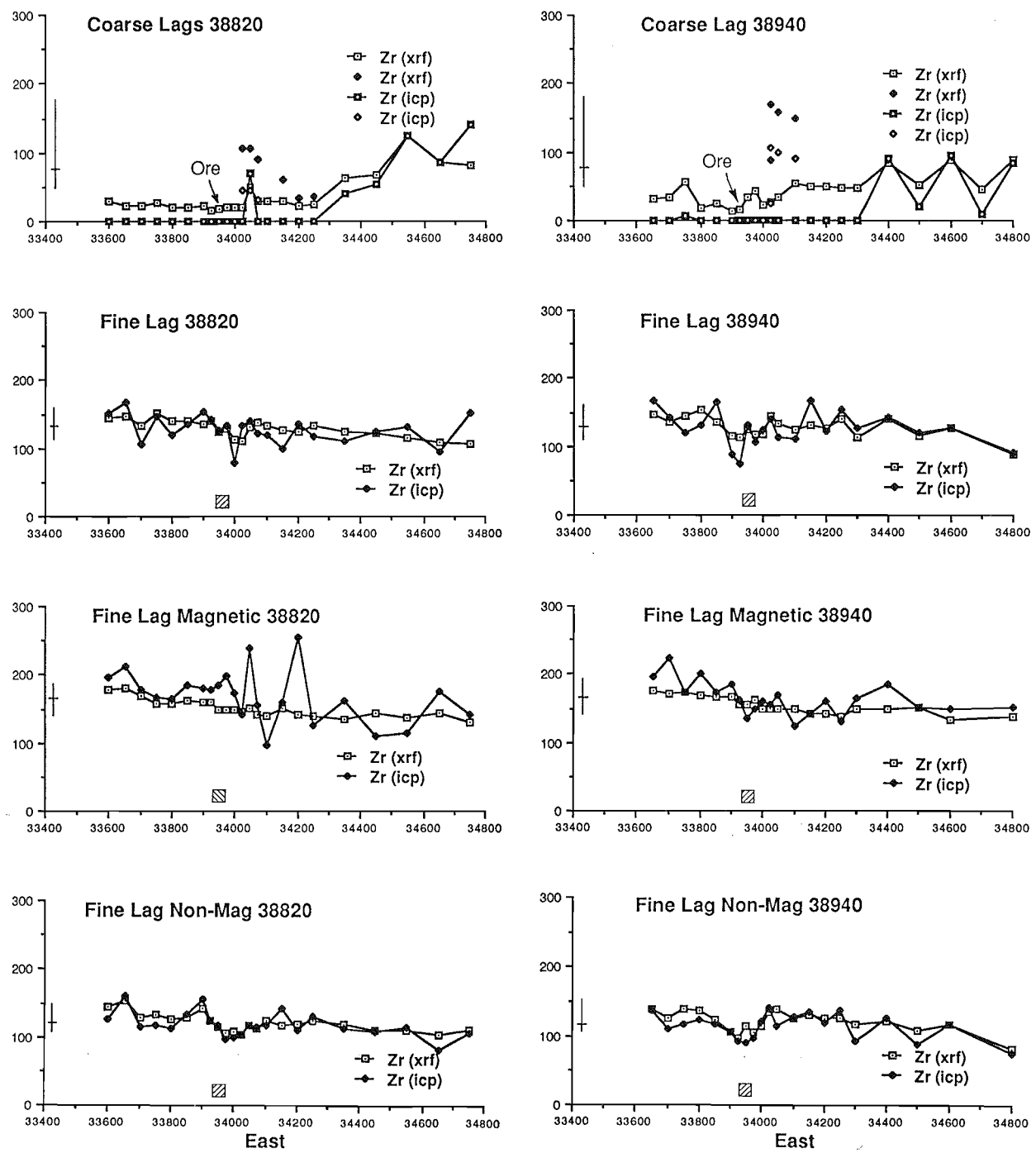


Y (ppm)



Zn (ppm)





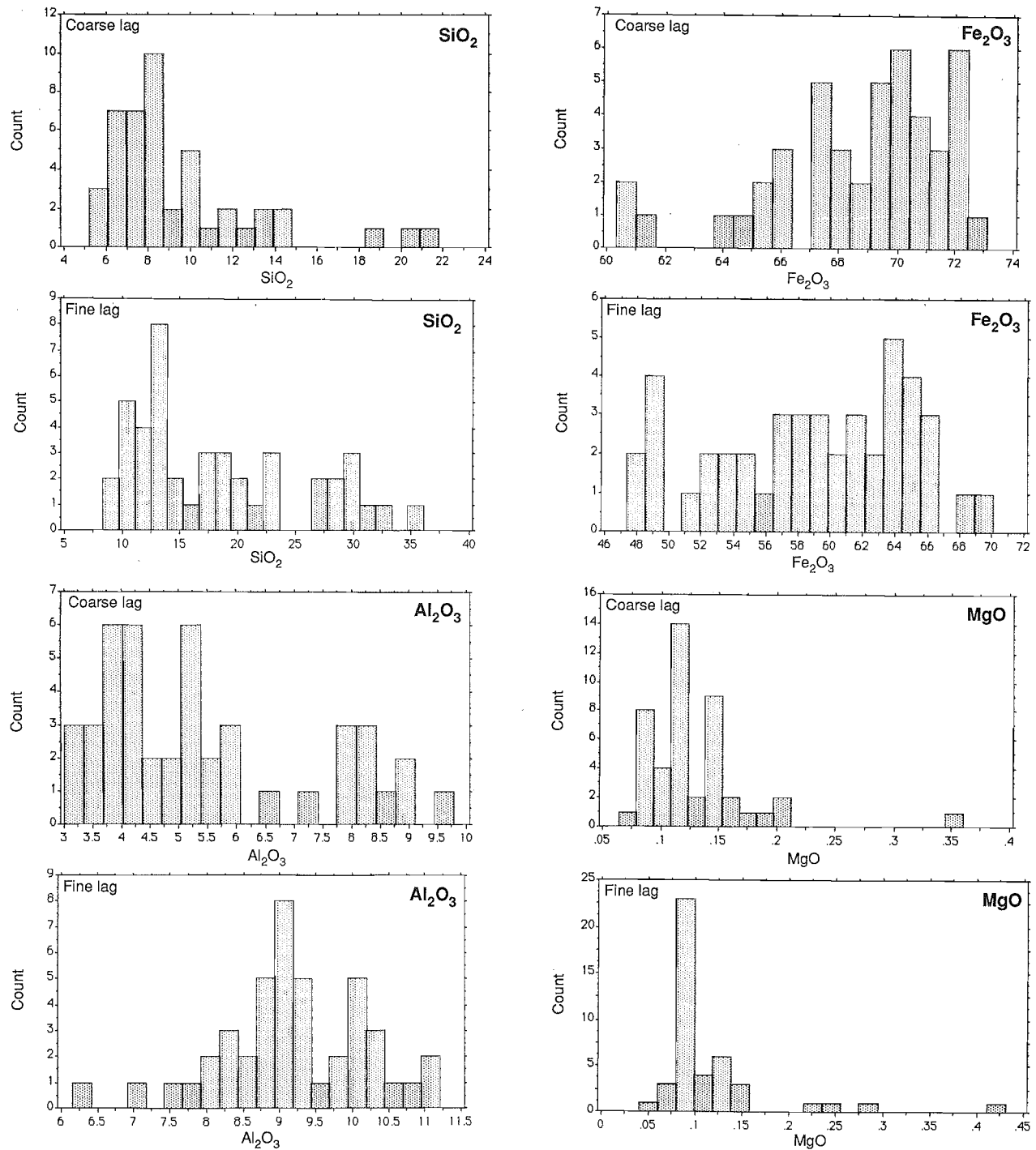
APPENDIX 4

Frequency Distributions

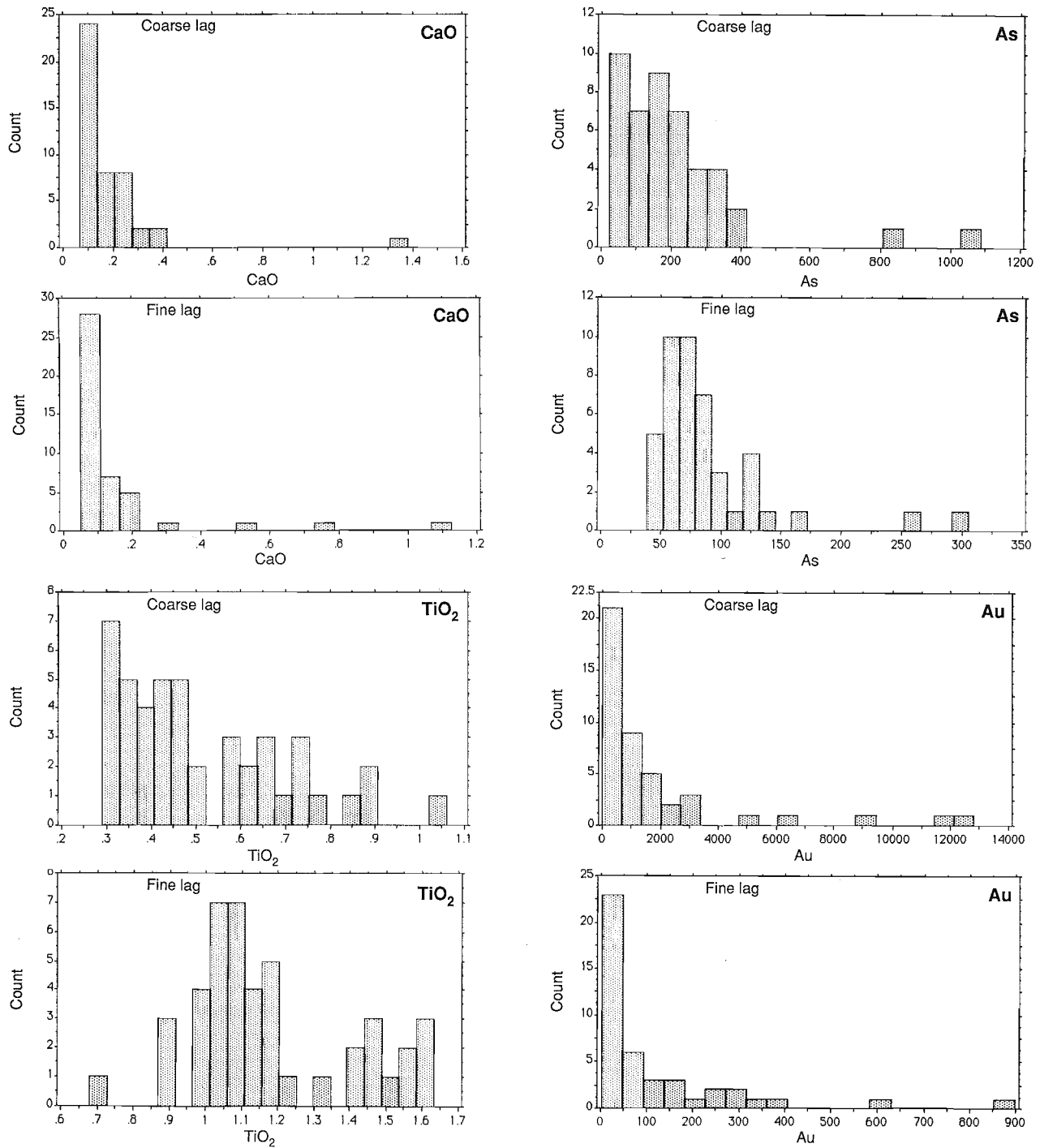
Oxides in weight %
Trace elements in ppm

Note:
Ag, Bi, Cd, In on page 8
Se, Sn, Zr on page 9

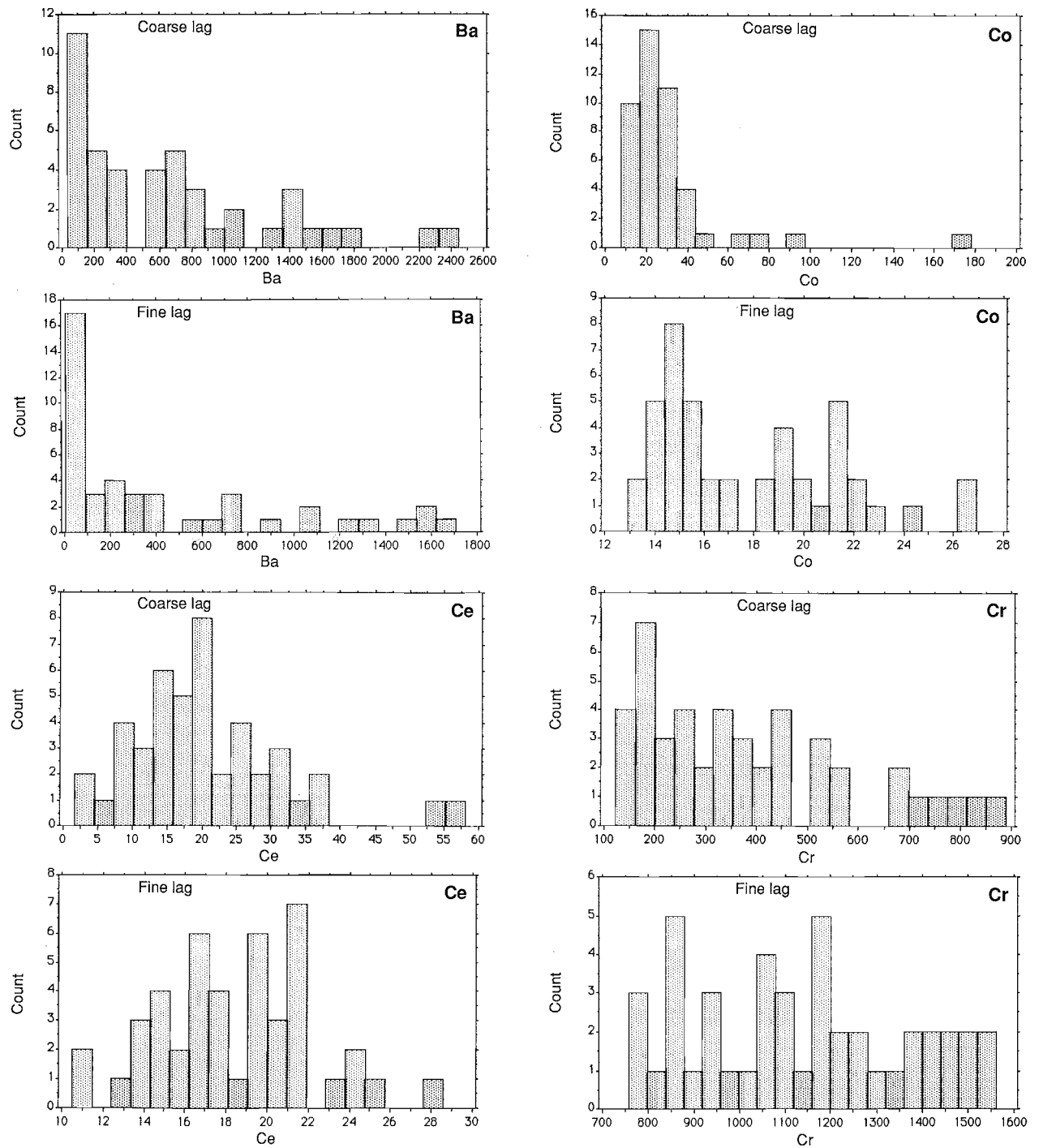
Si, Al, Fe, Mg



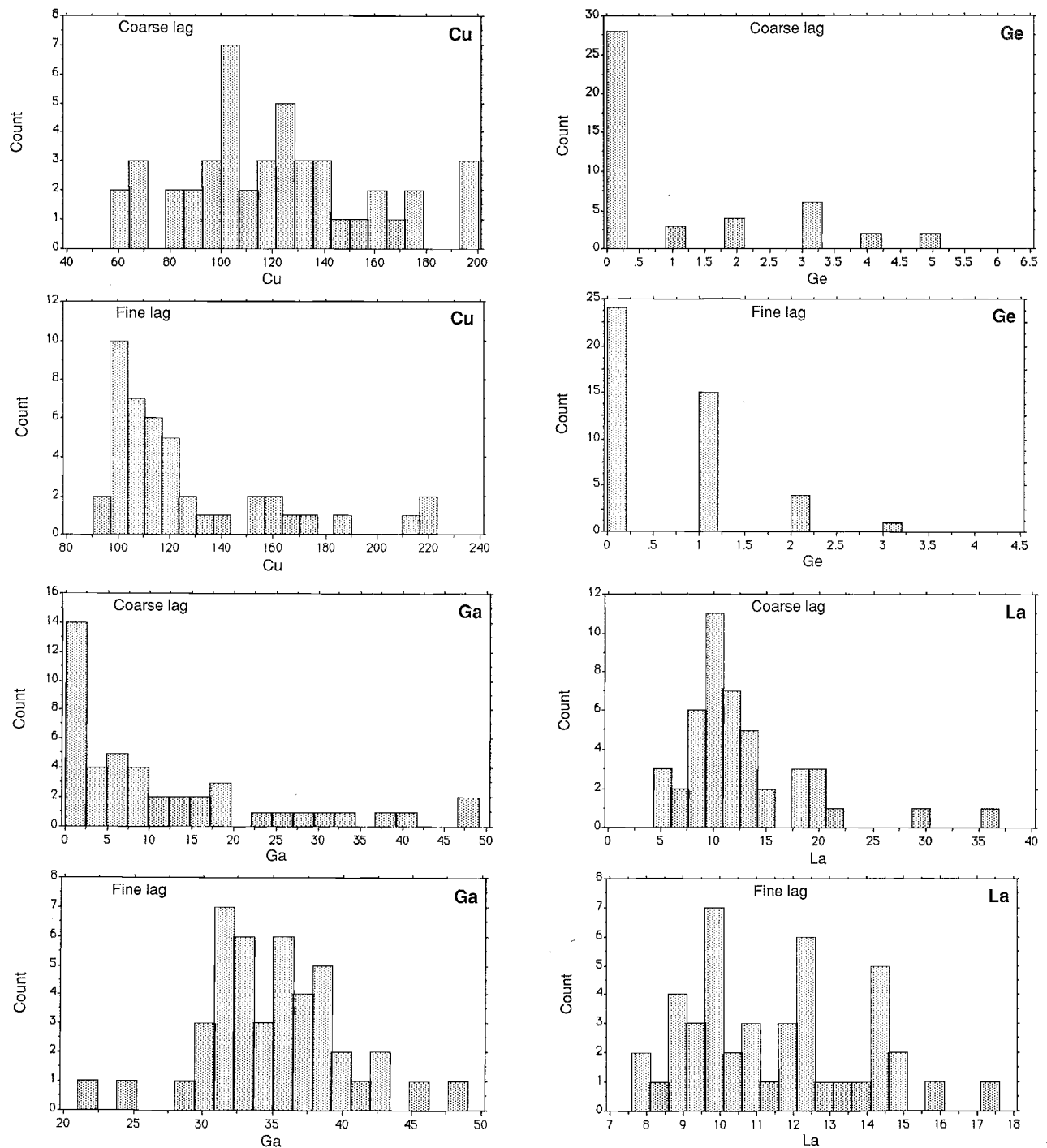
Ca, Ti, As, Au



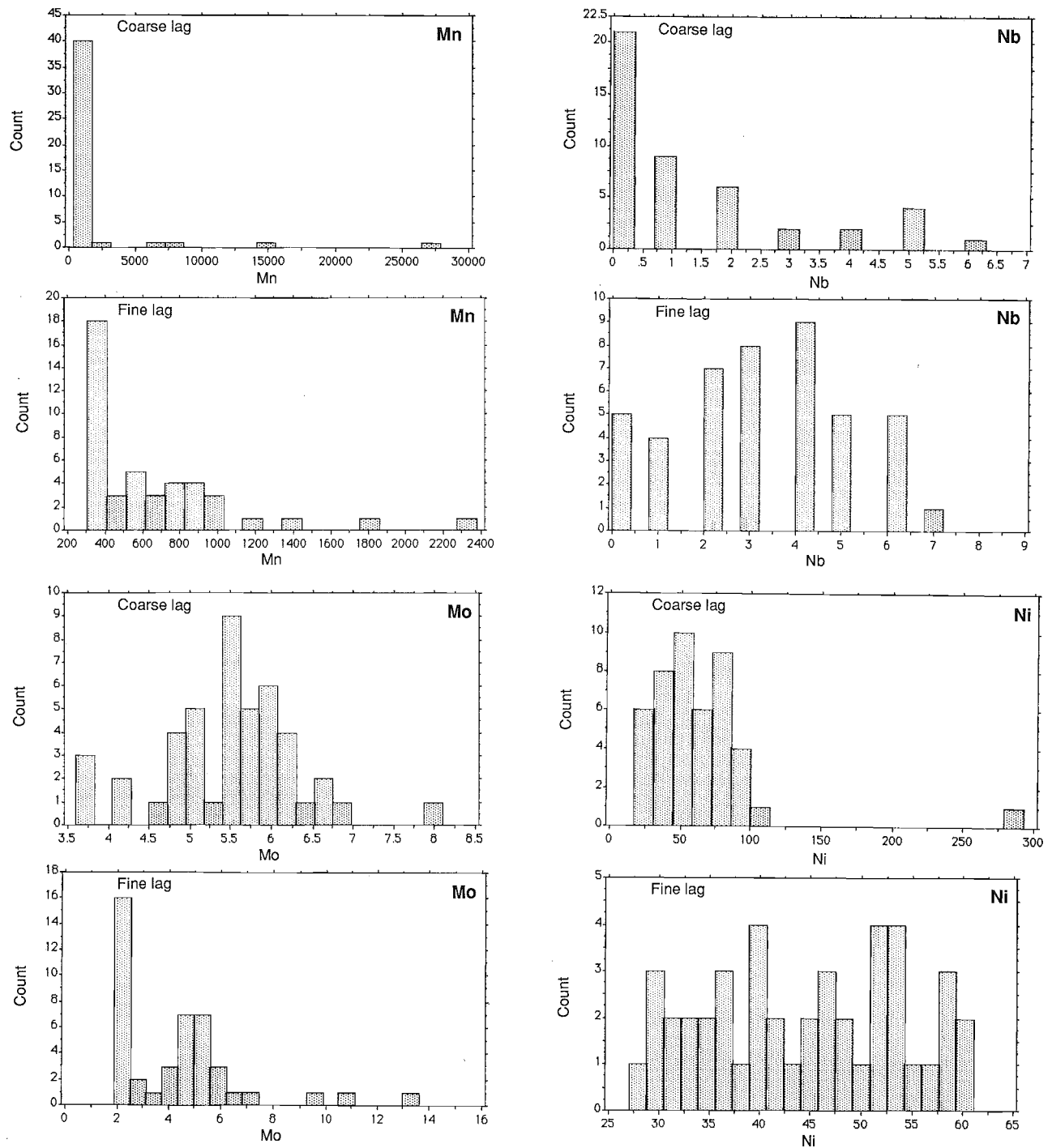
Ba, Ce, Co, Cr



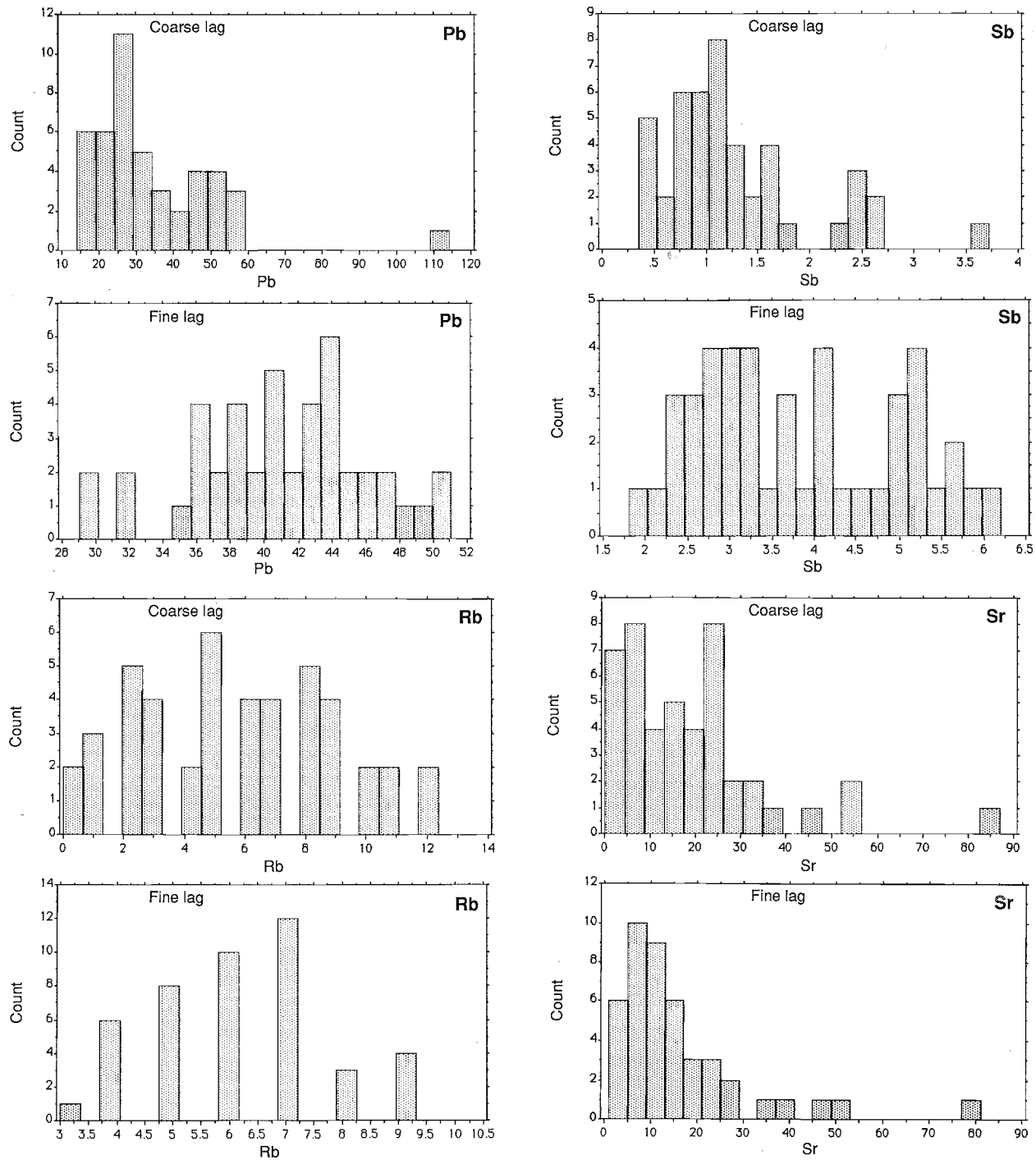
Cu, Ga, Ge, La



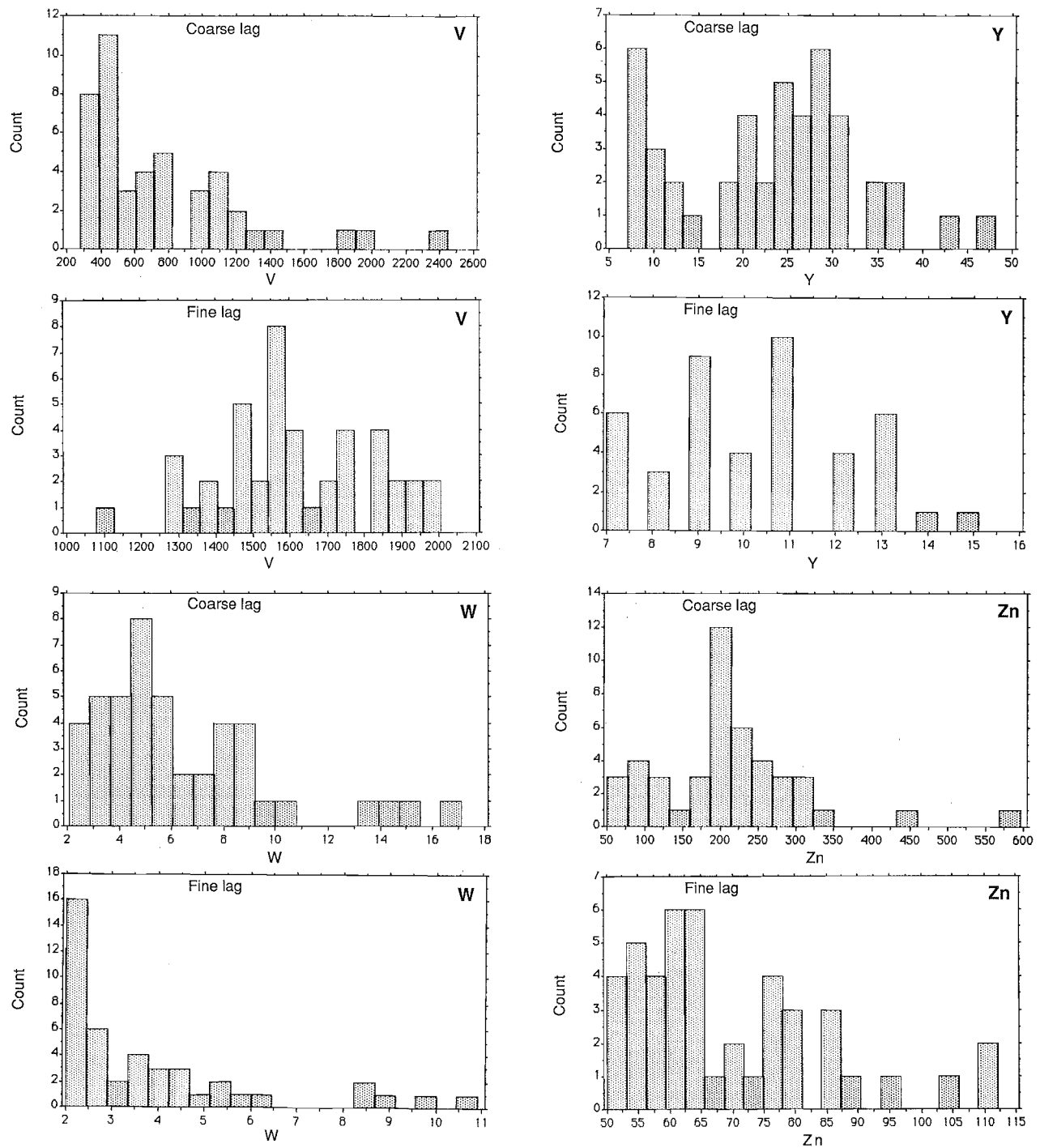
Mn, Mo, Nb, Ni



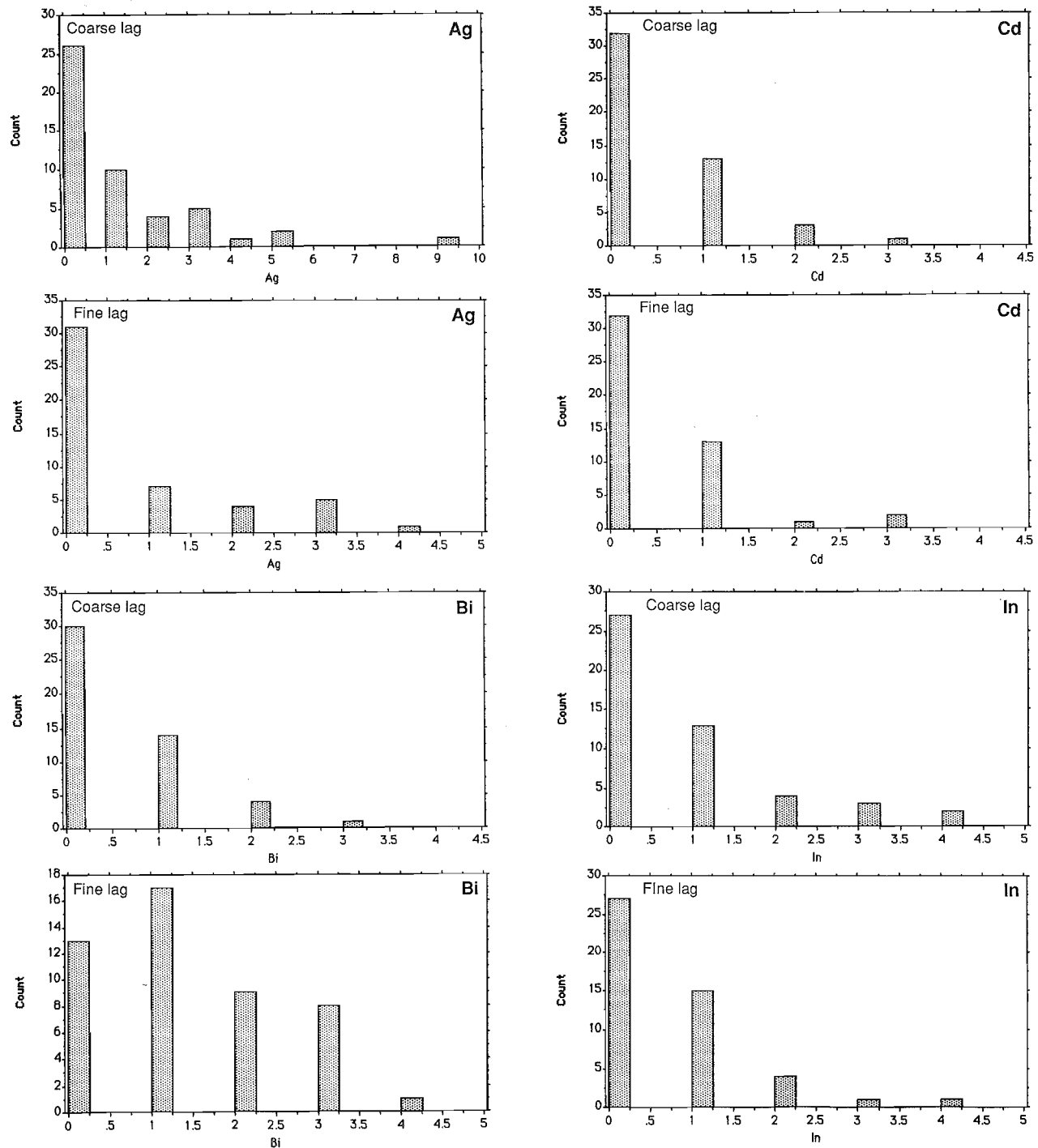
Pb, Rb, Sb, Sr



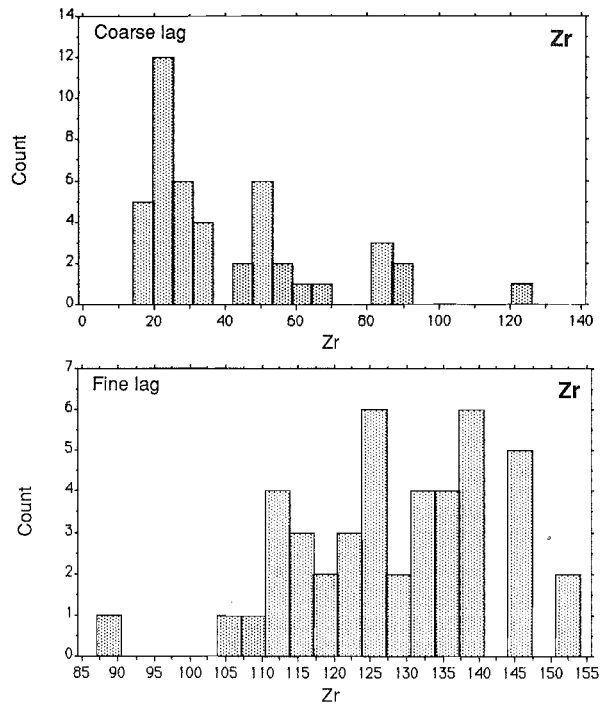
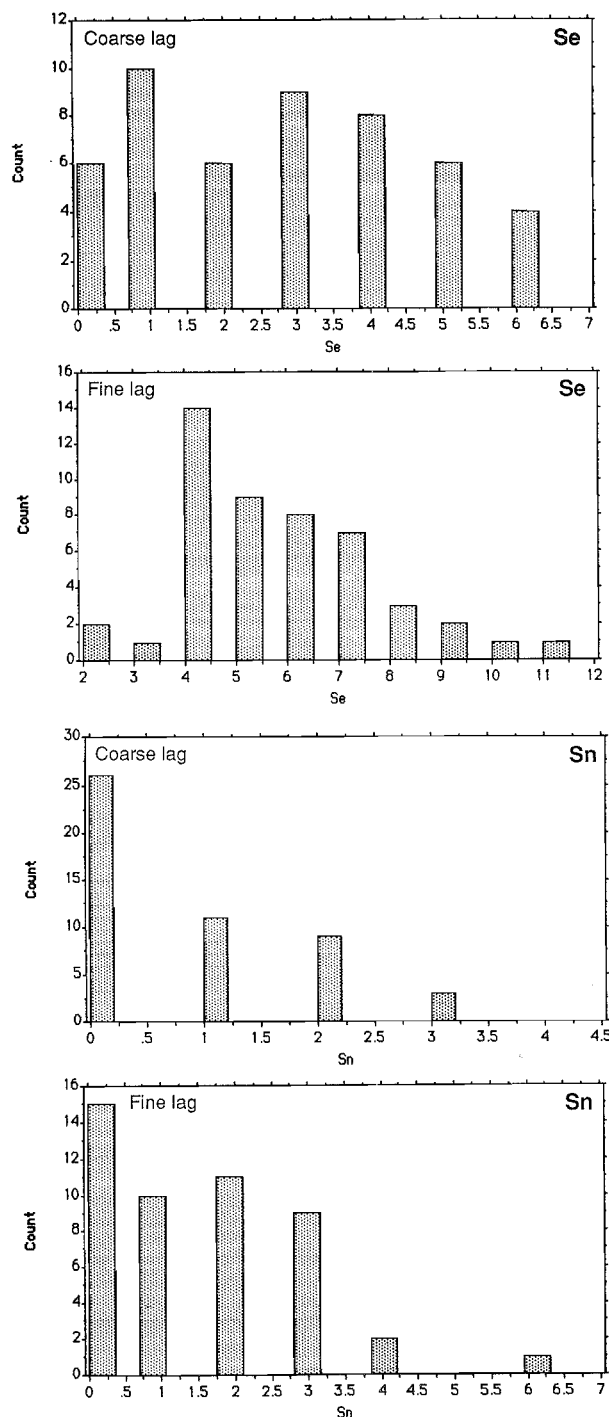
V, W, Y, Zn



Ag, Bi, Cd, In



Se, Sn, Zr



APPENDIX 5

Systematic Petrography

APPENDIX 5

SYSTEMATIC PETROGRAPHY

Detailed petrographic description of the coarse and fine lags is dealt with here on an individual specimen basis. The essential features of this petrographic investigation have been summarised in the main body of the report. Photographs of the internal structures of the lag fragments are shown in Figure 6. Their micro-fabrics are shown in Figures 7 and 8. Specimen numbers correspond to the library numbers in Appendices 1 and 2.

INTRODUCTION

Many of the lag fragments are lithorelics. Though iron minerals, principally goethite with some hematite, have almost completely replaced their original mineralogy, recognisable fabrics have survived in places. Where some hardy minerals have been preserved, these are relics; where iron replacement is complete and only the mineral fabric is preserved, these are pseudomorphs. The relics are invariably iron-stained mica ($\text{Si}=\text{Al}>\text{K}$ by SEM). The pseudomorphs are more difficult to determine but probably are after kaolinite (some of which may be authigenic), after kaolinite interlaminated with illite, and after smectite.

Where these pseudomorphed mineral fabrics have been destroyed, only secondary iron structures remain. In places there is evidence for several cycles of iron solution and deposition. Some goethite forms colloform, delicately banded structures, in places interlaminated with hematite, as a sequence of linings on the walls of open spaces which, in places, have been completely or almost completely filled.

Hematite occurs overtly, as small lozenge-shaped crystals, colloform layers and as poikiloblasts, but it also occurs covertly, with goethite, as an ultra fine-grained product, apparently produced by goethite dehydration. This has lead to a wide variety of goethite colours and reflectances, from dull brownish-grey, through lead-grey, to goethites of increasing brightness as dehydration progresses. It has lead to a greater hematite content in the samples than is immediately apparent from polished section study. The dehydration process is accompanied by a volume change, leading to dehydration cracking or to a porous appearance. This process has been discussed by Morris (1985), who described the process as selective, in that goethite pseudomorphs after quartz were the most easily transformed, followed by silicate and then carbonate pseudomorphs. In the iron ores of the Hamersleys, it appears to be due to long exposure of the goethite above the water table and is most prevalent near the surface. This is equally applicable to ferruginous nodules, which seem to have first formed in the mottled zone and, by gradual deflation of the surface, arrived in a lag accumulation.

COARSE LAG

The petrography of the coarse lag was made difficult by its inhomogeneity. Though the exteriors of lag fragments appear to be quite similar, cut sections show a wide variety of colours and fabrics. This variation is due to inherent inhomogeneity in the source of the lag, differences in subsequent weathering history (replacement by iron oxides) and mixing by lateral dispersion at the surface. Thus it was necessary to section at least four coarse lag fragments (A - D) to gain a representative petrographic impression. Each sectioned fragment is described and then the four sections, comprising the lag sample, are summarised.

Specimen 08-93

Black ferruginous lag

Co-ordinates 34025E 38820N

Located over lateritic duricrust

A

Internally the lag fragment is mottled yellow and honey-brown and contains a few irregular vesicles, each with an internal goethite lacework. The section shows small patches of goethite pseudomorphs after layer silicates. They form finely-laminated short stacks, with an aspect ratio of 1 : 5, in a confused fingerprint structure. These pseudomorphs are set in a patchy, darker, probably secondary goethite, with strong internal reflections. The rock is slightly porous.

B

The inside of the lag fragment is dark red-brown to mauve-brown and is pocked with vesicles (2-3 mm), some of which are filled with yellow-brown and red-brown ferruginous clay and others with white agate. The section shows a wispy, matted fabric of layer silicate remnants, interspersed with homogenous goethite. The pseudomorphed, layer silicate fabric shows some short stacks and is similar to specimen 08-93A but with more distortion.

C

The fragment is internally dark honey-brown and porous. It is pocked with open vesicles and others which are agate-filled. A few relict shreds of mica, interspersed with short stacked, layer silicate pseudomorphs, are set in a large proportion of colloform, fibrous goethite (Figure 7C). The specimen is very porous and the vesicles are lined with colloform goethite.

D

The inside of the fragment is blue-grey and mottled. The section shows complex goethite replacement of a fabric which contains both relict mica and layer silicate pseudomorphs with a short stacked fabric. This fabric has been replaced by several goethite generations and finally by a last goethite generation characterised by globular to polygonal bright grains.

Three of the sections from this specimen show a confused fingerprint fabric, comprising short stacks of pseudomorphed layer silicates. These are in various stages of preservation from invasive secondary iron and many are distorted. They appear to have been derived by replacement of a matted mass of original ragged and sutured uralitic amphibole, or its weathering clay mineral products, and the fabric was probably mafic. One specimen, C, is rich in mica relics, is probably related to the black shales of the nearby orebody and could have been relocated by down-hill easterly dispersion (40 m).

Specimen 08-104

Black ferruginous lag

Co-ordinates 33850E 38940N

Located over footwall mafic rocks

A

The inside of the fragment is a deep honey-brown, mottled with yellow-brown, and shows a preserved schistosity (Figure 6A). There are a few open vesicles. The section shows small islands of mica relics and finer-grained, layer silicate pseudomorphs, set in a mass of secondary goethite (Figure 7A). This later goethite forms bands, probably paralleling the original schistosity. The grain size of the layer silicate pseudomorphs vary considerably. Sub-angular irregular and lozenge-shaped grains of hematite occur, associated with goethite, in areas rich in layer silicate relics. Some of these hematite grains show re-entrant boundaries.

The rock is quite porous and secondary goethite forms fibrous, colloform linings to irregularly-shaped vesicles. At one location a lenticular blob of gold was found with secondary goethite on the edge of a small vesicle (Figure 7G). Microprobe analyses are available of the matted goethite, the layer silicate pseudomorphs (Table 5), the secondary goethite (Table 5, Volume I) and the colloform goethite.

B

The fragment is internally deep red to blue-black, very fine grained and flinty. Cauliflower-like secondary goethite structures predominate (Figure 6G). Styolitic veins, some filled with black goethite, cut the fabric, which is also set with agate-filled vesicles. The section is dominated by secondary goethite structures. It shows numerous cauliflower-shaped to lensoid cavities in a dark, very fine-grained goethite, which have been filled with a coarser-grained, slightly fibrous goethite. The coarser grained goethite infilling appears to have been partly dehydrated and shows cracking. There are also numerous vermiform vesicles, lined with fibrous goethite, and some have been infilled by agate. Secondary iron structures dominate this fragment and it seems to have been derived from a surface ironstone.

C

The fragment is fine grained and a deep honey-brown. Some veining is associated with dark, secondary goethite and chains of open vesicles. This rock consists predominantly of a goethite replacement of a matted layer silicate, forming globular patches (Figure 7C). There are a few irregular and lozenge-shaped grains of hematite.

D

The inside of the fragment is dark honey-brown. It consists largely of even-grained secondary goethite, with a few not very distinct islands of matted, layer silicate pseudomorphs with a fine-grained matted fabric. Parts are quite porous and a fine-grained colloform goethite has filled the voids and this goethite is fibrous near the margins of the voids (Figure 8D). A small speck of gold was seen in this later goethite. The extent of the infilling goethite is very evident under the binocular microscope.

The sections from this location (B - D) are dominated by secondary iron structures, though two (C and D) show a few islands of matted, layer silicate pseudomorphs which may be related to an original mafic fabric. Section A is dominated by mica relics, contains visible gold and has probably been relocated downhill by westerly dispersion (90 m) from the black shale of the orebody.

Specimen 08-108

Black ferruginous lag

Co-ordinates 33975E 38940N

Located over orebody

A

The section shows a very large quantity of coarse-grained mica relics, set in slightly-porous goethite. A small goethite vein cuts the fabric. Microprobe analyses have been made of the mica relics (Table 5) and of the goethite surrounding the mica relics (Table 5), some of which appear to contain mica on a sub-micron scale. Also the goethite of the vein has been analysed by microprobe (Table 5).

B

The inside of the fragment is very porous and is a deep red-brown. Small clusters of relict mica are visible under the binocular microscope. It is porous and is set with open vesicles. The section shows a very large proportion of coarse-grained mica relics (Figure 7A) set in goethite. Some of the secondary goethite shows colloform structures.

C

The fragment is dark brown and is very fine grained internally. It shows a weakly-preserved schistosity but this has been extensively taken over by secondary iron (Figure 6F). There are also a few arcuate vesicles, largely filled with goethite and silica. The section is similar to that of specimen 08-108B but it contains much less relict mica and much more late goethite, which is colloform near voids. There are a few lozenge-shaped hematite crystals scattered in the goethite.

D

The inside of the fragment is dark honey-brown, mottled with yellow-brown and has a preserved, and probably folded, schistose fabric (Figure 6B). It is set with open vesicles and is cut by ferruginous, clay-filled fractures. The section contains a very high proportion of fine-grained, layer silicate

pseudomorphs (Figure 7B) in goethite with a small proportion of mica relics. The mica relics are quite discrete from the layer silicate pseudomorphs, which are probably after kaolinite, though some are probably after interleaved kaolinite and illite (Robertson and Eggleton, in prep.). A few lenticular grains of gold appear in place of parts of some mica layers (Figure 7B) and a gold grain was also seen on the edge of a small vesicle (Figure 7H).

All the sections show mica relics and one shows layer silicate pseudomorphs after probable kaolinite or interstratified kaolinite and illite. This is typical of the fabric of the black shales of the orebody (Robertson and Gall, 1988), though no recognisable garnet pseudomorphs were found. The colours of the insides of the lag fragments differ from those overlying mafic rocks, in tending to a deep red-brown rather than honey-brown. Binocular microscopic examination shows some mica relics.

Specimen 08-113

Black ferruginous lag

Co-ordinates 34150E 38940N

Located overlying ultramafic schists

A

The inside of the fragment consists of several components. Yellow-brown to brown islands, with a schistose fabric, are permeated by very fine-grained, dark red goethite. There are several open and partly clay-filled vesicles, joined by fractures, which form solution channels. The section shows a porous mass of goethite, set with mica relics. A few patches and laths of hematite occur. Voids are lined with fibrous bright goethite and a small grain of gold was found on the edge of one vesicle. A small fragment of goethite breccia is attached to one part of the section. Goethite cementing this breccia is darker and clearly later than the goethite of the rest and it contains fragments of intensely corroded quartz.

B

The fragment interior is honey-brown and is very fine grained. Some very small mica relics are visible. Other parts show colloform goethite and vermiform vesicles, some of which are partly filled with agate, others with red-brown ferruginous clay. Parts of the section are rich in very coarse mica relics ($\text{Al}=\text{Si}>\text{K},\text{Fe}$) and in accordion-like, vermicular, layer silicate pseudomorphs. Others consist largely of several phases of colloform goethite. The vermicular structures have been largely replaced by goethite ($\text{Fe}>>\text{Al}$). They are set in very fine-grained goethite which has penetrated between the pseudomorphed, layer silicate sheets. In places, sheets of mica are preserved within the structure. A fair proportion of the goethite matrix appears to fill, what was at one time open cavities, with colloform goethite ($\text{Fe}>>\text{Al}$). A few small, bright, sieve-like grains of hematite occur.

C

The overall appearance of the fragment interior is a deep red-brown, mottled with blue-black and slightly porous. The section shows little but porous goethite and some bright poikiloblasts of hematite. There are few recognisable layer silicate pseudomorphs, though high magnification suggests a matted fabric, with a few very small mica relics, with a confused fingerprint structure (Figure 7D). Some voids have been filled with lead grey, colloform, delicately-banded goethite.

D

The inside of the fragment consists of brown to yellowish-brown goethite and dark, blue-black, metallic goethite with a strong, though distorted, preserved schistosity. It is penetrated by numerous vermiform vesicles, some of which are filled with ferruginous clay and hardpan and others with an open breccia of angular goethitic fragments, set in a partial matrix of ferruginous clay and hardpan (Figure 6J).

The goethitic areas show a few patches of layer silicate pseudomorphs ($\text{Fe}>>\text{Al},\text{Si}$) with a short stack fabric. This is set in a dark grey goethite. Some parts are replaced and invaded by at least two secondary goethite phases. A small grain of gold was seen lying just below the surface of the resin, filling a small vesicle in the hardpan. The matrix of the hardpan is clay ($\text{Al}=\text{Si}>\text{Fe}$).

Sections A and B contain appreciable quantities of mica relics and seem related to the orebody. Accordion-like authigenic kaolinites have been described by Williams, Turner and Gilbert (1955) from fireclays and in interstratified kaolinite and micas produced from granite weathering (Robertson and Eggleton, *in press*). These are almost identical to the goethite pseudomorphs after accordion-like layer silicates in section B. The fabric of the underlying ultramafic rocks is difficult to determine but it is probably shown by sections C and D. It appears to be very similar to but finer-grained than that which characterises the mafic rocks. The presence of gold in a vesicle in a hardpan matrix is evidence of some very late gold mobility.

Specimen 08-117

Black ferruginous lag

Co-ordinates 33747E 39311N

Located in regional background at NW corner, overlies probable ultramafics

A

The fragment interior is honey-brown, very fine grained and slightly mottled. The section is porous and consists largely of secondary goethite.

B

The inside of the fragment consists of islands of preserved schistose, yellow-brown material, which is veined and set in deep honey-brown goethite (Figure 6C). A few open vesicles are lined with dark brown goethite. The section shows a matted, very fine-grained fabric of layer silicate pseudomorphs, set in a brighter goethite. A few vermiform vesicles are lined with fibrous goethite. Some hematite lozenges occur.

C

The fragment consists internally of deep mauve-brown, very fine-grained material, dotted with black specks. A few open vermiform vesicles are lined with goethite. The overall fabric is porous. The section shows numerous very fine-grained relics of layer silicate with expanded-book structure, surrounded by secondary goethite, which is set with accordion-like, layer silicate pseudomorphs. There are also numerous vermiform voids and poikiloblasts of hematite.

D

The interior of the fragment has parts which are honey-brown and schistose. Remnants of a shattered quartz vein cut part of the fragment and this has, in turn, been veined and penetrated by fine-grained goethite. There are some pockets which are rich in secondary, colloform, vesicular goethite. The section shows a few lithorelics, which occur as islands in goethite. The lithorelics consist of fine-grained rather shredded, indeterminate silicate remnants, which are strongly aligned in a schistose structure. The fabric is cut by vein quartz and this in turn is cut and shattered by veins of later goethite, which forms colloform structures around voids.

Though secondary goethite structures have obscured much of the original fabrics, the porous fabric and very fine-grained nature of the layer silicate pseudomorphs and relics may typify the underlying ultramafics.

Specimen 08-118

Black ferruginous lag

Co-ordinates 34172E 39314N

Located in regional background, NE corner, overlying presumed ultramafics

A

The fragment interior consists of two grey-brown, fine-grained bands, separated by a quartz-rich layer. All these layers have a sugary appearance (Figure 6D). It is a silicified fragment of BIF, consisting largely of fine-grained, granular, polygonal quartz. Goethite fills a few fractures and forms patches in the fabric. There are a few grains of hematite, probably after magnetite.

B

The inside of the fragment is mottled with yellow-brown and red-brown and has a schistose fabric. It is set with open and clay-filled, vermiform vesicles. The overall fabric is porous. The section shows a very fine-grained mat of layer silicate pseudomorphs, that has been invaded by patchy colloform goethite, showing dehydration cracks. Colloform goethite forms complex, banded linings on some vesicles, some of which have been filled by a yellow to reddish ferruginous clay, others are unoccupied.

C

The fragment interior is mauve-blue and very fine grained. The section shows a coarse-grained fabric of mixed mica relics and goethite pseudomorphs after layer silicates. This is set with vermiform voids, surrounded by secondary goethite.

D

The inside of the fragment is mottled red-brown and blue-black and is very fine grained. The overall fabric is porous. Much of the section comprises a mat of very fine-grained, layer silicate pseudomorphs. This is cut by solution cavities, some of which are infilled by patches of later goethite and red ferruginous clay.

Sections B and D have the usual porous fabric and consist of fine-grained, matted, layer silicate pseudomorphs, typical of ultramafics. Sections A and C are probably exotic. This sample site is located within 20 m of the main road.

Specimen 08-119

Black ferruginous lag

Coordinates 33545E 38146N

Located in regional background, SW corner, underlying rocks unknown

A

The fragment interior is blue-grey, very fine grained, and porous. It is set with irregular vermiform vesicles, some of which are open and others lined with brown, ferruginous clay. The section reveals many very fine-grained mica relics, set in goethite. Some voids are lined with a layer of goethite, which is free of layer silicate inclusions. This fragment has a partial cutan of slightly brighter, partly dehydrated goethite, which still contains numerous relics. The overall fabric is porous.

B

The fragment is elongate and has a granular internal fabric. Inside, it is honey-brown and fine grained. The section is very porous. There appear to be blade-like remnants and pseudomorphs of matted layer silicates but it is difficult to determine their origin.

C

The inside of the fragment is a deep, slightly mauve to red-brown and is very fine grained. The section consists of very fine-grained, layer silicate pseudomorphs, set in secondary goethite. The overall fabric is porous.

D

The fragment interior is dark mottled blue-grey and is set with open and agate-filled vesicles. The section shows only a few very fine-grained wispy remnants of layer silicates, the large proportion is occupied by mottled secondary goethite.

The very fine-grained nature of the layer silicate pseudomorphs suggest an underlying ultramafic.

Specimen 08-120

Black ferruginous lag

Co-ordinates 34290E 38110N

Located in regional background, SE corner, underlying rock unknown, ? Permian glacials

A

The inside of the fragment is red-mauve and very fine grained and it has an indistinct cutan, which shows as an area in which the goethite has taken a slightly higher polish. The section consists of an extremely fine-grained mat of layer silicate pseudomorphs, set with a few vermiform solution cavities.

B

The fragment interior is mauvish brown and contains a few, apparently polymictic, fragments set in an apparently arenaceous matrix (Figure 6E). The fragment has a partial and gradational rim of bright metallic goethite. The section shows an overall fabric suggestive of a number of angular lithorelics, some of which are indistinct, set in what appears to be a matrix containing other, smaller fragments (Figure 7E). The rock could have been a sedimentary breccia. One fragment in the rock contains a very fine-grained mat of layer silicate remnants, set in goethite. There has been extensive replacement by massive goethite in the matrix.

C

The fragment is red-brown to mauve and porous. It contains a few round fragments about 3 mm across. The section shows very porous goethite, containing rare relics of wispy, very fine grained, layer silicate remnants, with a swirled fabric. There appear to be several different fabrics in the section suggesting fragments and a matrix.

D

The fragment is mottled dark grey and metallic and is very fine grained. It has an indistinct cutan, which has taken a higher polish than the core. A few coarse-grained mica relics and minor wispy, very fine-grained, layer silicate pseudomorphs occur in much bright goethite. The fragment has a rim of bright goethite, which grades into the very slightly less bright goethite of the core. Numerous vermiform voids are set in the fabric.

It is tempting to suggest that the apparent sedimentary breccia fabrics seen in B and C could reflect the underlying glacial sediments. On the other hand, the complex nature of the ferruginisation process could well mimic such a fabric. These lag fragments are unique in having distinct cutans and this could reflect a slightly increased content of hematite near the margins of the fragments.

Specimen 08-124

Khaki lag

Co-ordinates 34025E 38820N

Located over lateritic duricrust

A

The interior of the lag fragment consists of dark, red-brown, schistose, porous nodules, mottled with bluish-grey, set in a yellow-brown, ferruginous clay (Figure 6H). The nodules are complex in detail, consisting primarily of platey mica relics and wispy, matted, layer silicate pseudomorphs, set in an early, brownish grey goethite. These are, in turn, penetrated and set in a brighter, porous goethite. There are numerous vermiform voids, some lined with a thin goethite cutan, and patches of recrystallised goethite.

The ferruginous clay matrix, surrounding the nodules, contains numerous smaller goethite nodules. Some goethite nodules contain mica relics and layer silicate pseudomorphs set in secondary goethite, others consist of porous goethite alone. The ferruginous clay matrix also contains hematite crystals and vermiform voids, some of which are lined with thin goethite cutans.

B

The section consists predominantly of one dark grey to red-brown nodule in which lie several solution cavities, filled with red-brown ferruginous clay. The whole fabric has been fractured and the fractures filled with yellowish ferruginous clay and white agate.

The nodule consists of layer silicate pseudomorphs, with a short stack fabric. In this fabric are set numerous vermiform voids, lined with colloform, fibrous goethite. In parts of the nodule, the secondary goethite predominates and relics of the original, layer silicate pseudomorph fabric survive as islands. Porous goethite, rich in crystals of hematite and quartz shards, forms a partial cutan to the nodule. Some parts of the nodule show partial rims of bright goethite. Clinging to some fragments are breccias of quartz, cemented by goethite and containing irregular crystals of hematite. The red-brown, ferruginous clay is rich in fragments of all the earlier components and contains vesicles lined with a thin goethite cutan.

C

The inside of the lag fragment consists of a porous mass of dark red-brown, nodular material, mottled with yellow-brown, and is slightly schistose. It is set with irregular, open vesicles. The nodular material consists of an older phase of goethite, pseudomorphing matted, layer silicate pseudomorphs (with a short stack fabric), partly surrounded and set in a porous, brighter goethite phase. The whole is set with goethite-lined vermiform voids and patches of brighter colloform goethite. Some of the goethite linings show hematite layers, with dehydration fractures (Figure 8B), on which a later generation of goethite has been precipitated.

D

The inside of the lag fragment consists of dark, red-brown to metallic grey, ferruginous, sub-angular nodules, set in red and yellow, ferruginous clay. The nodules consist of a porous goethite, containing very fine-grained mica reliefs. These are set with poikiloblasts of hematite. There are at least two phases of ferruginous clay, one enclosing fragments of the other. The ferruginous clay contains fragments of the ferruginous nodules as well as shards of quartz and crystals of hematite. Strings of vermiform vesicles occur within the ferruginous clay, forming solution channels, which are lined with thin goethite cutans.

The yellow-brown and red-brown ferruginous clay phases have been investigated by XRD (see Section 7.1.2). They consist largely of kaolinite, with a lesser quantity of goethite, some hematite and a trace of quartz.

These sections show two phases, goethite-rich nodules and their enclosing ferruginous clay. The nodular material contains minor reliefs of mica and predominant pseudomorphs of layer silicates. The layer silicate fabric is typical of mafic rocks. These sections illustrate the complex later history of the lag, when it was contained within the lateritic duricrust. Partial cutans on the ferruginous nodules suggest multiple precipitation and solution of goethite, before the ferruginous clay was precipitated. The ferruginous clay contains fragments of all previous phases. Goethite linings of vesicles, within the ferruginous clay, indicate that goethite precipitation was, in part, a very late phase.

Specimen 08-130

Khaki lag

Co-ordinates 34025E 38940N

Located over lateritic duricrust

A

The lag pebble is a red, ferruginous, clay pisolith with a yellow, ferruginous, clay cutan. The red clay is highly ferruginous ($\text{Fe} > \text{Al} = \text{Si}$) and is set with small hematite poikiloblasts and patches of goethite. Small vesicles in the ferruginous clay are lined with very thin colloform goethite and solution cracks are lined or filled with a similar material. The yellow ferruginous clay cutan is gradational to the red ferruginous clay of the core, it is darker in normally reflected light and has the same set of inclusions.

B

This is a pisolith with an orange coloured core, a dark, red-brown, inner rim and a yellow cutan. The contact between the inner rim and the core is, in all places, gradational but the contact between the yellow cutan and the red inner rim is, in places, sharp and in others gradational. The ferruginous clay

of the orange coloured core has a very variable clay to iron ratio. Goethite has replaced the clay most intensively in the vicinity of numerous vesicles, most of which are lined with goethite. The orange, ferruginous, clay core also contains poikiloblasts of hematite and small goethitic nodules, which do not show any original rock fabric. The dark red rim is more goethite-rich than the core and is lighter, in normally reflected light, than both the core and the yellow outer rim.

C

This is a red, ferruginous clay nodule with a partial yellow rim. It contains included, earlier, rimmed pisoliths, unrimmed lithorelics, dark, ferruginous nodules and quartz shards. The ferruginous nodules consist largely of secondary goethite, with no recognisable original rock fabrics. The pisoliths consist of a ferruginous clay similar to the matrix but differ slightly in grain-size, extent of goethite replacement (the pisoliths are richer in goethite) and overall fabric. Both the yellow and the red ferruginous clays contain crystals of hematite.

D

This is a red, ferruginous, clay fragment, containing numerous pisoliths and lithorelics, and is partly surrounded by a yellow to reddish, ferruginous clay, with an oolitic fabric, that also contains lithorelics, with yellow ferruginous clay cutans (Figure 6I). It seems likely that the oolitic, ferruginous clay is an infilling of a vesicle, which contained fragments of lithorelics. The cutans were formed on these fragments by precipitation of yellow ferruginous clay. The red ferruginous clay contains angular fragments of ferruginous nodules (Figure 8F), showing no recognisable original rock fabric, and numerous hematite crystals. Some pisolith inclusions have a very similar composition to the matrix but most are more goethite rich. Chains of vermiciform vesicles and cracks in the red ferruginous clay form solution channels. A diffuse halo of goethite penetrates the ferruginous clay surrounding these solution channels.

The yellow, ferruginous clay has a strongly oolithic structure (Figure 8G). Crystals of hematite are scattered throughout. Pisolith and ferruginous nodular inclusions in the oolithic, ferruginous clay are similar to those found in the red, ferruginous clay, though some mica reliefs are preserved.

This suite of samples covers a late phase in the formation of the duricrust. Red, ferruginous clay was formed around ferruginous nodules, probably after saprolite collapse in the lateritic horizon. The red, ferruginous clay could have been a goethite-bearing, yellow, ferruginous clay originally but dehydration of part of the goethite component to hematite could explain the red colour. The later, yellow, ferruginous clays and cutans may have formed by solution of the red ferruginous clay, followed by deposition of a ferruginous goethitic clay as cutans and oolithic masses. Alternatively, they could have formed by *in situ* hydration of the minor hematite component of the goethitic clay, due to penetration of water along grain boundaries. Goethite has been precipitated into the ferruginous clay from solution channels, which formed as fractures, linking vesicles.

Specimen 08-133

Khaki lag

Co-ordinates 34025E 38940N

Located over lateritic duricrust

A

The interior of the lag pebble consists of red, ferruginous clay with a few small pisolithic inclusions, dark, ferruginous nodules and shaly quartz. The ferruginous clay is set with irregular crystals of hematite, fragments of nodular, porous goethite and some vesicles.

B

This section shows a red, ferruginous clay-fragment, which contains a ferruginous lithorelic. The lithorelic consists of islands of grey goethite, set with mica reliefs, in turn set in lead-grey secondary goethite. The latter goethite is cut by numerous dehydration cracks. The red, ferruginous clay, which is

set with small hematite crystals, is cut by chains of vermicular vesicles and solution cracks from which goethite has diffused into the ferruginous clay (Figure 8H).

C

The lag fragment is of red, ferruginous clay, with inclusions of angular, goethitic lithorelics and a yellow pisolith with a thick cutan. The lithorelics show remnants of matted, layer silicate pseudomorphs and some mica relics, set in porous goethite. One lithorelic has a thick partial goethitic cutan, with included crystals of hematite. Another lithorelic contains only mica relics, set in goethite. The pisolith is more goethite-rich than the matrix and it has a rim which is particularly goethite-rich.

The surrounding red, ferruginous clay, is slightly coarser grained than its enveloping, yellow, ferruginous clay cutan. Both the cutan and the red, ferruginous clay core contain crystals of hematite.

D

The mottled, red-brown nodule contains matted, layer silicate pseudomorphs, set in porous goethite. The whole is set with vermicular voids and solution channels which are unlined.

This suite, except for D, is similar to specimen 08-130. D is related to fabrics seen in specimen 08-124.

Specimen 08-438

Black ferruginous lag

Co-ordinates 34700E 38940N

Located in local background, over either ultramafics or Permian glacial sediments

A

This is a deep honey-brown lithorelic, mottled with yellow-brown and shows a preserved schistose fabric. It consists of matted, layer silicate pseudomorphs, with a short stack fabric, set in secondary goethite. A small patch of fractured quartz is intensely veined with goethite. There are also some vermicular vesicles.

B

This fragment is also a deep honey-brown, rather cellular relic. It contains a few matted, layer silicate pseudomorphs, which occur as islands in later and brighter goethite, which in turn contains vermicular, fibrous, accordion-like structures (Figure 7F), apparently after recrystallised kaolinite (compare with Figure 9). The whole is set with numerous vesicles which are lined with colloform goethite and some are filled with a ferruginous clay and a quartz breccia, cemented by colloform goethite.

C

This is a dark mauve-brown nodule, set with open and clay-filled vesicles. It has an indistinct but wide cutan which has taken a slightly better polish than the core. It contains a few islands of matted, layer silicate pseudomorphs, set in secondary goethite. Numerous vermicular vesicles are scattered throughout and are lined with fibrous goethite.

D

This consists largely of pinkish, iron-stained quartz and granular iron ore, some showing cubic outlines. The quartz has a granoblastic polygonal fabric and is dotted with euhedral hematite, probably pseudomorphing magnetite crystals. Some areas of colloform goethite fill voids left by pyrite. This appears to be an exotic BIF fragment, veined with quartz.

The fabrics of three of these sections contain relatively coarse-grained pseudomorphs, after matted layer silicates, in confused fingerprint structures, suggesting underlying mafic rocks, but one is exotic. An alternative interpretation could be that they, together, represent a polymictic rock (Permian glacial). This dilemma is a limitation to the interpretation of lag petrography.

Specimen 08-443

Black ferruginous lag

Co-ordinates 34650E 38820N

Located in local background, over either ultramafics or Permian glacial sediments

A

The section shows a mixture of numerous, wispy mica relics and dull goethite pseudomorphs of layer silicates, set in brighter goethite. The overall fabric is matted. The mica relics have been analysed by microprobe (Table 5) as well as the goethite surrounding the mica relics.

B

The interior of the fragment is a complex, mauve-brown, porous nodule with a broad, shiny goethite cutan and contains scattered mica relics and some layer silicate pseudomorphs, set with patches of porous secondary goethite. It has numerous, unlined vesicles and a cutan of bright goethite about 0.2 mm wide. Attached to the lithorelic is a patch of clay-rich hardpan, containing and cementing smaller ferruginous nodules, with fabrics of lithorelics and cutans. The hardpan is set with casts of probable carbonates, now filled with epoxy resin.

C

The interior of this fragment is fine grained, deep honey-brown and has a preserved, slightly schistose fabric. It contains a few islands of very fine-grained, matted, layer silicate pseudomorphs, some with a short stack fabric, set in predominant secondary goethite. A few lozenge-shaped patches of hematite are scattered about.

D

This is a red-brown fragment with patches of hardpan. It contains islands of matted, layer silicate pseudomorphs and mica relics, set in variable proportions of secondary goethite. A few lozenge-shaped hematite crystals are scattered in the fabric.

The layer silicate fabrics suggest underlying mafic rocks, though the *caveat* attached to Specimen 08-438 applies equally here.

FINE LAG

Petrography of the fine lag was carried out on polished grain mounts of 100 - 200 grains so that only one polished block was needed for each sample site. The same sample sites were used as for the coarse lag, so that they can be compared. There was no fine lag available at site 34700E 38940N, so the site 100 m to the west was substituted.

Specimen 08-216

Co-ordinates 33975E 38940N

Located over orebody

The lag is highly heterogeneous (see Frontispiece), containing a wide variety of granule fabrics and colours. Lithorelics vary from honey-brown to deep mauvish red-brown and show preserved schistosities and islands of original metamorphic fabric cut by secondary goethite. Deep brown secondary goethite granules abound. Granules related to the lateritic duricrust vary from yellow-brown to red-brown. A few have cutans of shiny goethite and others are filled with small vesicles.

The section shows a few granules with included mica relics and layer silicate pseudomorphs. In some, the silicate pseudomorphs are difficult to discern as replacement of the pseudomorph is almost complete and a weak and very fine-grained swirled fabric is all that remains. A few kaolinite pseudomorphs show accordion-like structures. Many grains show porous secondary goethite and a few botryoidal structures of alternating layers of goethite and hematite (Figure 8E).

Specimen 08-212

Co-ordinates 33850E 38940N

Located over footwall mafic rocks

The section shows a high proportion of lithorelics, many showing layer silicate pseudomorphs and a few have confused fingerprint structures. Mica relics are rare. Granules showing an indistinct, very fine layer silicate fabric are common. Some granules show partial cutans of grey goethite but many grains show only secondary goethite, in which porous, vein and colloform structures are common.

Sample 08-201

Co-ordinates 34025E 38820N

Located over lateritic duricrust

A large proportion of the granules are lithorelics. Recognisable fabrics include platey mica relics and layer silicate pseudomorphs. Secondary structures include porous goethite, partial goethite cutans and oolitic clay.

Specimen 08-221

Co-ordinates 34150E 38940N

Located over ultramafic schists

Many granules are lithorelics, showing mixed layer silicate pseudomorphs, mica relics and preserved schistosity. Secondary features include bright goethite cutans, grey, clay-bearing goethitic cutans, veining, oolitic material, permeation of goethite outward from cracks in ferruginous clay granules and porous goethite.

Specimen 08-447

Co-ordinates 34600E 38940N

Located in local background, over either ultramafics or Permian glacial sediments

Quartz fragments are very slightly more abundant than usual. The lithorelics contain little mica and the layer silicate pseudomorphs are very fine grained. Some accordion-like goethite pseudomorphs after kaolinite were found.

Specimen 08-453

Co-ordinates 34650E 38820N

Located in local background, over either ultramafics or Permian glacial sediments

Like specimen 08-447, the quartz content is slightly higher than usual. The lithorelics show fine-grained, layer silicate pseudomorphs and rare mica relics. Secondary features include cutans and porous goethite.

Specimens 08-225 to 08-228

Co-ordinates 33747E 39311N: 34172E 39314N: 33545E 38146N: 34290E 38110N

*Located in regional background over probable ultramafics: over presumed ultramafics:
underlying rock unknown: underlying rocks unknown*

The fine lags from the regional background samples have a far higher proportion of red-brown and yellow-brown granules to black granules. Lithorelics show very fine-grained, layer silicate pseudomorphs. Other primary features are a few wispy mica relics and some preserved schistosity. Secondary features include dull, porous and bright, massive goethite, as well as cutans. Specimen 08-227 showed one granule with a confused fingerprint fabric. The clay granules show considerable veining by dark grey goethite. Colloform goethite is found cementing fragmented yellow ferruginous

clay. Some granules show internal ooliths, which are concentrically banded and are set in ferruginous clay.

In summary, the fine lag shows similar features to the coarse lag. Fabrics that can be related to the underlying lithologies can be discerned and all the later secondary goethite and ferruginous clay features are preserved. It is difficult to follow the complex history of the lag from a petrographic study of the fine lag alone. The historical evidence is more fragmentary and this is inherent in the small size of the granules. The wide variety of lag fabrics, colours and structures in the specimens are an added distraction (see Frontispiece). Greater dispersion of the fine lag is apparent from the wide variety of lithorelict fabrics encountered in each specimen, though, in a general way, these fabrics parallel those found in the coarse lag.

APPENDIX 6

Correlation Matrices

Correlations of $> \pm 0.3$ are significant
(95% confidence)

APPENDIX 7

Detailed Geochemical Examination of Cellular Ironstone, Calcrete and Red-Brown Clay

Oxides in weight %
Trace elements in ppm

**DETAILED GEOCHEMICAL EXAMINATION OF CELLULAR
IRONSTONE, CALCRETE AND RED-BROWN CLAY**

A sample of fine lag, from above the orebody on line 38940N, which contained significant quantities of both the cellular ironstone component and fragments of calcrete, was selected for detailed study of its minor, non-magnetic components. Small samples (6 -10 g) of the red- and yellow-brown clays, calcrete and cellular ironstone were laboriously hand picked from the sample with tweezers and analysed. The results are presented in the attached Table, where they are compared to the complete sample of the fine lag and to the magnetic and non-magnetic components of the fine lag.

As would be expected, high levels in Ca, Mg and Sr are restricted to the calcrete component. The calcrete has a Ca/Mg ratio of 13 : 1. The Ba anomaly is not related to the calcrete but probably lies in the black ferruginous lag component and is, thus, likely to be a useful indicator element.

The cellular ironstone is anomalous to strongly anomalous in the target elements As, Au, Co, Cu, Mn Sb, Se and Zn, compared to the other components, and this is where anomalies in these elements are expected to lie. This component appears to represent a gossan component in the lag.

COMPARISON OF COMPONENTS OF FINE LAG SAMPLE 08-0217

Material	Sample Numbers			Co-ordinates		ICP	ICP	XRF	ICP	ICP	ICP	XRF	ICP	INAA
	Field No	Lab Seq	Lib No	East	North	SiO ₂	Al ₂ O ₃	Fe ₂ O ₃	Fe ₂ O ₃	MgO	CaO	TiO ₂	TiO ₂	As
Fine Lag	BC 330	L08-00216	08-0217	34000	38940	17.50	8.71	56.33	58.00	0.42	1.08	1.19	0.87	304
Nonmag Comp	BC 730	L08-00238	08-0259	34000	38940	19.00	9.67	55.47	59.80	0.48	1.13	1.20	0.92	327
Magnetic Comp	BC 830	L08-00269	08-0298	34000	38940	7.08	7.25	72.91	74.10	0.19	0.37	1.33	0.90	114
Cellular Ironst	BC 330.2	L08-01470	08-1471	34000	38940	8.58	4.96	70.48	70.35	0.31	1.01	0.56	0.46	946
Calcrete	BC 330.1	L08-01471	08-1470	34000	38940	24.95	5.87	7.01	7.36	2.28	29.34	0.44	0.41	36
Red-brown Clay	BC 330.3	L08-01472	08-1472	34000	38940	16.83	19.48	44.32	45.1	0.5	0.58	2.29	1.91	254

Material	Lib No	INAA Au	ICP Ba	INAA Ce	INAA Co	ICP Cr	INAA Cr	ICP Cu	XRF Cu	INAA La	ICP Mn	XRF Mn	INAA Mo	XRF Nb
Fine Lag	08-0217	0.288	885	17.5	14.1	771	793	221	219	9.1	1032	895	6.6	6
Nonmag Comp	08-0259	0.148	795	14.3	18.6	772	766	205	236	9.6	1132	1024	5.1	5
Magnetic Comp	08-0298	0.004	1712	21.3	11.3	1234	1444	75	60	13.0	755	669	4.1	6
Cellular Ironst	08-1471	0.396	552	11.4	23.4	346	457	484	506	7.1	1401	1136	1.1	4
Calcrete	08-1470	0.137	211	10.6	6.3	117	142	26.9	42	8.3	255	278	4.1	1
Red-brown Clay	08-1472	0.040	682	12.5	10.5	752	877	136	165	6.2	795	664	3.9	7

* XRF Analyses in bold

Material	Lib No	ICP Ni	XRF Ni	INAA Sb	INAA* Se	XRF Sr	ICP V	XRF V	INAA W	XRF Zn	ICP Zr	XRF Zr
Fine Lag	08-0217	67	29	3.6	11.0	48	1233	1714	6.2	75	125	118
Nonmag Comp	08-0259	43	31	3.5	11.0	43	1218	1716	2.9	79	121	114
Magnetic Comp	08-0298	53	38	7.9	5.0	49	1404	2010	4.0	32	161	149
Cellular Ironst	08-1471	18.3	24	6.9	14.6	45	684	887	11.2	125	100	65
Calcrete	08-1470	24.5	26	0.5	3.5	289	159	166	1.7	27	68.6	69
Red-brown Clay	08-1472	36.8	36	2.2	6.8	34	1396	1701	12.3	65	190	189

APPENDIX 8

Geochemical Data Disc

This DOS formatted 360 kb disc contains four ASCII files:

- | | |
|--------------|---|
| REPT27R.TAB | A tab- (ASCII 9) delimited file which can be read by Microsoft Excel and similar spreadsheets. |
| REPT27R.QRT | A comma-delimited file which can be read by Borland's Quattro. |
| REPT27RA.DAT | A fixed field formatted file which contains Field No, Lab Sequence No, Sample No, Type, Map Ref, Easting, Northing and Date in the format A6, 1X, A9, 1X, A6, 2X, A4, 1X, A8, 1X, I5, 1X, I5, 1X, I5. Data begins on line 7. |
| REPT27RB.DAT | A fixed field formatted file which contains the sample No and 44 analytes in the format A6, 44(1X, F10.3). Data begins on line 5. A list of the analytes, together with methods, units and detection limits, are given in the header. |